TECHNISCHE UNIVERSITÄT WIEN

Imperial College London

DIPLOMA THESIS

Synthesis and characterisation of redox-active conjugated macrocycles

conducted at the **Department of Chemistry**

at **Imperial College London**

under supervision of

Dr Florian **Glöcklhofer**

and

Prof Martin **Heeney**

and

Prof Johannes **Fröhlich**

by

Martina Rimmele, BSc

01326153

December 4th, 2019

Martina Rimmele

An important feature of the chemical universe is that the tree of possible structures is denumerable. At the same time, the playground of chemical structures is subject to systematic elaboration, through the decoration of an underlying skeleton by functional groups of some stability. Very quickly a multitude turns into a universe - of structure and of function.

- Roald Hoffmann/Henning Hopf [1]

Acknowledgements

Zunächst möchte ich mich bei **Prof. Johannes Fröhlich** bedanken, dass er diese Diplomarbeit betreut hat. Außerdem möchte ich mich bei **Prof. Martin Heeney** vom Imperial College in London bedanken, dass er mich in seiner Forschungsgruppe aufgenommen hat und mir somit die praktische Durchführung dieser Diplomarbeit ermöglicht hat.

Mein wohl größter Dank gilt **Dr. Florian Glöcklhofer**, sowohl für die ausgezeichnete Betreuung der Diplomarbeit als auch für die jahrelange Unterstützung und das große Vertrauen, dass er mir entgegenbrachte.

Ich möchte mich außerdem bei der **Heeney Group** und auch bei der **McCulloch Group** in London bedanken, dass sie mich so herzlich aufgenommen haben und auf jede meiner Fragen eine Antwort hatten. Besonders möchte ich mich bei **Notina, Pete, Tom, Max, Mark** und **Charlotte** für die Unterstützung bedanken und dafür, dass sie dafür gesorgt haben, dass sich der Frust über nicht gelungene Reaktionen immer schnell wieder gelegt hat. Die Zeit im Labor wäre ohne sie sicher nicht so lustig gewesen.
Bei **Matthias** und **Katharina** möchte ich mich für die Hilfe und Unterstützung innerhalb des Projekts bedanken, sowie für die lustigen Stunden die wir gemeinsam im Labor verbracht haben.
Ich möchte mich auch bei der **Fröhlich Gruppe** bedanken, dass sie mir bei sämtlichen Anliegen geholfen haben.

Meinen Freunden **Barbara**, **Dorian** und **Eva** möchte ich dafür danken, dass sie London zu einem Zuhause für mich gemacht haben.

Bei meinen Studienkollegen, insbesondere **Anna**, **Vroni**, **Emil** und **Andi**, möchte ich mich für die unzähligen Lernsessions und Mittagspausen bedanken. Ohne sie wäre die Zeit an der Uni nur halb so unterhaltsam gewesen. **Michi** möchte für die vielen Diskussionen und Tipps danken.

Lilli und **Felix** möchte ich dafür danken, dass sie stets für mich da waren und es immer geschafft haben, mich von der Uni abzulenken. Ohne sie hätte ich die stressige Zeit während des Studiums sicher nicht überstanden. Auch **Hannah** und **Ricci** bin ich unglaublich dankbar, dass sie beide immer ein offenes Ohr für meine Probleme hatten.

Mein ganz besonderer Dank gilt meinen Eltern **Andrea** und **Andreas** und meiner Schwester **Madlen**, dafür dass sie immer an mich glauben und ich in jeder Lebenslage auf ihre Unterstützung zählen kann.

Abstract

Fully conjugated macrocycles have attracted much interest during the past few years, as the demand for new materials in nanotechnology is continuously rising. Due to the variety of excellent properties that they can show, they are most suitable for application in the area of organic electronics. However, they are surprisingly underexplored regarding various state-of-the-art applications in this area. This may be due to the lack of straightforward syntheses and the often low yields of cyclisation reactions.

In the course of this work macrocycles with four different cavity sizes were synthesised. Furthermore, the effect of different alkyl chain lengths on the properties of the macrocycles were investigated.

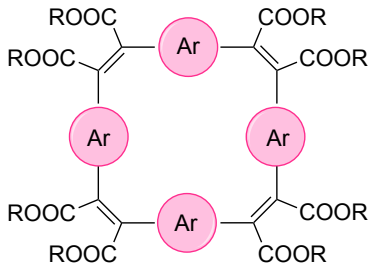

Fully conjugated macrocycle with different aromatic units were synthesised. Aromatic units include benzene, naphthalene, anthracene and pyrene.

The macrocycles were prepared *via* Perkin cyclisation of diacetic acid and diglyoxylic acid precursors, for which synthetic routes had to be developed.

The obtained molecules were characterised by absorption and photoluminescence measurements. Moreover, in collaboration with the Institute of Physical Chemistry at the Polish Academy of Sciences, the redox properties of the macrocycles were analysed by cyclic voltammetry (CV) measurements.

Further conversion of the ester groups to other functional groups, such as cyano groups, was tested using model compounds designed specifically for this purpose.

Model compounds for an alternative approach to conjugated macrocycles with cyano groups *via* Benzoin condensation and further conversion were also prepared. First attempts to convert these model compounds were carried out.

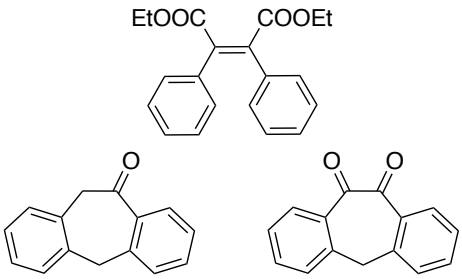

Model compounds for testing and optimising the reactions for the conversion of cyclisation products to conjugated macrocycles with cyano groups. Top: Perkin model compound, bottom: Benzoin model compounds.

Abbreviations

Besides common abbreviations in the English language and chemical element symbols, the below listed short forms are used.

CPP	Cycloparaphenyl
CV	Cyclic voltammetry
DBU	Diazabicyclo[5.4.0]undec-7-ene
DCM	Dichloromethane
DMF	Dimethylformamide
EA	Ethyl acetate
GPC	Gel permeation chromatography
HOMO	Highest occupied molecular orbital
LUMO	lowest unoccupied molecular orbital
MeCN	Acetonitrile
MIEC	Mixed ionic electronic conductor
OPD	Organic photodetector
OPV	Organic photovoltaic
PCC	Pyridinium chlorochromate
PCE	Power conversion efficiency
PE	Petroleum ether
THF	Tetrahydrofuran
TLC	Thin-layer chromatography

Table of contents

A Formula scheme

A.1 Synthesis of precursors for Perkin cyclisation

A.1.1 Synthesis of 2,6-dibromoanthracene

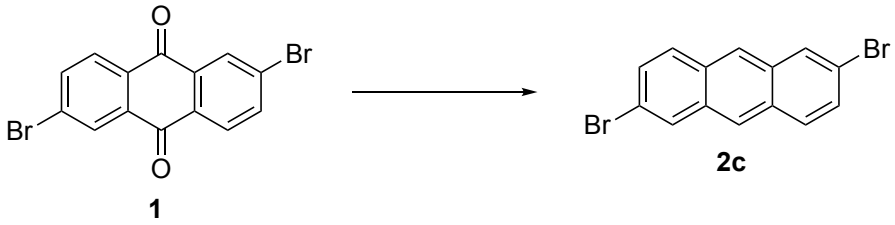

A.1.2 Diethyl glyoxylates

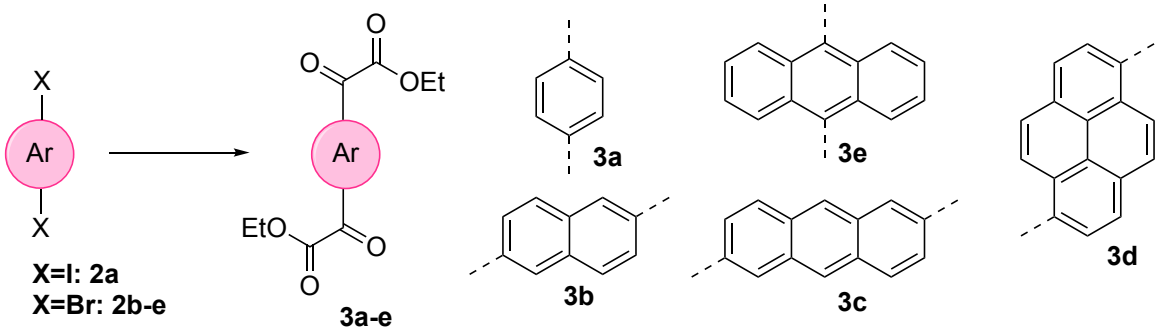

A.1.3 Diglyoxylic acids

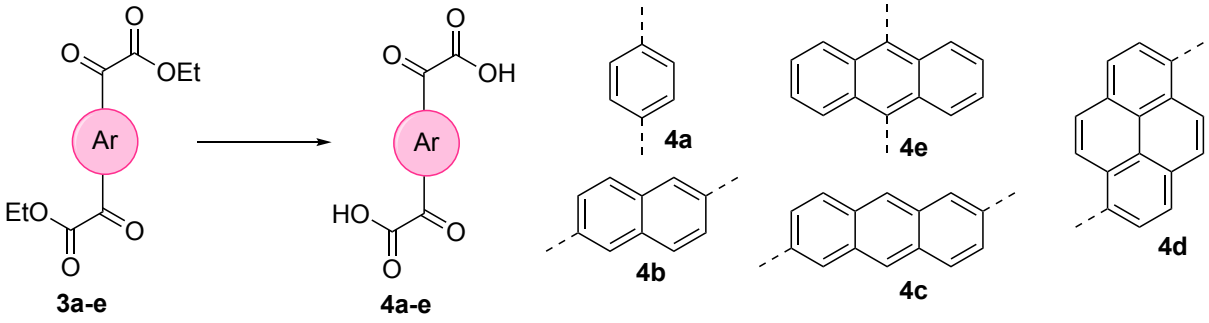

A.1.4 Diacetic acids

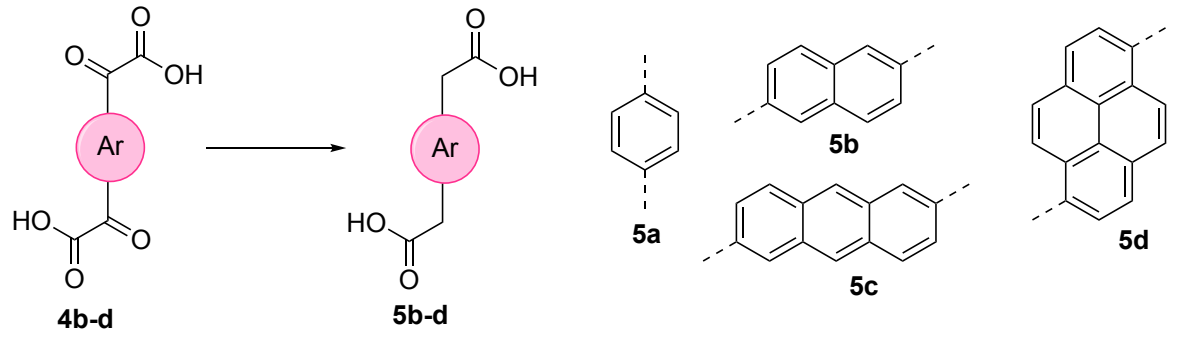

A.2 Synthesis of macrocycles

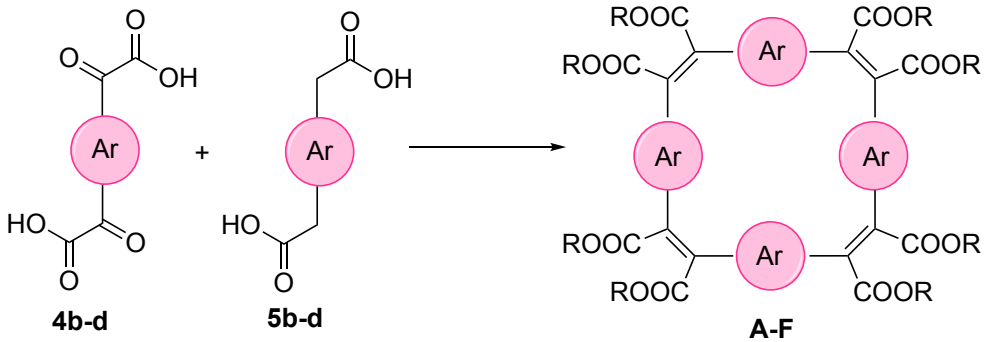

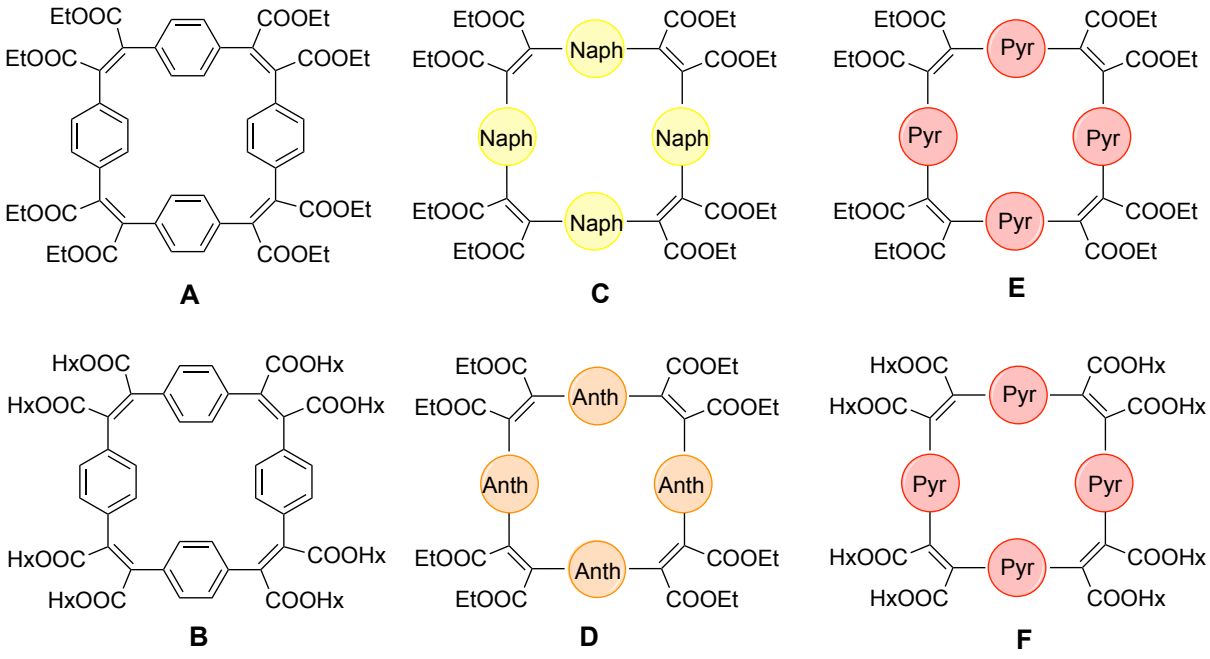

A.3 Synthesis and conversion of Perkin model compound

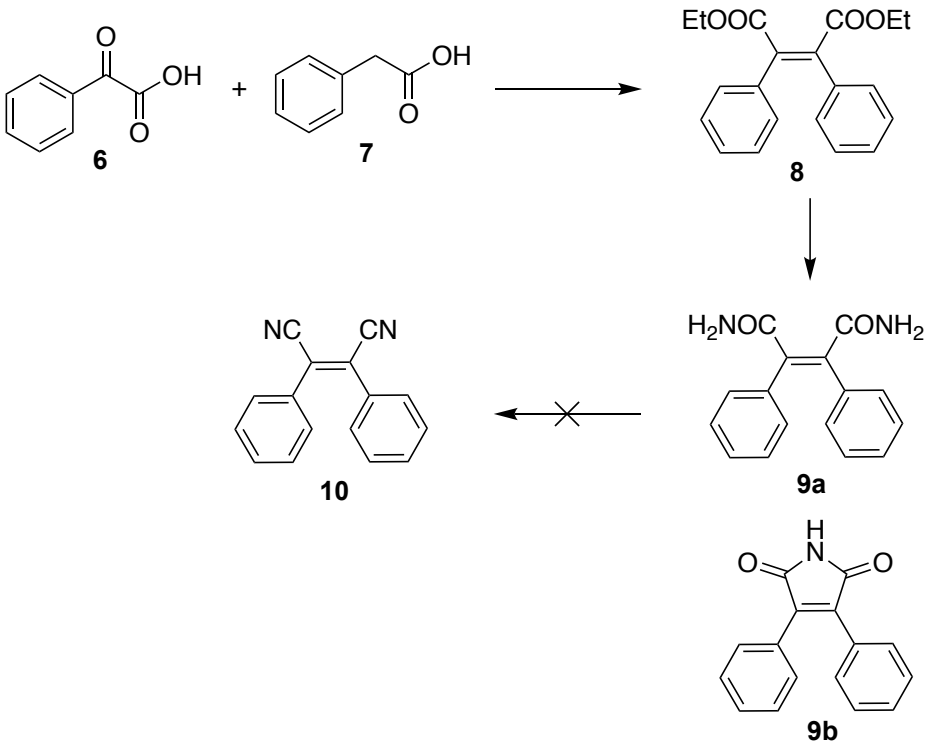

A.4 Synthesis and conversion of Benzoin model compounds

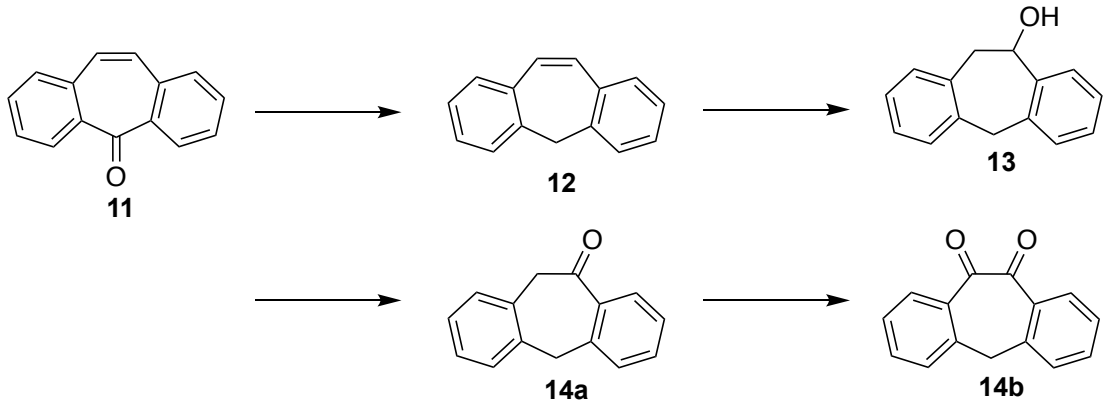

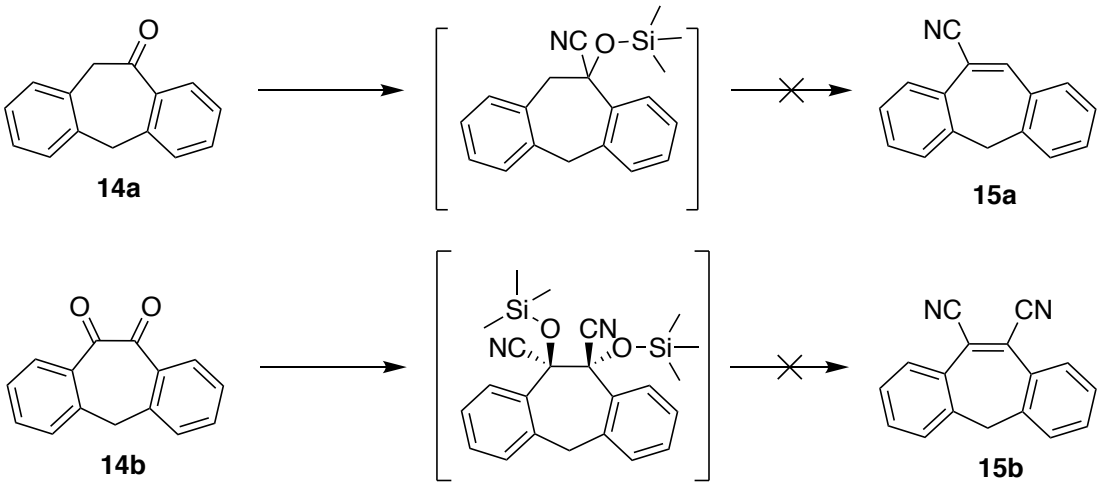

B Introduction

B.1 Conjugated macrocycles

Macrocycles have attracted much interest during the past few years, as the demand for new materials in nanotechnology is insatiable. Due to the variety of excellent properties that they incorporate, they are most suitable for the application in organic electronics, such as in organic battery electrodes, electrochemical transistors, electrochromic devices and light-emitting electrochemical cells.[2, 3]

Macrocycles belong to a group of unique carbon-based molecules, that are hard to synthesise due to the limited number of suitable C-C-bond formation reactions. In order to synthesise these structures, clever methods need to be developed.[4]

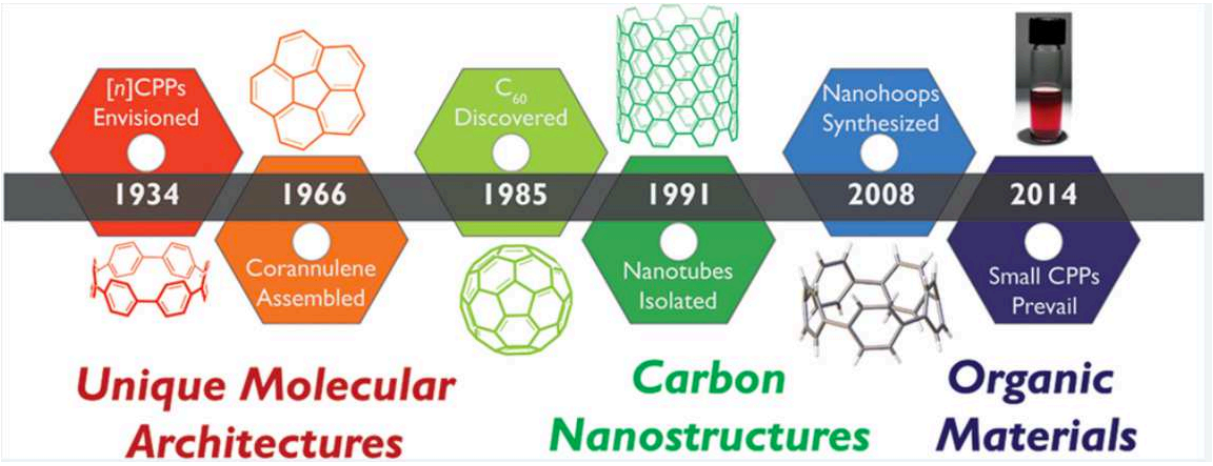

Figure 1: Timeline of the development of unique carbon-based architectures that could be of great value in the application of organic electronics.[4]

Macrocycles are fully conjugated systems, that can be regarded as infinitely conjugated π-systems.[5] Furthermore, many are regarded as shape persistent, which means that they are non-collapsible and geometrically well-defined. In addition, they exhibit repeating units as well as low conformational flexibility.[6] The strain and lack of conformational flexibility is mainly responsible for the hierarchical self-assembly, hence the macrocyclic structure facilitates intermolecular contact and strong π-interactions enable self-assembly into tubular structures.[7] The formation of tubular superstructures is especially advantageous as the channels might be capable of conduction ions. If ion-conduction properties are present, they can be classified as mixed ionic-electronic conductors (MIEC).

In addition, the shape-persistency can also enable them to host electronically useful guest-molecules in the cavity, which makes them feasible candidates for photodetector applications.

B.1.1 Cycloparaphenylenes

Cycloparaphenylenes (CPPs) are a type of macrocycle that are also referred to as carbon nanohoops [8]. They can be seen as the smallest possible armchair carbon nanotube. Owing to the high strain that is present in the CPPs, the synthesis remained challenging for synthetic chemists for many years.[9] In 1934, Parekh and Guha were the first to attempt the synthesis of CPPs. However, their route, the desulphurisation of macrocyclic p,p′-diphenylene disulphide by heating with copper, was not successful. Some 60 years later, Vögtle tried various routes in order to synthesise CPP (see Figure 2), e.g. Wittig reaction followed by Diels-Alder, “shotgun” Kumada macrocyclisation and intramolecular McMurry coupling. Unfortunately, all of those approaches remained unrewarding. [4]

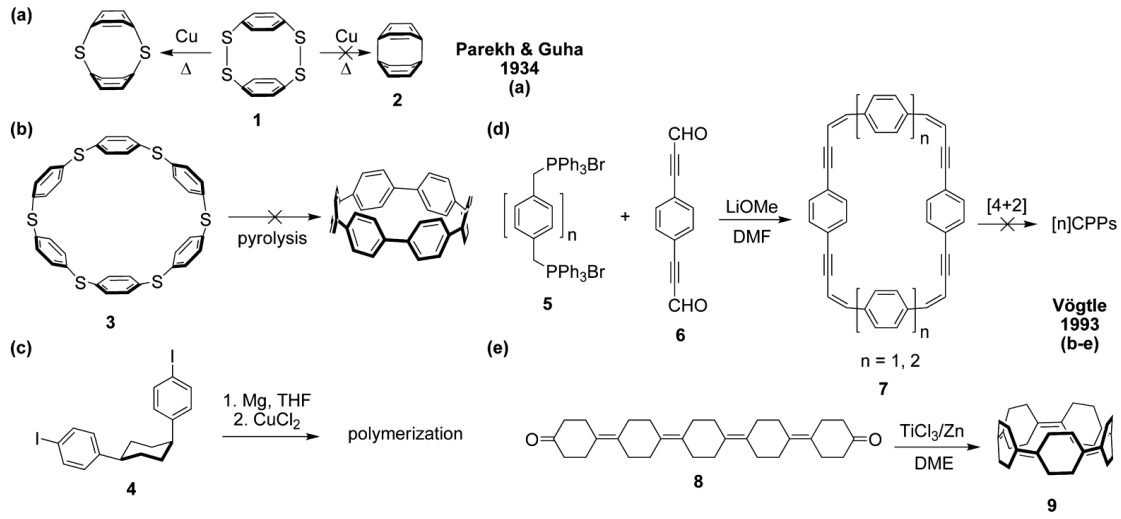

Figure 2: Multiple approaches to synthesise CPPs. a) Pareck and Guha synthesised macrocycle 1 and tried to desulphurise by heating with Cu. b) Pyrolysis of macrocyclic aryl sulfide. c) Kumada coupling of 4 lead to polymeric product. d) Vögtle tried to synthesise CPPs via Wittig reaction and subsequent intermolecular Diels-Alder reaction. e) Intramolecular McMurry coupling to yield 9. In this last approach traces of macrocycle 9 were isolated. [4]

Another 15 years later, Jasti and co-workers published a synthetic protocol to CPPs of different sizes.[8] They were able to obtain the nanohoops in just four steps (Figure 3), starting from 1,4-diiodobenzene by gradually increasing the strain in the molecule. The slightly strained cyclic intermediates (12-14) were converted to CPP with lithium naphthalide. The driving force to overcome the strain energy is provided by aromatisation.[8]

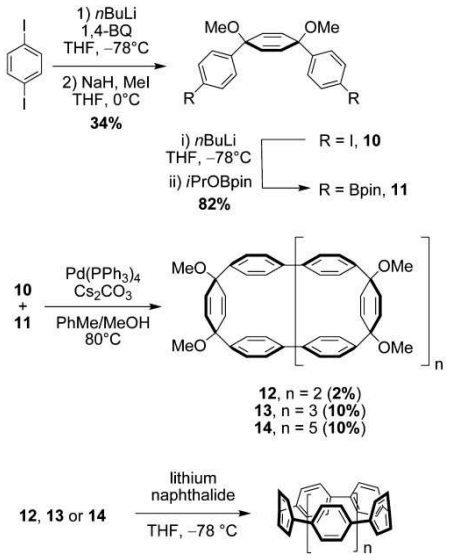

Figure 3: Synthesis of CPPs by Jasti and co-workers[4]

B.1.2 Electronic structure and aromaticity

Conjugated macrocycles can feature unusual electronic and electrochemical properties. For example, paracyclophanetetraenes, which are composed of linked benzene units connected at the 1,4 positions by vinylene units, and related compounds exhibit exciting redox properties. Using the Hückel rule it can be estimated whether a planar cyclic molecule shows aromatic or antiaromatic properties. A macrocycle is considered aromatic if it possesses a circuit [4n+2] π-electrons. Formally, paracyclophanetetraenes in their neutral state are antiaromatic due to their number of π-electrons in the periphery [4n] (see Figure 4). [10] Upon twofold reduction, a system consisting of [4n+2] π-electrons is created, a dianion, and is considered superaromatic, or globally aromatic. Global aromaticity is defined as a state of higher electronic stability due to cyclic movement of π-electrons in the perimeter of the molecule.[10, 11] Tetra- and even hexaanions can be created upon further reduction. It is expected, that those large and stable cyclic anions exhibit exceptional magnetic characteristics. [11]

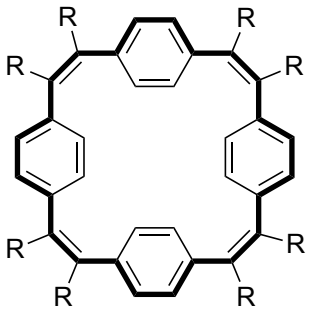

Figure 4: Fully conjugated substituted macrocycle with 24 π-electrons in the perimeter (in bold).

B.1.3 Molecular self-assembly

As mentioned above, self-assembly of macrocycles into supramolecular aggregates such as 2D layers, 3D nanostructures, tubular channels, discotic liquid crystals, host-guest complexes and porous organic solids has been observed.[5, 12] Self-assembly describes a process, in which a supramolecular structure forms spontaneously from its components and is held together by non-covalent forces. The main forces that come into play are hydrogen bonding and π-π-stacking. Moreover, an additional important feature that strongly influences the assembly, is the presence of side groups that are attached to the macrocycle. Those affect the supramolecular assembly behaviour. For instance, if the side groups are polar and tend to orientate orthogonally (see Figure 5, left), the formation of tubular structures is more favoured. In contrast, if the polar functional groups are pointing to the outside (see Figure 5, centre), the arrangement into 2D networks is more likely. Macrocycles with functional groups that are pointing inside the cavity (see Figure 5, right) tend to act as host molecules for smaller molecules or ions.[13]

Figure 5: Different orientations of the side groups (functional groups) that are attached to the macrocycles lead to distinctive motifs after self-assembly [13]

The formation of tubular channels is especially interesting for application in organic electronics as the channels might be capable of conducting ions. Furthermore, the channels are also capable of hosting guest-molecules. The size of the cavity is regarded as the main characteristic that determines the binding of certain cations, e.g. by π-cation interactions. π-cation interactions are

crucial in the regard of molecular recognition, catalysis, ion channels, in materials science and biological processes.[14] The strength of the π-cation bond is dependent on both, the π-system and the cation (size and charge). Dinadayalane et al. found that the interaction strength of the π-system and the cation decreases in the following fashion: $Be^{+2}>Mg^{+2}>Ca^{+2}>Li^{+}>Na^{+}>K^{+}$, and that the binding strength increases if the number of rings fused to benzene increases.[15] The rattling motion (out-of-plane motion) through the pores of carbon-based conjugated ring systems was further studied computationally by Shekar et al. They found that in theory, a rattling motion of Li^{+} ions is only hindered by a relatively small energy barrier (~ 4 kcal/mol, energetically comparable to the inversion of NH_3) and thus should be observable experimentally.[16]

Another issue that is influenced by macrocycle size, is the HOMO-LUMO energy gap. It was found, that the band gap of cycloparaphenylenes narrows with decreasing macrocycle size (see Figure 6).[4]

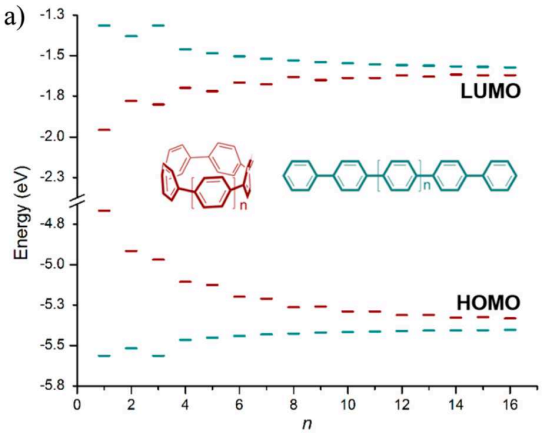

Figure 6: Calculated HOMO and LUMO energy levels of cyclic (red) and acyclic (blue) p-phenylenes [4]

To stress the experimental evidence of tubular channels formed by macrocycles, Figure 7 shows the crystal structure of cyclotetrabenzoin, synthesised by Ji and co-workers by benzoin condensation.[12]

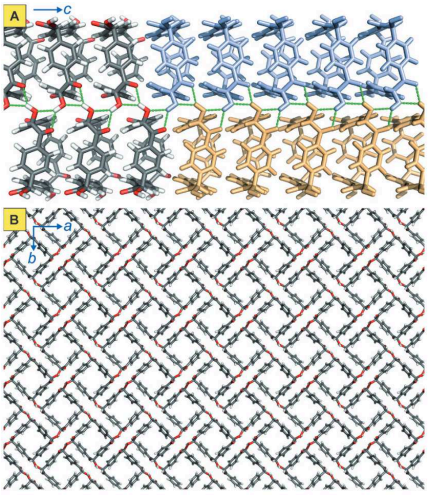

Figure 7: Crystal structure of cyclotetrabenzoin. A) Two columnar assemblies, hydrogen bonds indicated in green. The right ones are coloured to highlight a single nanotube. B) Extended crystal structure viewed along the crystallographic c axis. Shows cluster of hydrogen bonded tubular structures and the pores. C (grey) O (red) H(white).[12]

B.1.4 Potential applications

B.1.4.1 Organic photodetectors

Semiconductor materials are appealing for the use in organic photodetectors (OPDs). OPDs are a promising approach to light detection owing to the tuneable absorption ability that ranges from ultraviolet to near-infrared in the light spectrum. The advantages lie in the straightforward device fabrication which is a general superiority of organic electronics, and compatibility with almost every substrate.[17] Therefore, light-weight and flexible devices can be fabricated.

The working principle of the diodes can be described in three steps (see Figure 8). Firstly, by the illumination of light an exciton pair is formed due to absorption of a photon, followed by diffusion of the exciton pairs to a donor-acceptor interface and subsequent charge separation on the interface. The thus obtained electrons can be trapped by the electrode and converted to an electric signal. This principle overlaps with the working principle of an organic solar cell, but in this type of devices the goal is to achieve a photocurrent signal, not electrical energy. In addition, an external electrical field is applied in order to decrease the energy barrier that occurs in the separation of the exciton to generate a charge pair.[17]

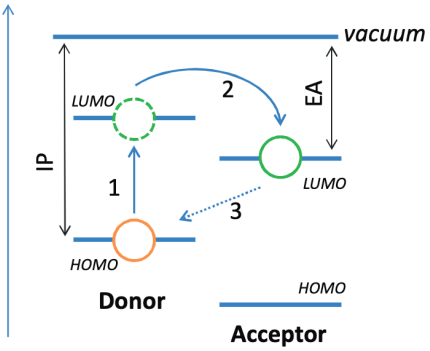

Figure 8: Working principle of a photodetector (photodiode): In the first step, by absorption of photons tightly bound electron-hole pairs (excitons) are generated, those excitons diffuse to a donor-acceptor interface where the charges are separated and the electrons are collected at the electrode where an electrical signal is generated.[17]

The use of rigid macrocycle molecules as the acceptor in the detector lowers the dark current and hence leads to higher photocurrent. Furthermore, due to the lack of end-groups in the macrocycles in contrast to conjugated polymers, the number of trap-sites for charge carriers is remarkably lower. Moreover, charged carriers can occur due to covalent defects in π-conjugated macrocycles and can thus lead to a higher dark current. This also takes place in fullerene-based OPDs as the fullerenes can dimerise and form radicals under illumination which can introduce free carriers as well. Various architectures were introduced to minimise dark current, but by the use of rigid macrocycles in the active layer the device architecture remains simple while at the same time a low dark current is achieved.[2]

B.1.4.2 Rechargeable batteries

Global energy consumption is continually increasing and therefore the demand for renewable energy sources as well as new materials capable of producing energy is rising. Many energy sources produce electricity periodically (e.g. photovoltaics), those rhythms often do not fit energy needs of society, thus there is a huge requirement of materials capable of storing tremendous amounts of electrical energy.[18] An approach to address the problem of sustainable energy storage would be rechargeable organic batteries. The advantage of this materials class is that they are independent of non-renewable components such as rare metals, as they are made of abundant and low-cost starting materials. Furthermore, the large specific capacities and the cost effectiveness make those materials an exciting candidate for future energy storage. Active materials for organic rechargeable batteries need to fulfil a few requirements, e.g. they have to be stable in the used environment upon reversible reduction and they need to host cations or anions reversibly. Moreover, they should not be soluble in the electrolyte. [19] As rigid macrocycles have exceptional electronic, physical and chemical

properties, not only due to the cavity, which is able to host cations, but also due to the electronical structure, they would be valuable candidates in battery testing.

B.1.4.2.1 Mixed ionic-electronic conductors

Organic mixed ionic-electronic conductors (MIECs) are a class of materials that exhibit electron and ion conduction properties, which make them applicable in batteries and fuel cells. Currently there are two groups that are associated as MIECs: ceramics and conducting polymers. Ceramics in general are far better ionic conductors than electronic conductors, for polymers the situation is the opposite (see Figure 9). Macrocycles might be capable of filling the gap between those two classes of materials.

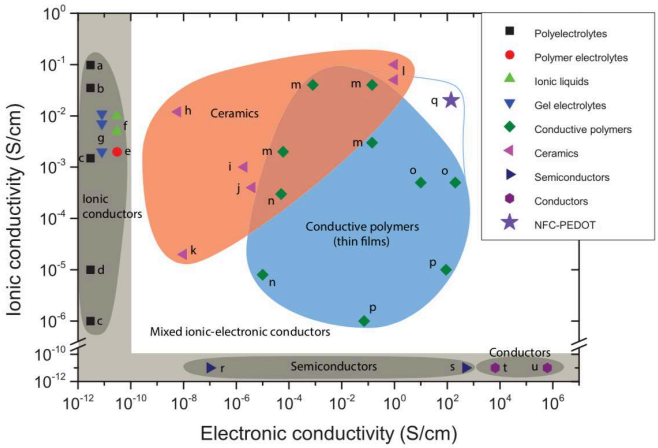

Figure 9: Comparison of different classes of materials with regard to their capability of ion and electronic conductivity.[18]

B.1.4.3 Organic photovoltaics

Organic photovoltaics (OPVs) are yet another way to renewable and clean energy production. Since the direct conversion of sunlight to electricity by organic materials is admirable, the call for new materials is getting louder. OPVs are currently fabricated from two distinctive materials, electron donor (p-type) and electron acceptor (n-type) materials. Under illumination, a strongly bound electron-hole pair is generated in the p-type material, which is then diffusing to an p- and n-type interface where the charges can be separated. The morphology of the active layer needs to be designed in a way that the diffusion length to the next interface is preferably short, in order to inhibit recombination and thus charge loss.[20]

Macrocycles were compared to their linear analogues in the application as n-type materials in OPVs. Devices based on macrocycles (see Figure 10) showed good morphologies and higher

electron mobility. In addition, macrocycles are more easily reduced compared to their linear analogues in this case.[21]

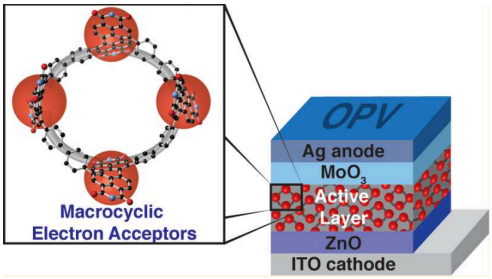

Figure 10: Device structure of an organic solar cell with a macrocyclic electron acceptor material in the active layer.[21]

The power conversion efficiency (PCE) achieved in those devices is more than doubled, which makes them suitable materials for further studies in these types of devices. The rise in PCE can be attributed to the better alignment of the macrocycles with the donor material, but still great phase separation. Furthermore, the macrocycles absorb more visible light and charges are more efficiently transported in the material.[21]

B.2 Aim of the thesis

The aim of this thesis was to synthesise macrocycles with different aromatic units in order to modify the cavity and characteristics of the compounds. Esters were introduced as functional groups as they might be suitable to be converted into other interesting functionalities such as imids and cyano groups. The method of choice for the cyclisation reaction was the recently reported fourfold [2+2] Perkin reaction of diglyoxylic acid and diacetic acid. Moreover, the new compounds were analysed in terms of their spectroscopic and electronic properties.

Another aim was to synthesise model compounds of the cyclisation products of two different cyclisation methods (Benzoin and Perkin cyclisation). Reactions for the conversion of the respective functional groups to imid and cyano groups were tested.

C Synthesis

C.1 Introduction

The synthesis of macrocycles is challenging since the number of cyclisation methods is limited and the yields are usually low.[5] Furthermore, the attachment of functional groups to the macrocycle backbone remains demanding, but two groups have recently published cyclisation protocols that pave the way to macrocycles with a variation of functional groups attached to the backbone.

Durola et al. have recently reported the synthesis of shape-persistent macrocycles by fourfold [2+2] Perkin reaction of a diglyoxylic acid and its reduction product diacetic acid.[22] By the use of either an esterification or imidification reagent, esters and imids can be directly synthesised.[23] The precursors can be prepared from the respective dibrominated aromatic species with *n*-BuLi and diethyl oxalate, followed by hydrolysis of the resulting ester and reduction of the diglyoxylic acid to the diacetic acid.[24]

The above mentioned route to a macrocycle with ester functionalities was published for pyrene as the aromatic unit, but can be adapted to a manifold of aromatic units of different sizes, such as benzene, naphthalene, anthracene (see Figure 11).

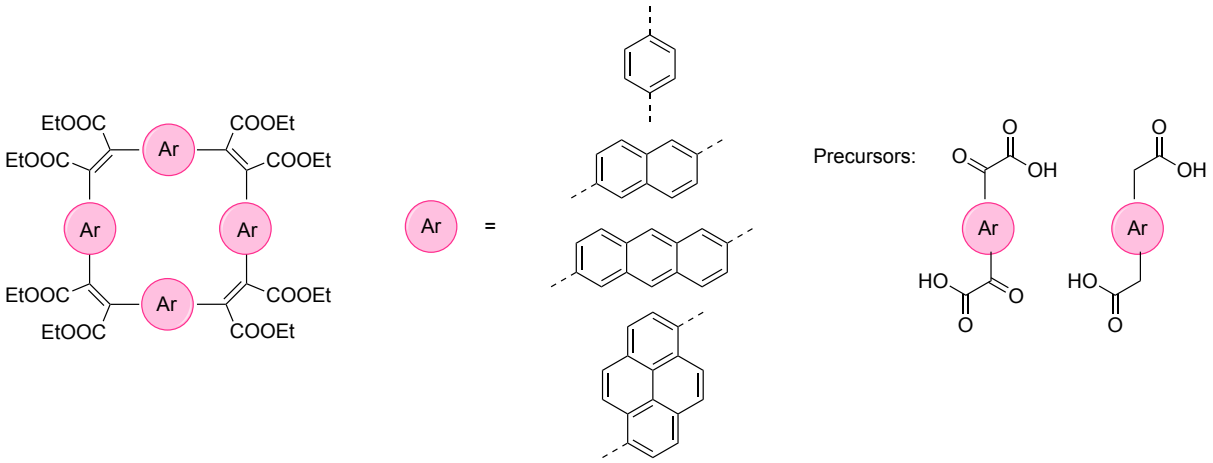

Figure 11: Macrocycles with different aromatic units in order to alter the characteristics such as cavity size. On the right: Precursors used for the Perkin cyclisation

Additionally, it was aimed at transforming the ester groups into amide groups, followed by dehydration of the amides to cyano groups. As these reactions need to be highly efficient due to the number of groups in one molecule, a model compound has been designed for the

optimisation of the reaction conditions prior to carrying out the reactions on the macrocycles (see Figure 12). The model compound **8** was made *via* Perkin reaction.

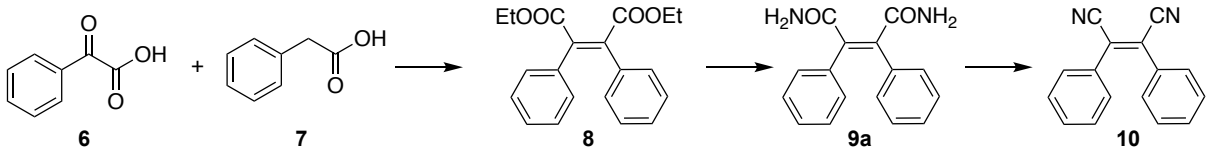

*Figure 12: Synthesis and intended conversion of model compound **8***

The other approach, in which the macrocycle is synthesised in just one step by benzoin condensation of terephthalaldehyde, was reported by Miljanić et al.[12] In this case, the first step of the modification of the functional groups of the macrocycle would be dehydroxylation of the α-hydroxy ketone to the ketone **14a**, followed by formation of the silylated cyanohydrin and the elimination of trimethylsilanol to obtain the desired monocyanated product **15a**. Another route, which leads to the cyclisation product with two cyano groups starts by oxidation of the of the α-hydroxy ketone to the diketone **14b**. Analogous to the monocyanated product, the next step is the formation of the silylated cyanohydrins and subsequent elimination of bis(trimethylsilyl)peroxide in order to obtain **15b**. To see whether this would be a possible approach to cyanated macrocycles, a model compound **16** was designed to test the reactions (see Figure 13).

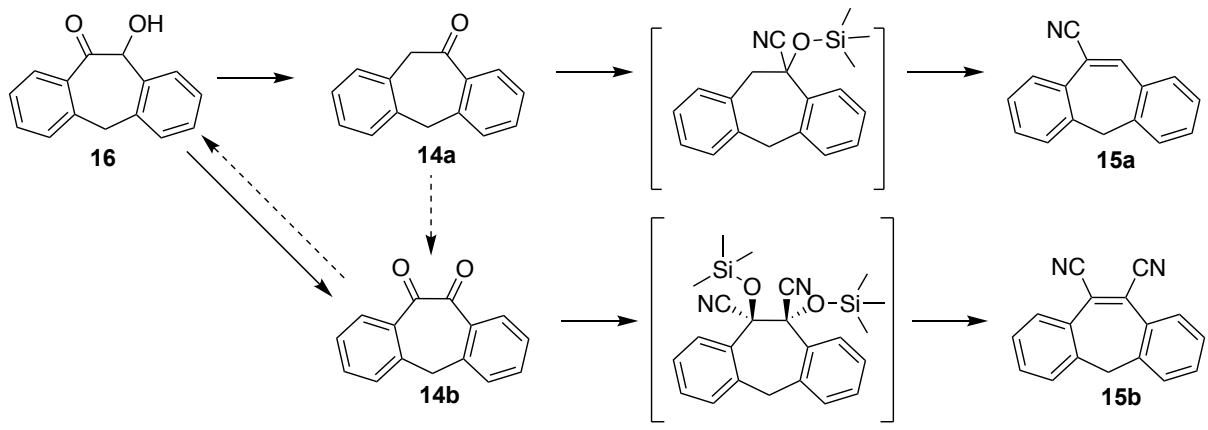

*Figure 13: Reactions to target compounds **15a** and **15b**, synthesis of model compound **16** in dashed arrows*

C.2 Synthesis of precursors for Perkin cyclisation

C.2.1 Synthesis of 2,6-dibromoanthracene

Using the reducing agent H_3PO_2, 2,6-dibromoanthraquinone **1** was sufficiently reduced to **2c** (Figure 14) in HBr and acetic acid. H_3PO_2 is a powerful reducing agent with phosphorus in the oxidation state +I. It is unclear how this reaction proceeds, but it may be assumed that in the first step the ketones are reduced to hydroxy groups by H_3PO_2 followed by protonation of the hydroxy groups and dehydration, whereby a carbocation is formed as an intermediate which is reduced by H_3PO_2 again.

Initially the reaction was refluxed for 5 days as proposed by Kang and co-workers who reported 54 % yield.[25] However, the yield was significantly higher if it was continuously refluxed for 7 days (75 %) or even 10 days (84 %). The colour was a strong indicator in this reaction, as the mixture turns dark grey after one day, and slowly gets of a lighter colour again. The highest yields were achieved if the reaction was refluxed until the colour was light yellow again.

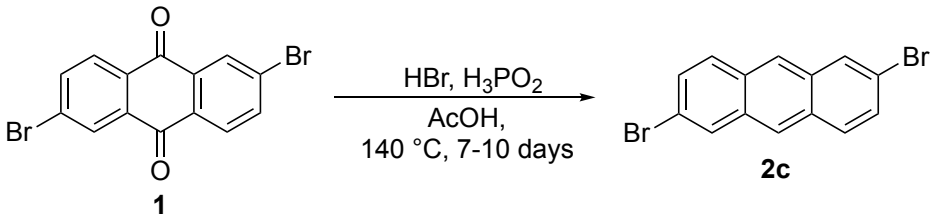

*Figure 14: Reduction of 2,6-dibromoanthraquinone **1** to 2,6-dibromoanthracene **2c** using the reducing agent H_3PO_2*

Before the successful synthesis of **2c** following the procedure outlined above, two other approaches were followed. The first of the unsuccessful approaches was in accordance with the publication of Guo et al.[26] The anthraquinone was treated with sodium borohydride (15.9 eq.) in Na_2CO_3 solution and *i*-PrOH overnight at r.t. (Figure 15). No product was obtained by this method.

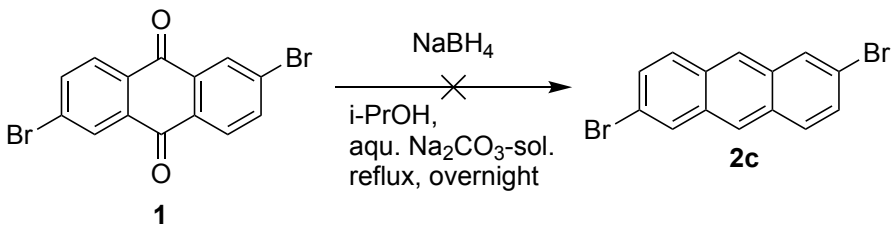

*Figure 15: Reduction of 2,6-dibromoanthraquinone **1** to 2,6-dibromoanthracene **2c** with $NaBH_4$ as reducing agent*

The second unsuccessful approach following a protocol by Klanderman and co-workers, also used $NaBH_4$ as reducing agent.[27] The anthraquinone is reduced in three subsequent steps comprising two reduction-dehydration sequences. In the first step the anthraquinone is reduced to 9,10-anthracenediol **IM1** by $NaBH_4$ in methanol (83 %). Subsequently, by treating with 5 N HCl the anthranol **IM2** is formed, which immediately rearranges to the anthrone **IM3** in a tautomeric reaction.[28] The anthrone **IM3** was isolated in 98 % yield, but the subsequent reduction with $NaBH_4$ in *i*-PrOH only gave very little, impure product.

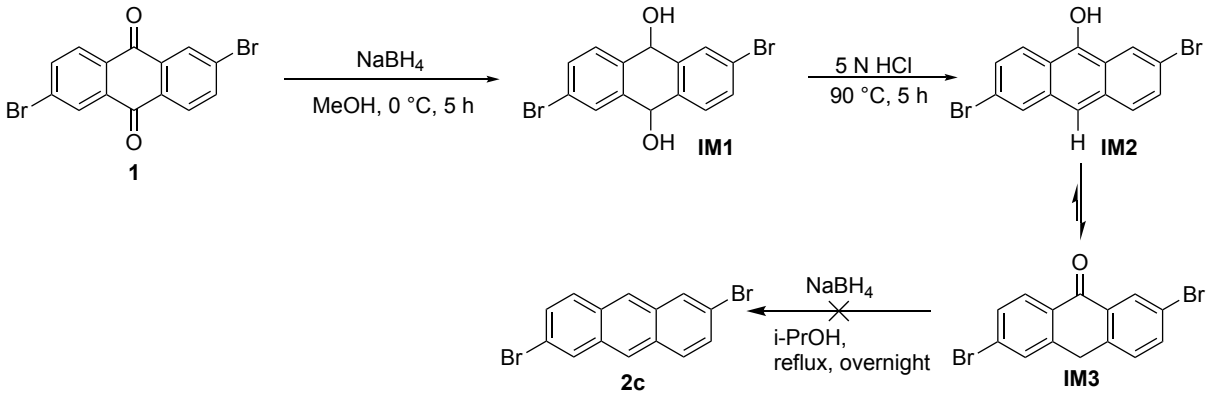

Figure 16: Reduction of 2,6-dibromoanthraquinone to 2,6-dibromoanthracene in three steps using NaBH4 as reducing agent

C.2.2 Benzene- and naphthalene-based diglyoxylate

3a and diethyl 2,6-naphthylglyoxalate **3b** were synthesised *via* lithium-halogen-exchange with *t*-BuLi (4 eq.) followed by quenching of the organometallic intermediates with diethyl oxalate (9.9 eq.) yielding **3a** (44 %) and **3b** (64 %) (Figure 17).

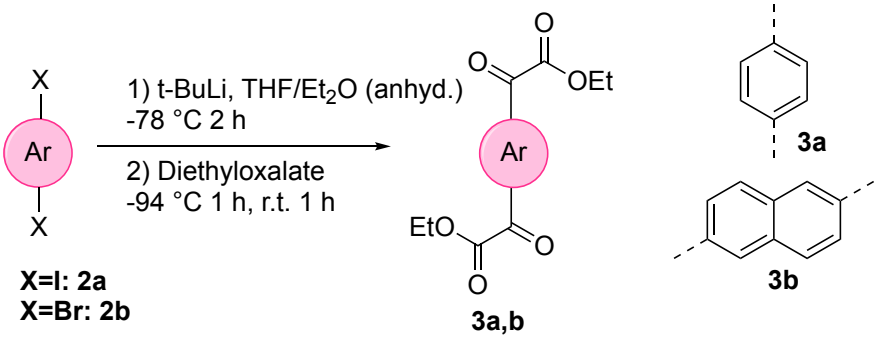

*Figure 17: Synthesis of diglyoxylate with different aromatic units. For the synthesis of **3b** anhyd. Et_2O was used as a solvent, for **3a** anhyd. THF was preferred*

The method for **3a** was adapted from a protocol that was reported by Durola et al.[29]. By replacing n-BuLi (4 eq.) by t-BuLi (4 eq.) the yield was increased remarkably. Initially, 1,4-

dibromobenzene was used instead of 1,4-diiodobenzene for the synthesis of **3a**, but the higher reactivity of the latter towards the *t*-BuLi increased the yield. The solvent was exchanged to anhyd. THF from anhyd. Et_2O as this resulted in slightly better yields. Initially, the crude product was isolated as an oil due to the non-reacted oxalate in the mixture that could not be separated by extraction. Some purification problems arose due to the large amount of oxalate, as it affects the separation by column chromatography. Therefore, the oxalate was first distilled off under high vacuum. The low yield can be attributed to the effort of achieving a very high purity of the compound, as the high purity is crucial in the cyclisation step. Furthermore, the product is prone to react with the lithiated intermediate species and the formation of side products occurs.

3b was synthesised in analogy to **3a**, except for the solvent. This synthesis was reported by Durola et al. before, but some of the parameters were optimised, due to the low yields achieved by using the proposed method.[30]

C.2.3 Anthracene- and pyrene-based diglyoxylate

Anthracene- and pyrene-based diglyoxylates were synthesised from dibrominated precursors by lithium-halogen exchange with *n*-BuLi (4 eq.) in anhyd. THF in the first step followed by quenching of the organometallic species with diethyl oxalate (9.9 eq.) (see Figure 18). The dibrominated precursors were commercially available, except for **2c**, which synthesis was described above. Durola et al. reported a protocol for the synthesis of diethyl pyrenylene-1,6-diglyoxylate **3d** which was followed with only few modifications, e.g. lithiation temperature was raised to -78 °C.[24] Although the reaction was performed multiple times, the published yield of 80 % could not be reproduced (yield of **3d**: 61 %).
Accordingly, anthracene-based diglyoxylates **3c** and **3e** were synthesised following the above-mentioned protocol as well, except that anhydrous THF was exchanged for anhydrous Et_2O as the solvent. Although ethanol was an appropriate solvent for the recrystallisation of **3d** and **3e**, it was not useful for the purification of **3c**, which was therefore purified by filtration over a pad of silica (with PE/DCM 1:1 and pure DCM).

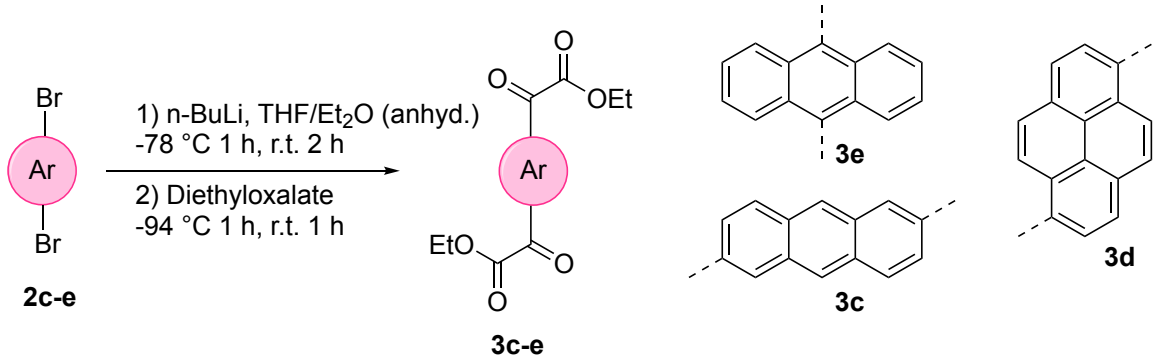

*Figure 18: Synthesis of diglyoxylates with different aromatic units. For the synthesis of **3c** and **3e** anhyd. Et_2O was used as the solvent, for **3d** anhyd. THF was preferred.*

C.2.4 Benzene- and naphthalene-based diglyoxylic acid

Diglyoxylic acids **4a** and **4b** were obtained in almost quantitative yields (**4a**: 96 %, **4b**: 99 %) by hydrolysis of the respective ester with aqueous 2 M NaOH (Figure 19). Prior experiments that were performed following a protocol by Durola et al. [30] in ethanol and with $NaHCO_3$ as a base were not satisfying due to low yields and severely impure products that could not be purified.

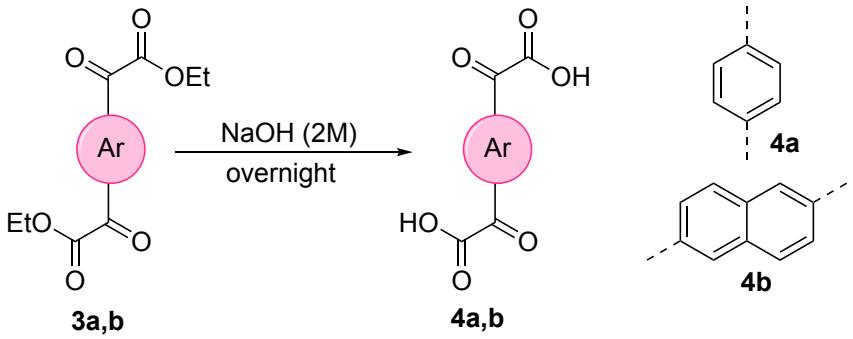

Figure 19: Hydrolysis of diethyl diglyoxylates with 2 M NaOH

Another approach to **4a** was by oxidising 1,4-diacetylbenzene with selenium dioxide (3 eq.), the so called Riley oxidation (see Figure 21), following a published protocol (Figure 20).[31, 32]

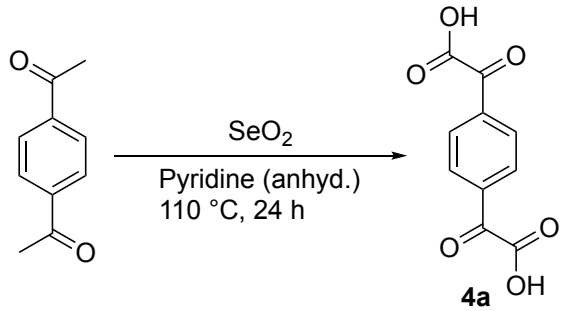

Figure 20: Oxidation of 1,4-diacetylbenzene with SeO_2

In the Riley oxidation, the α-position of a carbonyl is oxidised; it starts with the attack of the enol tautomer on the selenium of selenium dioxide, followed by elimination of water and the attack of an equivalent of water. In the last step, selenic acid is eliminated and the free 1,2-carbonyl product is obtained. [33]

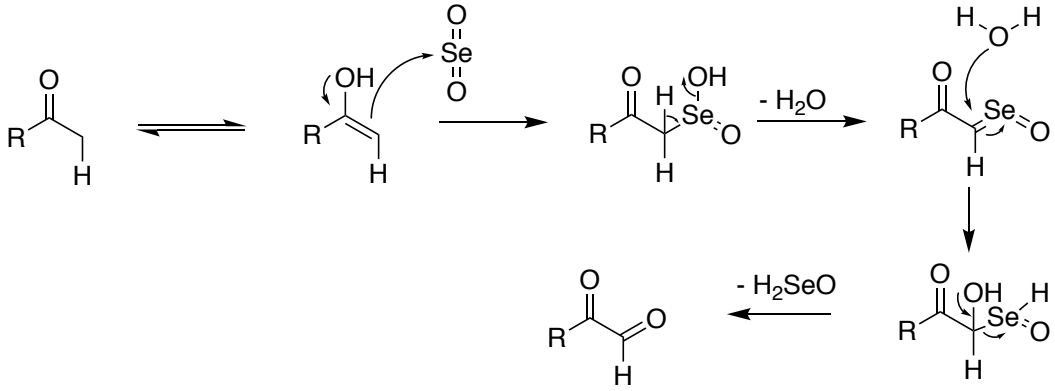

Figure 21: Mechanism of the Riley oxidation with SeO_2

After the oxidation to the 1,2-diketone the compound was further oxidised to the oxocarboxylic acid. Initially a geminal diol is formed by base catalysed addition of water to the aldehyde. Subsequently, the geminal diol is oxidised to the carboxylic acid by SeO_2 (see Figure 22).

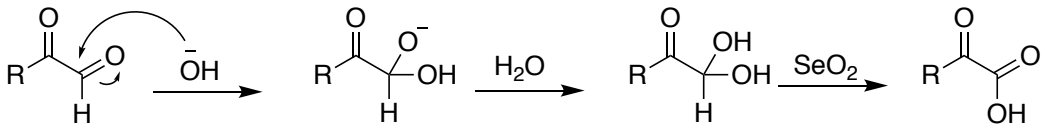

Figure 22: Further oxidation of the 1,2-diketone to the carboxylic acid via a geminal diol.

Zhang and co-workers prepared the mono-oxocarboxylic acid which simply precipitated from an acidified solution after basic extraction. However, due to the stronger solubilising effect of two acid groups, **4a** did not precipitate after acidification and was hence isolated *via* an additional extraction with *n*-ButOH, which can be used to separate polar substances from an aqueous solution by extraction. The obtained product appeared to be very hard to purify due to its high polarity. Nevertheless, the formation of the product could be confirmed by ^{1}H-NMR

(Figure 23) by comparison with the spectrum of pure **4a** obtained by hydrolysis of ester **3a**, as the signal for the aromatic protons at 8.15 ppm was detected. In summary, by oxidation of 1,4-diacetylbenzene with SeO_2 a full conversion could not be achieved but the reaction may be feasible for other oxocarboxylic acids.

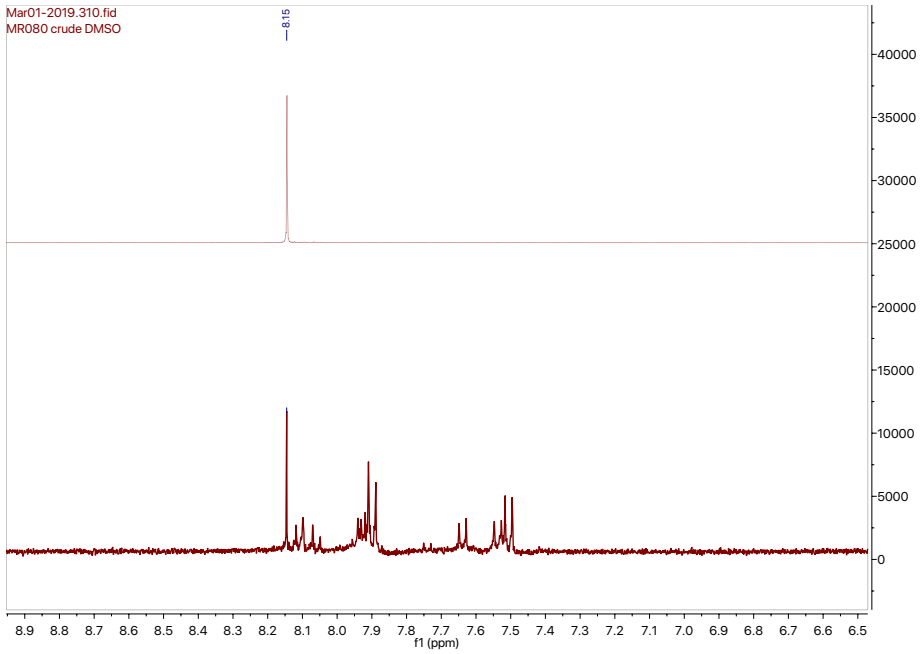

*Figure 23: Stacked ^{1}H-NMR experiments of pure **4a** obtained by the hydrolysis method (top) and crude **4a** obtained via oxidation with SeO_2 (bottom)*

C.2.5 Pyrene- and anthracene-based diglyoxylic acid

Hydrolysis of the esters **3c**, **3d** and **3e** with $NaHCO_3$ in H_2O and EtOH was performed according to a procedure by Durola et al.[29] The reaction yielded the free acids **4c**, **4d** and **4e** in almost quantitative yields (99 %, 90 % and 93 %, respectively).

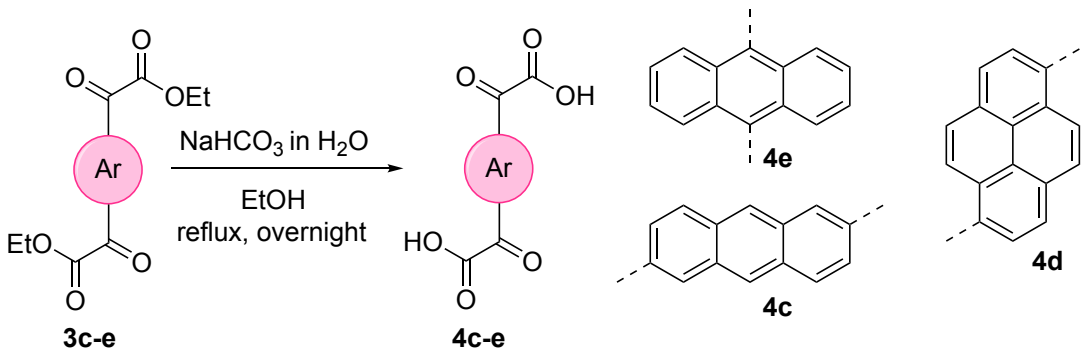

Figure 24: Hydrolysis of diethyl diglyoxalates with $NaHCO_3$

C.2.6 Reduction of diglyoxylic acids to diacetic acids

Durola et al. published a procedure for the reduction of diglyoxylic acids to diacetic acids using a system of NaI and H_3PO_2.[29] Sodium iodide acts as the initiator in this reaction, as it forms I_2 that reacts with H_3PO_2 to form HI which is the active reducing agent. In the first step the keto group is reduced to the alcohol, whereby the reduction regenerates iodine, which is again reduced by H_3PO_2. Thus, iodine is only required catalytically as the actual reducing equivalents are provided by H_3PO_2.[34] The reduction products **5b**, **5c** and **5d** were isolated in moderate to excellent yields (54 %, 77 % and 94 %, respectively) by filtration.

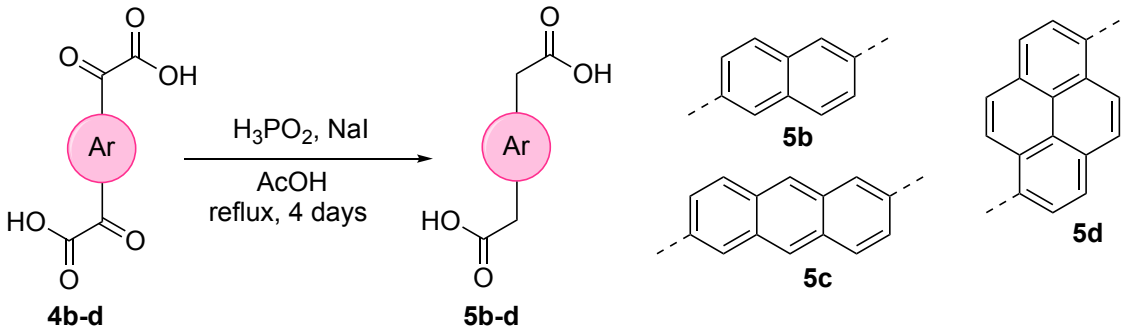

Figure 25: Reduction of diglyoxylic acids to diacetic acids with NaI and H_3PO_2

The same conditions were applied in an experiment with diglyoxylic acid **4e**, but the product could not be obtained analogously. Hence another method was tried that was suggested by Provot and co-workers using NaI and TMSCl as the reducing species.[35] In contrast to the mechanism described above, the active species under these reaction conditions is not HI, but the equimolar ratio of NaI and TMSCl.

^{1}H-NMR of the isolated product revealed that it was a mixture of starting material and product, but due to the difficulty of separating the resulting diacetic acid from starting material the synthesis and isolation of this compound was not studied any further.

C.3 Synthesis of macrocycles

The macrocycles were synthesised by fourfold [2+2] Perkin reaction, which was recently published by Durola et al.[22]

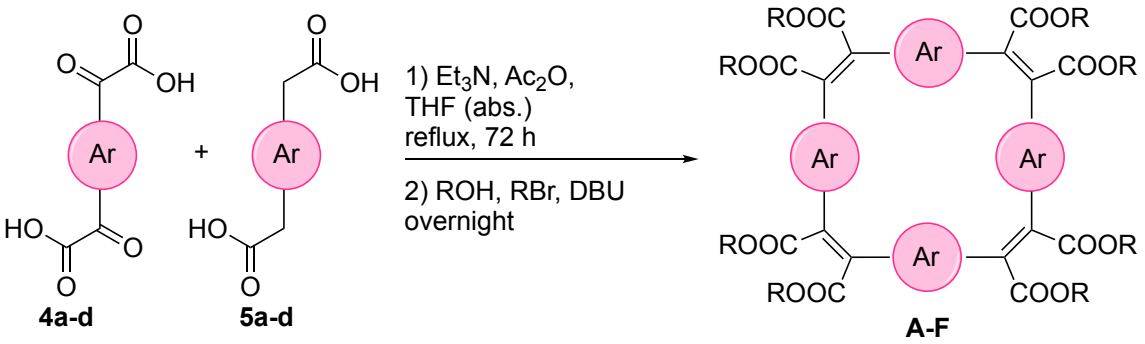

Figure 26: Synthesis of macrocycles via [2+2] Perkin reaction with Et_3N and Ac_2O in THF and subsequent ring-opening and esterification with an alcohol and the respective alkyl bromide as well as 1,8-Diazabicyclo[5.4.0]undec-7-ene (DBU).

The two monomers, diglyoxylic acid and diacetic acid were suspended in THF (anhyd.) and triethyl amine and acetic anhydride were added and the mixture was heated to reflux for three days. Subsequent, the anhydrides were opened and esterificated using an alcohol and the respective alkyl bromide and 1,8-diazabicyclo[5.4.0]undec-7-ene (DBU). The mechanism of the cyclisation is a Perkin reaction followed by base catalysed opening of the anhydride moiety (see Figure 31) and is explained in more detail on page 26.

As the formation of macrocycles competes with the formation of linear oligomers and polymers, the expected yields are usually low. Furthermore, the purification of the cyclic target molecules is difficult, as their properties are similar to the linear by-products. To increase the probability of a ring closing reaction instead of linear chain growth the concentration of monomers in the reaction mixture was kept low (0.005 mol/L). In addition, the use of a syringe pump was investigated in the case of macrocycle **A**, as both starting materials for the synthesis of this macrocycle (**4a** and **5a**) were soluble in anhyd. THF. In this approach, the monomers were dissolved in 20 mL anhyd. THF and added dropwise (2 mL/h) to a refluxing mixture of triethyl amine and acetic anhydride in anhyd. THF *via* a syringe pump. Durola et al. claim that using a syringe pump increased the yield from 25 % to 52 % in their reaction.[29] However, such an effect on reaction yield was not observed in this case; the yield of macrocycle **A** prepared by the conventional method without the use of a syringe pump (16 %) was almost equal to the yield achieved by the use of a syringe pump (17 %).

In total, six different macrocycles with four different cavity sizes, as a result of the use of four different aromatic units, and two different alkyl chains were synthesised (see Figure 27). For

the synthesis of **A**, **C**, **D** and **E**, ethyl bromide and ethanol were used in the ring opening step of the synthesis in order to obtain the ethyl esters, whereas in case of **B** and **F** hexyl bromide and hexanol were used instead.

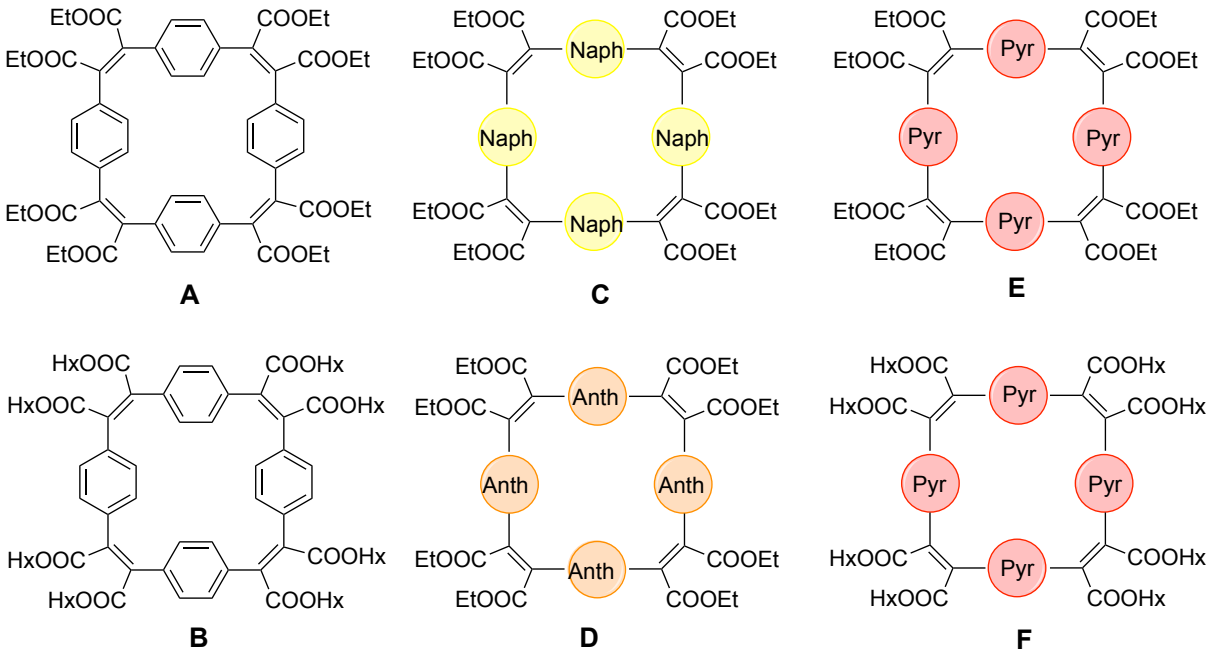

Figure 27: Overview of the prepared macrocycles with different cavity sizes and alkyl chains. Abbreviations: Anth: anthracene, Naph: naphthalene, Pyr: pyrene.

The reaction mixture was quenched in 1 M aqu. HCl and extracted with chloroform. The thus obtained crude products were purified by recycling gel permeation chromatography (GPC), in which the components are separated and recycled over the column multiple times in order to improve the separation. How well this worked can be seen in Figure 28, where the crude compound **A** is displayed below (dark red) and purified **A** is shown above (light red). Another example, where the ^{1}H-NMR spectra of macrocycle **E** are displayed, is shown in Figure 29. Durola and co-workers claimed that macrocycle **E** was purified *via* column chromatography on silica with DCM/PE (3:1) [22], hence this was tested but a separation was not possible. However, the purification of the compounds by the recycling GPC was successful and macrocycles of high purity were obtained.

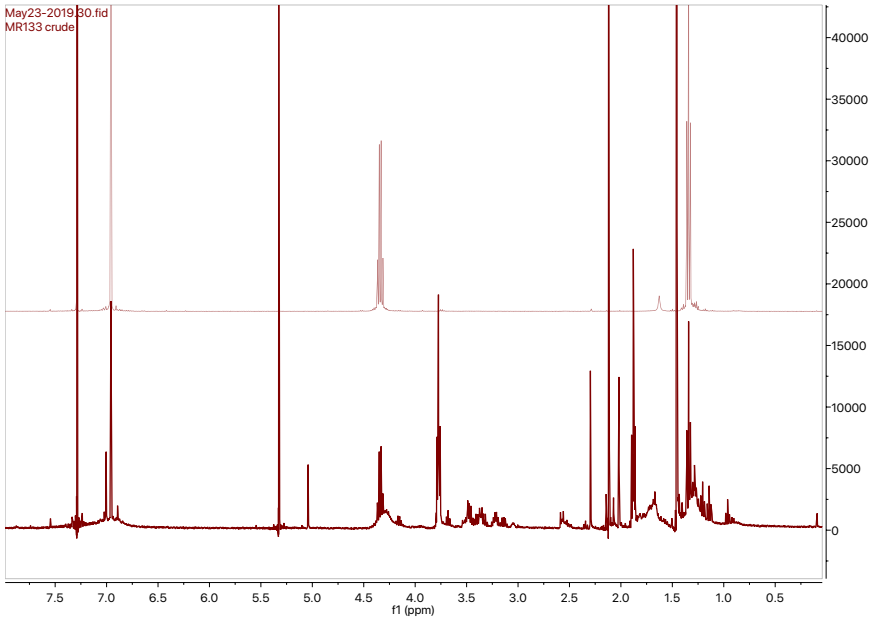

*Figure 28: ^{1}H-NMR spectra of the crude **A** below (dark red) and the purified **A** above (light red).*

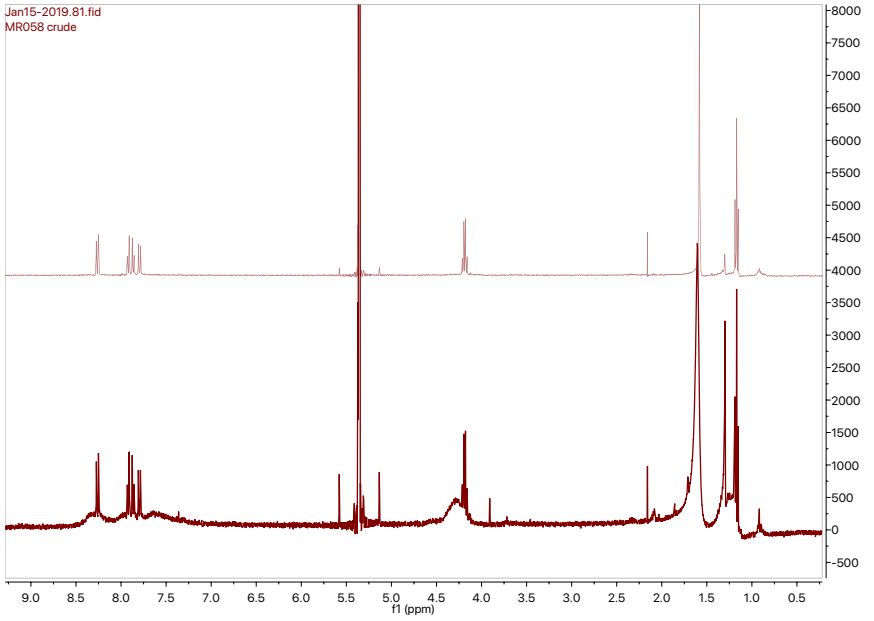

*Figure 29: ^{1}H-NMR spectra of the crude **E** below (dark red) and the purified **E** above (light red).*

Table 1 shows an overview of the yields that were obtained for the respective macrocycles. The reason why the yield obtained for **E** is significantly lower than the yield recently published [22], remains inexplicable, because in general, the ^{1}H-NMR of the crude looks comparable and the purification method has been improved.

Table 1: Yields of the respective macrocycles after purification

	A	**B**	**C**	**D**	**E**	**F**
Yield	17 % w/ pump 16 % w/o pump	8 %	8 %	7 %	8 %	5 %

C.4 Synthesis and conversion of model compounds

Two model compounds were designed on which the functionalisation reactions were tested and optimised prior to carrying them out on the macrocycles. The Perkin model compound was synthesised in order to investigate whether the ester groups can be transformed to imide or cyano groups.

An alternative approach to a conjugated macrocycle with cyano groups would be by benzoin condensation of terephthalaldehyde and further conversion of the resulting functional groups. Model compounds were designed for this route as well and conversion of the ketone and hydroxy groups to cyano groups was tested on these compounds.

C.4.1 Perkin model compound

C.4.1.1 Preparation of Perkin model compound

In a Perkin reaction with acetic anhydride and triethyl amine, phenylacetic acid **7** and phenylglyoxylic acid **6** reacted to give **8** (see Figure 30).[29] The starting materials were suspended in THF (anhyd.) and Et_3N and Ac_2O were added to the mixture. After 24 h, the ester **8** was formed by addition of DBU, EtOH and EtBr. Purification by column chromatography with DCM/hexane yielded the diethyl 2,3-diphenylmaleate **8** in satisfying yield of 79 %.

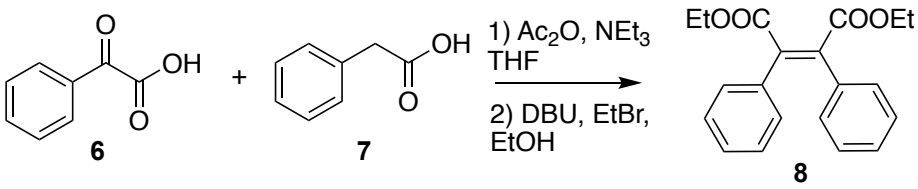

Figure 30: Preparation of Perkin model compound

In the macrocycle the configuration of the double bond is Z, hence it needs to be assured that the configuration of the double bond in the model compound is Z as well. One look at the reaction mechanism (see Figure 31) of the Perkin reaction shows that the configuration is Z for certain, as the cyclic intermediate **IM4** is formed and subsequently opened in a S_N2 reaction catalysed by DBU.

In the first step of the mechanism phenyl glyoxylic acid and phenylacetic acid are acetylated by acetic anhydride, followed by deprotonation of the acidic position of phenylacetic acid. Subsequently, the Perkin reaction takes place. An intramolecular reaction occurs in which the anhydride **IM4** is formed. Hereafter, the cyclic anhydride moiety is opened base-catalysed by

an alcohol whereas a carboxylic ester-acid is formed first, followed by reaction with the ethyl bromide to the diester **8**.[36]

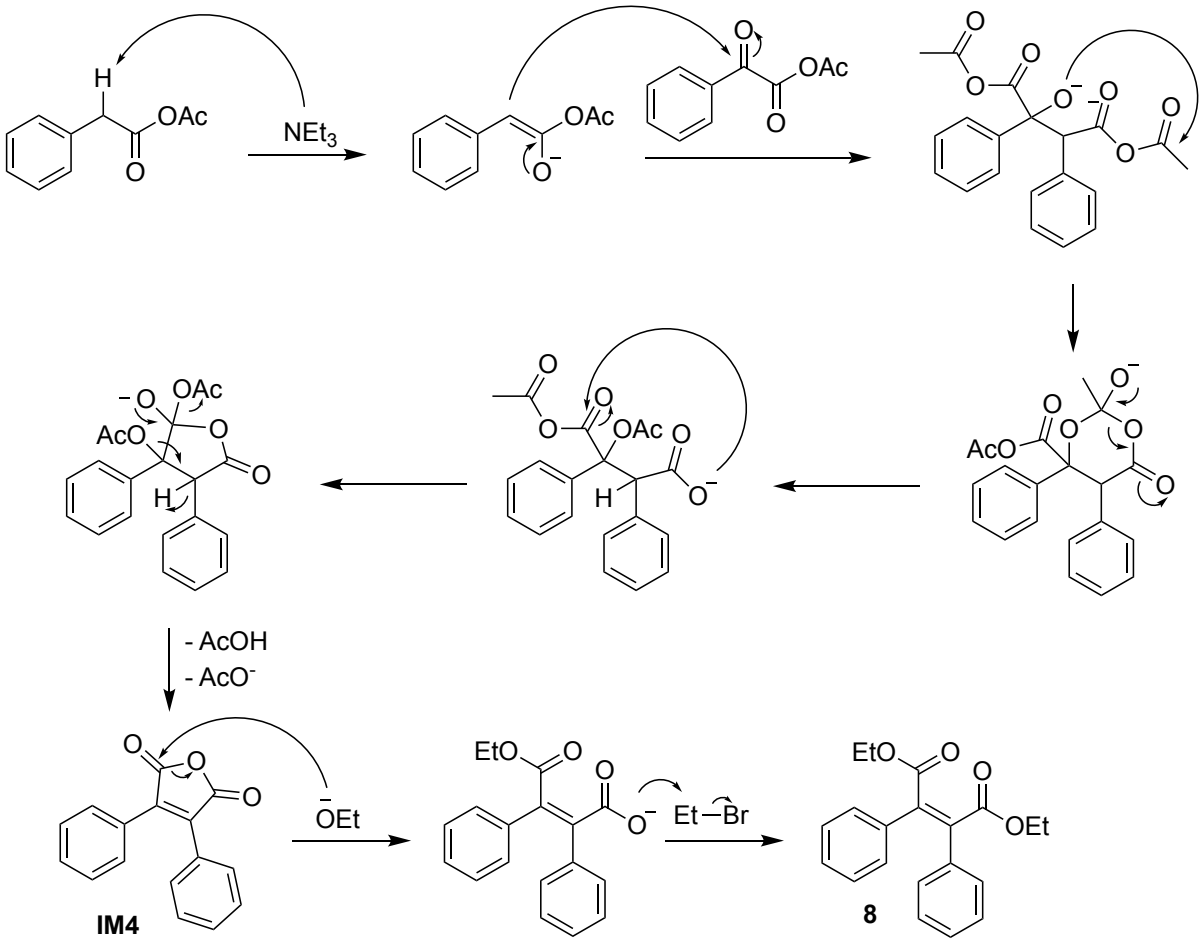

Figure 31: Assumed mechanism of the Perkin reaction with Et_3N and Ac_2O. Subsequent anhydride opening with EtOH, EtBr and DBU.

C.4.1.2 Conversion of Perkin model compound

To investigate whether a conversion of the ester groups in the Perkin cyclisation product to cyano groups would be possible, different approaches were tested on the model compound. The idea was to first convert the ester to amide groups, followed by the dehydration to cyano groups. The first attempt to convert the functionalities was carried out according to Barrett and co-workers, who proposed a method to convert ester into amide groups on a pyridazine.[37] When those conditions were applied and the reaction controlled *via* thin-layer chromatography (TLC), a product formation was not observed. Therefore, NaCN was added as a catalyst to the reaction mixture, which also did not seem to improve the reaction as described before.[38]

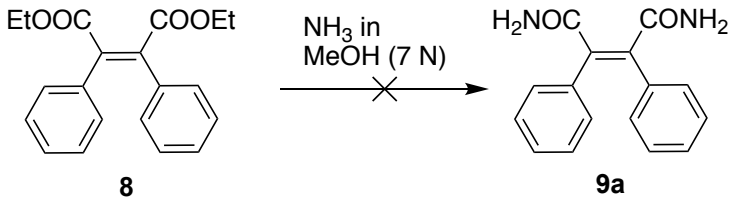

*Figure 32: Conversion of Perkin model compound to diamide **8** with NH_3, which was not successful also not after multiple different attempts*

Derdour and co-workers synthesised amides by treating esters with formamide and solid potassium tert-butoxide under microwave irradiation.[39] It was observed that not **9a** is formed as was expected, but imid **9b** (see Figure 33**)**.

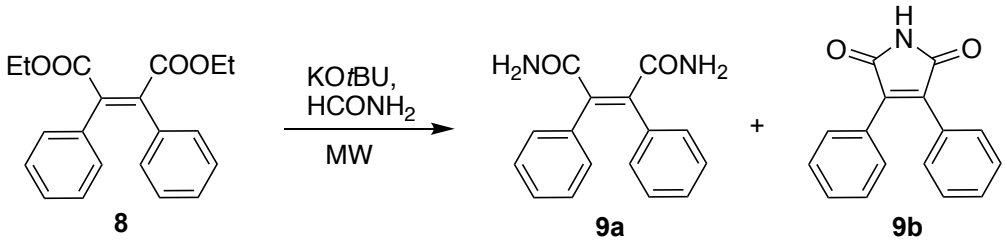

*Figure 33: Attempted synthesis of diamide **9a** by treating **8** with KOtBu and $HCONH_2$ under microwave irradiation. Furthermore, side product **9b** is shown, which was the main product.*

The microwave conditions were optimised for the synthesis of **9b**. It was found that 120 °C for 1 h provides the highest yields of the imid. Furthermore, a method to open the imid ring moiety was tested, to the reaction mixture was added NH_3 in water and stirred for some days, or heated in the MW, but these attempts were not successful.

Moreover, an additional signal with δ 8.95 ppm was detected in the ^{1}H-NMR, which could not be explained at first. However, this peak can be explained by the formation of side product **9b** (see Figure 34), as suggested in the reaction mechanism of Tummala et al.[40]

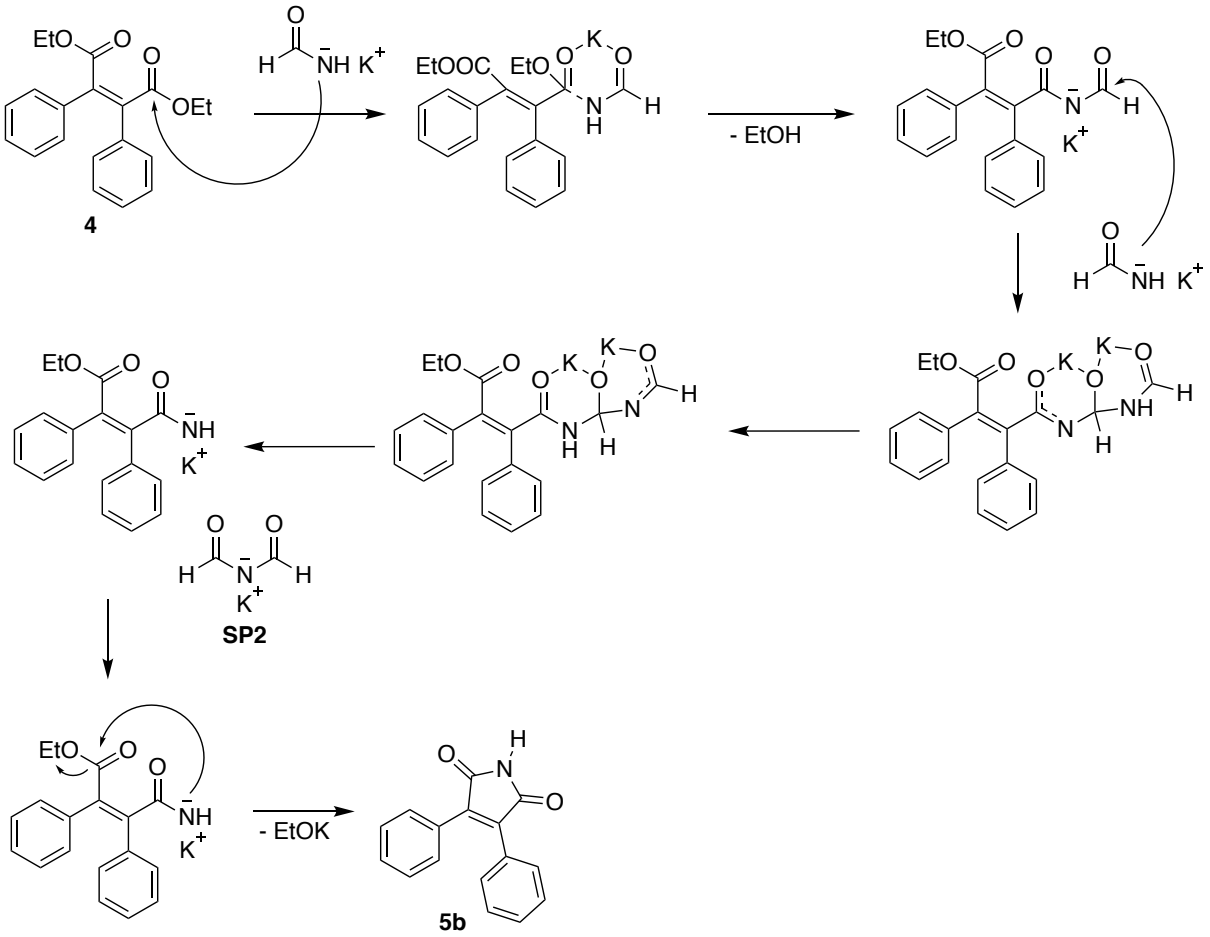

Figure 34: Mechanism of the imid formation with formamide and KOtBu under microwave irradiation

The protons of this potassium salt give a signal in the ^{1}H-NMR which was assigned clearly to the signal at 8.95 ppm, according to Soller and co-workers.[41] To get rid of the salt in the final product, acetic acid was added to the mixture after it was cooled down after the MW, the product crystallised overnight and could simply be filtered off and **9b** was obtained in 73 % yield.

C.4.2 Benzoin model compounds

As an alternative route two benzoin model compounds were synthesised. It was desired to convert the ketone functionalities to cyano groups.

C.4.2.1 Preparation of benzoin model compounds

Model compounds **14a** and **14b** were synthesised following a route published by Linders and co-workers.[42] The first step is the reduction of the ketone with $LiAlH_4$ and $AlCl_3$ in order to obtain **12** in excellent yield (92 %). By treating $LiAlH_4$ with $AlCl_3$ an even more reactive reduction agent is formed, AlH_3. Following, **13** is synthesised in a hydroboration reaction with BH_3 (formed in-situ) and subsequent addition of H_2O_2 to the organoborane. After filtration

through a pad of silica with PE and EA, **13** was isolated in excellent yield (98 %). The alcohol **13** was further oxidised to the respective ketone **14a** with PCC (pyridinium chlorochromate), which yielded 48 % after column chromatography. In a Riley oxidation **14a** was oxidised with SeO_2 in acetic acid to give **14b** in 86 % yield (see mechanism of Riley oxidation in Figure 21).

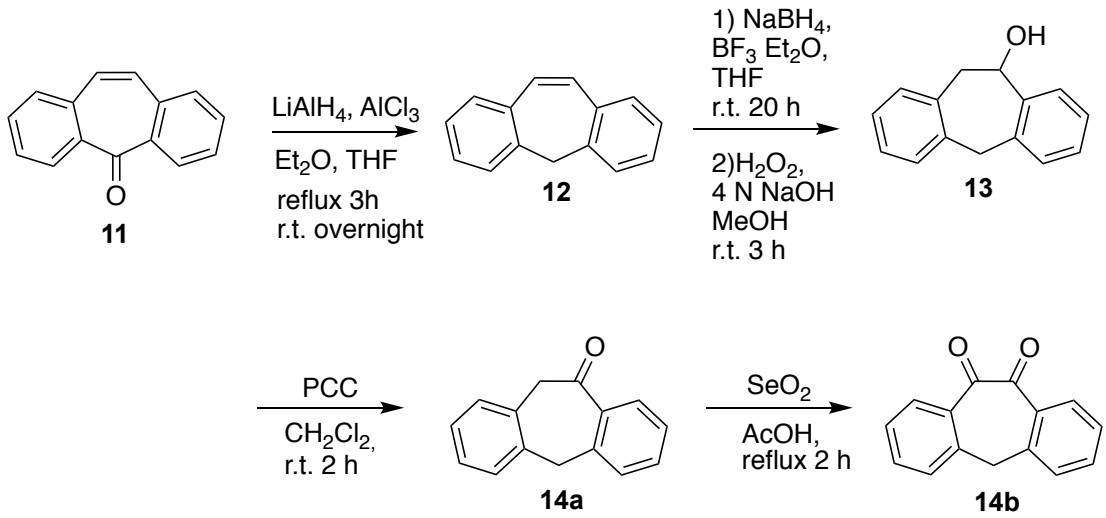

*Figure 35: Synthetic route to model compounds **3a** and **3b***

Furthermore, it was tried to synthesise the actual model compound **16** from **14b** in three different ways. As first attempt, **14b** was treated with 0.25 eq. of $NaBH_4$ as Kaupp and co-workers suggested, although they performed the reaction solvent-free.[43] The reaction was monitored by TLC, after extraction with EA a mixture of starting material **14b** and **17** were obtained.

As an alternative, Shi et al. claim that the diketone could be selectively reduced to the hydroxyketone with $TiCl_4$ and Zn-powder.[44] In this attempt, no reaction took place and just starting material **14b** was isolated.

Finally, following a protocol by Faridbod et al. that presents the reduction of diketones by treatment with Zn-powder and sat. aqu. NH_4Cl-solution in THF was also not successful.[45]

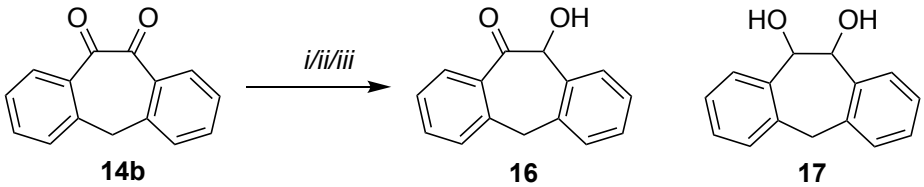

*Figure 36: Attempted reduction of **14b** to **16**. i)NaBH4, THF (anhyd.), 0 °C to r.t.; ii) TiCl4, Zn, THF (anhyd.), r.t. 10 min. iii) Zn, sat. aqu. NH_4Cl-sol., THF, r.t., 140 min. In attempt i) side product **17** was obtained.*

To conclude, benzoin model compound **16** could not be synthesised *via* the presented routes. There are other possibilities for a single reduction published by Shimizu et al. and Hashimoto et al. but due to a lack of time these were not studied further.[46, 47]

Another possibility for the synthesis of **16** would be to start from 1,2-phenylenedimethanol **18** and prepare dialdehyde **19** in four steps according to Kim and co-workers (Figure 37).[48] **16** could then be formed in the next step by benzoin condensation.

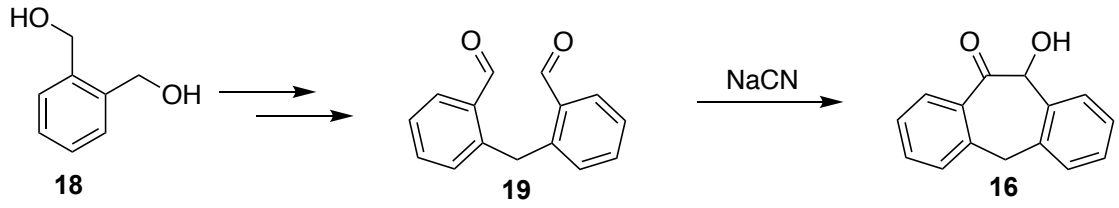

*Figure 37: Possible alternative synthetic route to synthetic route to **16** starting from 1,2-phenylenedimethanol **18***

C.4.2.2 Conversion of benzoin model compounds

The conversion of the keto groups to cyano groups according to Glöcklhofer et al. was tested on the model compounds.[49] In the first step, the cyanohydrin was formed using TMSCN and catalytic amounts of KCN, followed by the attempted elimination of the trimethylsiloxy group with PBr_3 in order to obtain the desired cyanated product **15b** (see Figure 38). The reaction was performed repeatedly, but **15b** could not be isolated. Initially, the reaction was performed in DMF (anhyd.), but the solvent was changed to MeCN (anhyd.) to see whether this could improve the reaction, but no product was isolated.

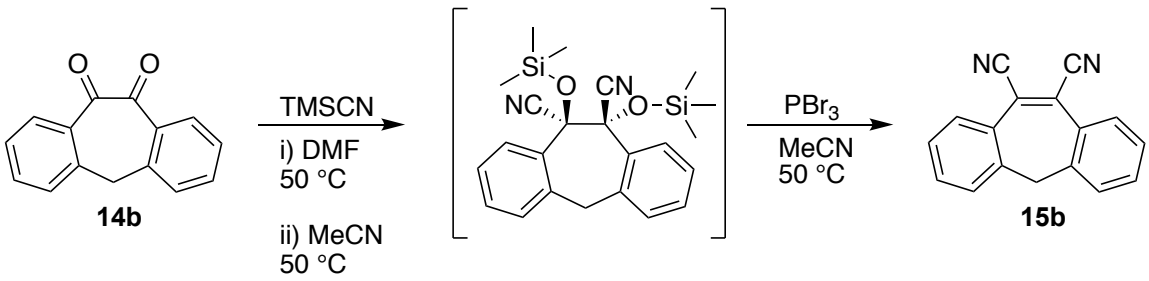

*Figure 38: Conversion of the keto groups to cyano groups and the formation of the alkene via elimination of the trimethylsiloxy groups on the model compound **3b***

Analogue to **15b**, the reaction was executed on **14a** as well and **15a** could not be isolated either.

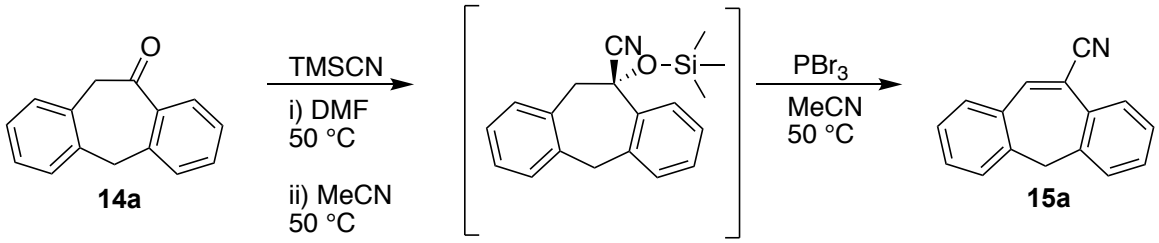

*Figure 39: Conversion of the keto groups to cyano groups and the formation of the alkene via elimination of the trimethylsiloxy groups on the model compound **3a***

D Characterisation

D.1 Spectroscopic characterisation

Absorption spectra were recorded on an Agilent Cary 60 UV-Vis Spectrophotometer and fluorescence spectra on a PerkinElmer LS55 spectrometer. All spectra were taken at room temperature under regular lab conditions from solutions in $CHCl_3$ at concentrations of 5 µM.

D.1.1 Absorption

Absorption spectra for macrocycles A-F were recorded and are displayed in Figure 40. The spectrum of macrocycle **E** is comparable to the spectrum in the literature [22] with two absorption maxima at 283 nm and 362 nm (see Table 2). In case of **A** and **B**, as well as **E** and **F**, there are no differences in absorption maximum for different alkyl chains on functional groups.

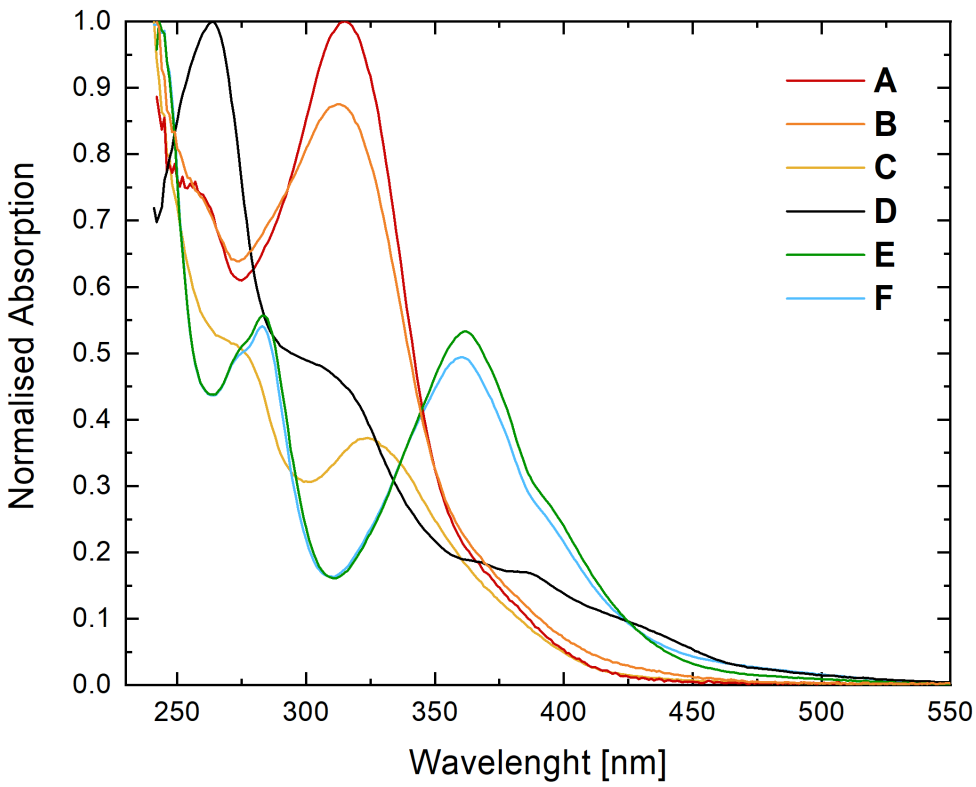

*Figure 40: Absorption spectra of macrocycles **A-F**.*

The optical bandgap was calculated from the absorption onsets (see Table 2). The band gap tends to decrease with increasing aromatic unit size.

Table 2: Determined absorption onsets of macrocycles A-F and resulting calculated optical band gap. For the calculation of the optical bandgap the formula E_g=1243/absorption onset was used.

	Absorption maxima [nm]	Absorption onset [nm]	Optical bandgap [eV]
A	315	355	3.50
B	313	355	3.50
C	275	402	3.09
D	263	466	2.67
E	283 and 362	437	2.84
F	283 and 360	431	2.88

D.1.2 Photoluminescence

Different excitation wavelengths, which were determined from the absorption maxima in the collected absorption measurements, were applied for the excitation of the molecules. In case of **A** and **B** the excitation wavelength was chosen varying from the absorption maxima, because the intensity could be increased, and the quality of the spectra was therefore improved. All spectra were recorded with an emission and excitation slit of 5 nm.

The recorded emission spectra of **C** and **D** are not satisfying which may be due to a non-optimal excitation wavelength.

In Figure 41, there are no obvious trends identifiable for the photoluminescence of macrocycles with different sized aromatic units. It can be observed though that the length of the alkyl chain on the ester, as expected, does not affect the emission behaviour.

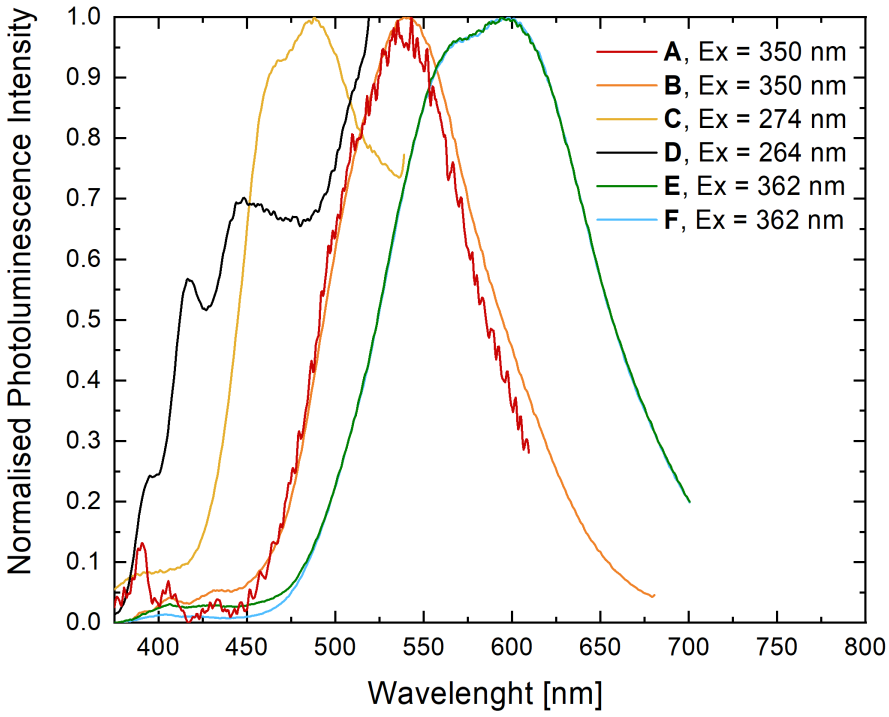

Figure 41: Photoluminescence spectra of macrocycles A-F.

The emission maxima of the compounds were determined, they are summarised in Table 3.

Table 3: Emission maxima of A-F.

	Emission maxima [nm]
A	536
B	539
C	488
D	417 and 444
E	594
F	598

D.2 Electrochemical characterisation

D.2.1 Cyclic voltammetry (CV)

Cyclic voltammetry measurements were carried out by Wojciech Nogala (Institute of Physical Chemistry, Polish Academy of Sciences) with a microelectrode setup in a glove box. The measurements were performed at a scan rate of 100 mV/s. The macrocycles were dissolved in dimethylformamide (DMF) with tetrabutylammonium hexafluorophosphate (NBu_4PF_6) added to the solvent (0.1 M) as supporting electrolyte to ensure sufficient conductivity.

The analysis of the resulting measurements was carried out by the author of this work. In order to determine the reduction or oxidation onset, two tangents were drawn at the baseline and the rising of the reduction and oxidation peaks and their intersection was identified. Ferrocene was used as internal reference material and the reduction onsets were plotted versus the oxidation onset of the internal ferrocene standard (Figure 42 to Figure 47). The oxidation of the macrocycles has not yet been analysed.

The measurements of the ferrocene oxidation and the analysis of the respective oxidation onsets can be found in the appendix (G.1).

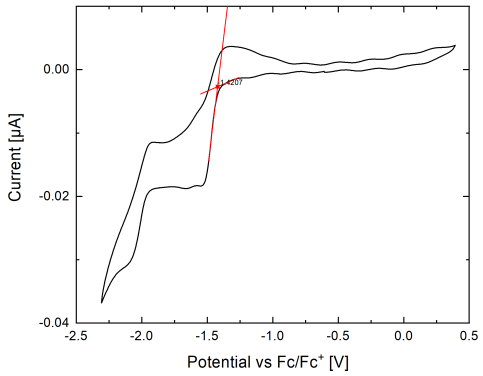

Figure 42: CV measurement of the reduction of A versus Fc/Fc⁺.

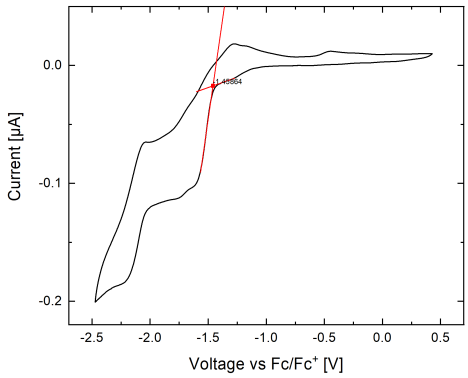

Figure 43: CV measurement of the reduction of B versus Fc/Fc⁺.

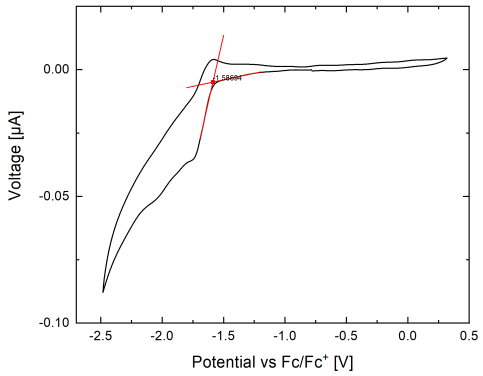

Figure 44: CV measurement of the reduction of C versus Fc/Fc⁺.

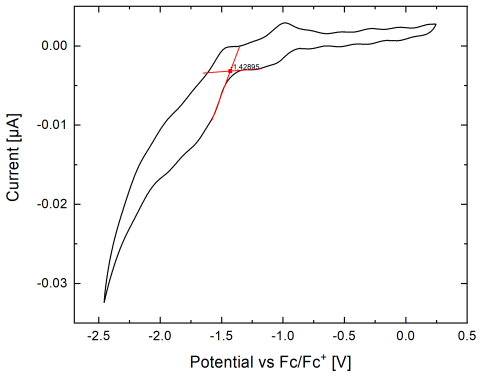

Figure 45: CV measurement of the reduction of D versus Fc/Fc⁺.

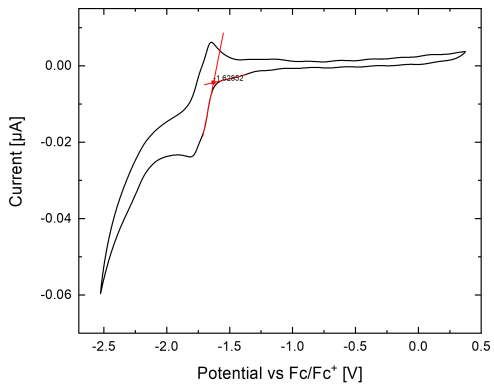

Figure 46: CV measurement of the reduction of E versus Fc/Fc⁺.

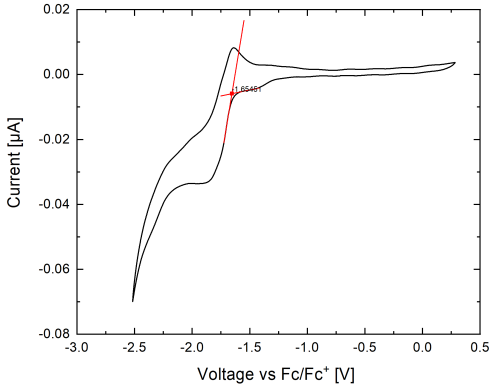

Figure 47: CV measurement of the reduction of F versus Fc/Fc⁺.

The calculated values for the HOMO and LUMO energy levels and the resulting electrochemical gaps are summarised in Table 4. HOMO energy levels were calculated subtracting the optical gap from the LUMO energy levels determined by CV. The optical gap

was determined by the absorption measurements (see Table 2), as only the reduction potential was measured for the macrocycles. All measurements were referenced to ferrocene with a HOMO energy level of -4,80 eV.

Table 4: Calculated LUMO energy levels from CV measurements, the optical band gap determined from absorption measurements, and the resulting HOMO energy levels.

	A	B	C	D	E	F
Reduction onset vs. Fc/Fc^+ [V]	-1,42	-1,46	-1,59	-1,43	-1,63	-1,66
LUMO [eV]	-3,38	-3,34	-3,21	-3,37	-3,17	-3,15
Optical band gap [eV]	3,5	3,5	3,09	2,67	2,84	2,88
HOMO (opt.) [eV]	-6,88	-6,84	-6,30	-6,04	-6,01	-6,03

The electrochemical gap, as expected, is not affected by the alkyl chain length, as can be seen by comparing the results for **A** and **B** and **E** and **F**. Moreover, the gap tends to narrow with larger aromatic unit size and the LUMO energy levels tend to increase with increasing size.

E Experimental section

E.1 Precursors for Perkin cyclisations

E.1.1 Diethyl 1,4-phenylglyoxalate (3a) and diethyl 2,6-naphthylglyoxalate (3b)

General procedure for **3a** and **3b**: [22, 30, 50]

1,4-Diiodobenzene **2a** (3.5 g, 329.90 g/mol, 10.6 mmol)/ 2,6-Dibromonaphthalene **2b** (3.04 g, 285.97 g/mol, 10.6 mmol) was dissolved in 150 mL anhyd. THF/Et_2O (properly degassed priorly) under nitrogen and cooled to -78 °C with an acetone/dry ice bath. *t*-BuLi (1.7 M in pentane, 25 mL, 42.5 mmol) was very slowly added *via* cannula transfer under vigorous stirring. The mixture was cooled to -78 °C for 2 h, afterwards it was cooled to -94 °C using an acetone/N_2(liq.) bath. diethyl oxalate (14.3 mL, 146.14 g/mol, 104.94 mmol) was added quickly, the reaction mixture was cooled to -94 °C for 1 h. Afterwards, it was slowly let warm to r.t. for 1 h. To quench the reaction, it was poured onto aqueous hydrochloric acid (200 mL). It was extracted with DCM (3 x 150 mL), the combined organic phases were extracted with sat. aqu. Na_2SO_3 solution (2 x 150 mL) (not necessary in case of **3b**) and dried over $MgSO_4$. The solvent was evaporated under reduced pressure and the remaining diethyl oxalate was distilled off under high vacuum. The compound was purified by column chromatography on silica gel using DCM/PE (1:1). In order to get rid of small traces of diethyl oxalate, the now crystalline product was suspended in hexane and filtered off.

Characterisation for diethyl 1,4-phenylglyoxalate **3a:**

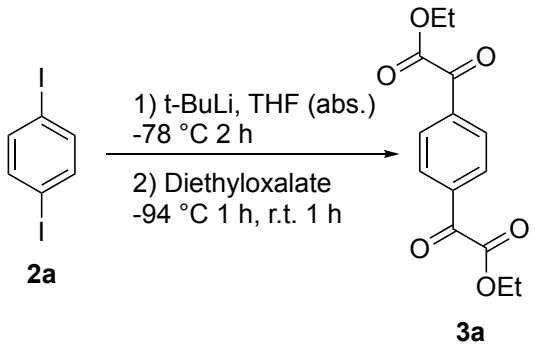

2a **3a**

The compound was isolated as slightly yellow crystals (1.30 g, 4.7 mmol, 44 %).

^{1}H NMR (400 MHz, Chloroform-*d*) δ 8.16 (s, 4H), 4.47 (q, *J* = 7.1 Hz, 4H), 1.44 (t, *J* = 7.2 Hz, 6H).

^{13}C NMR (101 MHz, Chloroform-*d*) δ 185.38, 162.92, 136.96, 130.47, 62.99, 14.28.

MS (ESI-TOF) *m/z*: 278 [M - H]. HRMS: calc. for $C_{12}H_9O_6$ [M]$^-$: 249.0399, found: 249.0390. (Difference of 29 which corresponds to an ethyl group).

Characterisation for diethyl 2,6-naphthylglyoxalate **3b:**

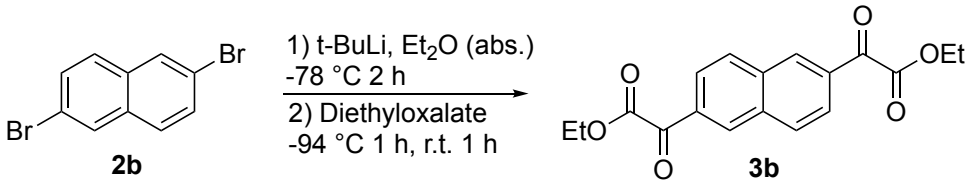

The compound was isolated as white powder (2.24 g, 6.8 mmol, 64 %).

^{1}H NMR (400 MHz, Chloroform-*d*) δ 8.62 (s, 2H), 8.15 (dd, *J* = 8.6, 1.6 Hz, 2H), 8.10 (d, *J* = 8.6 Hz, 2H), 4.52 (q, *J* = 7.1 Hz, 4H), 1.47 (t, *J* = 7.1 Hz, 6H).

^{13}C NMR (101 MHz, Chloroform-*d*) δ 185.88, 163.48, 135.43, 132.84, 132.77, 131.03, 125.56, 62.88, 14.33.

MS (CI) *m/z*: 329 [M + H]. HRMS: calc. for $C_{18}H_{16}O_6$ [M]$^+$: 329.1020, found: 329.1020.

E.1.2 1,4-phenyldiglyoxylic acid (4a) and 2,6-naphthyldiglyoxylic acid (4b)

General Procedure for **4a** and **4b**:

2 M NaOH was added to the respective ester and stirred overnight. The mixture was acidified to pH 1 with 4 M aqueous hydrochloric acid and extracted with Et_2O (3x). The combined organic layers were dried over $MgSO_4$.

1,4-Phenyldiglyoxylic acid **4a:**

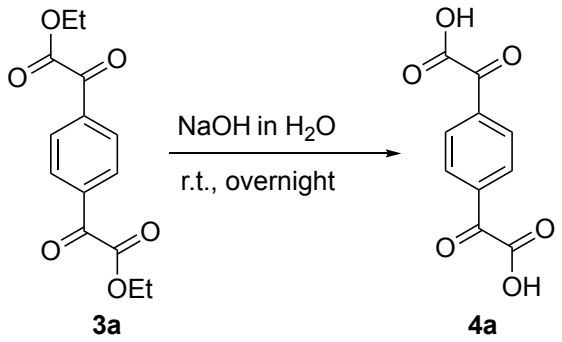

3a **4a**

Synthesis according to general procedure using 2 M NaOH (4 mL) and **3a** (0.4 g, 278 g/mol, 1.4 mmol).

4a was isolated as pure white powder after evaporating the solvent under reduced pressure (0.30 g, 1.4 mmol, 96 %).

^{1}H NMR (400 MHz, DMSO-d_6) δ 8.14 (s, 4H).

^{13}C NMR (101 MHz, DMSO-d_6) δ 187.79, 165.02, 136.32, 130.13.

MS (ESI-TOF) *m/z*: 221 [M - H]. HRMS: calc. for $C_{10}H_5O_6$ [M]$^-$: 221.0086, found: 221.0093.

2,6-Naphthyldiglyoxylic acid **4b:**

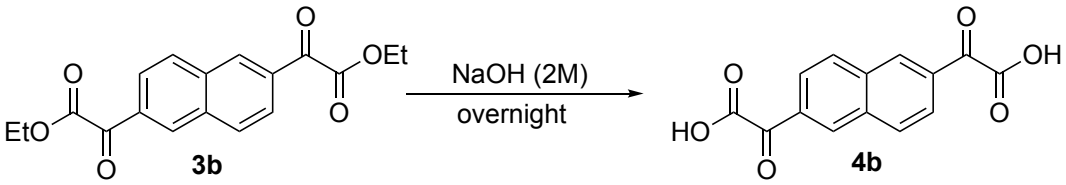

Synthesis according to general procedure using 2 M NaOH (30mL) and **3b** (1.5 g, 328 g/mol, 4.6 mmol).

4b was isolated as white powder after evaporating the solvent under reduced pressure (1.23 g, 4.5 mmol, 99 %).

^{1}H NMR (400 MHz, DMSO-d_6) δ 8.72 (s, 2H), 8.42 (d, J = 8.5 Hz, 2H), 8.08 (dd, J = 8.5, 1.7 Hz, 2H).

^{13}C NMR (101 MHz, DMSO-d_6) δ 188.42, 165.62, 134.81, 132.17, 131.98, 131.16, 124.76.

MS (ESI-TOF) *m/z*: 271 [M - H]. HRMS: calc. for $C_{14}H_6O_6$ [M]$^-$: 271.0243, found: 271.0236.

E.1.3 2,6-naphthalenediacetic acid (5b), 2,6-anthracenediacetic acid (5c) and 1,6-pyrenylenediacetic acid (5d)

General procedure for **5b**, **5c** and **5d** (according to [51]):

The respective glyoxylic acid (1 eq.) and NaI (1.2 eq.) were dissolved in acetic acid in a microwave vial. 50% aqueous H_3PO_2 (2.6 eq.) was added and the mixture was degassed properly for 15 min and afterwards heated to reflux under nitrogen for 4 days. After cooling to r.t., water (THF in case of **5d**) was added and the white precipitate was filtered off.

2,6-naphthalenediacetic acid **5b:**

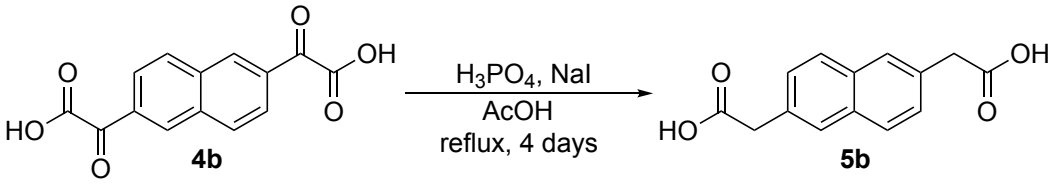

Synthesis according to the general procedure using **4b** (0.5 g, 272.21 g/mol, 1.8 mmol), NaI (0.33 g, 149.89 g/mol, 2.2 mmol), acetic acid (10 mL), 50% aqueous H_3PO_2 (0.5 mL, 66.0 g/mol, 4.8 mmol) and water (2 mL).

5b was isolated after drying as white powder (0.24 g, 1.0 mmol, 54 %).

^{1}H NMR (400 MHz, DMSO-d_6) δ 12.33 (s, 2H), 7.81 (d, J = 8.4 Hz, 2H), 7.74 (s, 2H), 7.41 (dd, J = 8.4, 1.6 Hz, 2H), 3.73 (s, 4H).

^{13}C NMR (101 MHz, DMSO-d_6) δ 172.43, 132.20, 131.54, 127.87, 127.19, 127.08, 40.56.

MS (ESI-TOF) *m/z*: 243 [M - H]. HRMS: calc. for $C_{14}H_{12}O_4$ [M]$^-$: 243.0657, found: 243.0661.

2,6-anthracenediacetic acid **5c:**

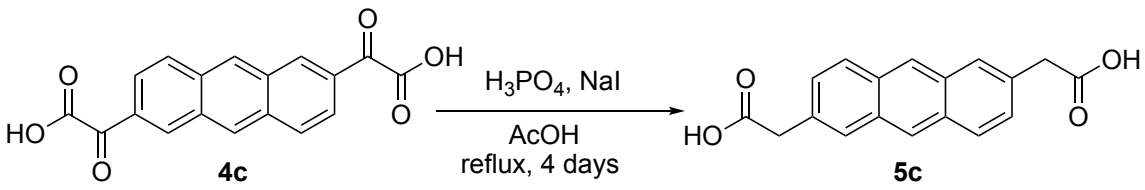

Synthesis according to the general procedure using **4c** (0.5 g, 322.27 g/mol, 1.55 mmol), NaI (0.22 g, 149.89 g/mol, 1.49 mmol), acetic acid (12.5 mL), 50% aqueous H_3PO_2 (0.5 mL, 66 g/mol, 4.8 mmol) and water (5 mL).

5c was isolated as off-white powder (0.35 g, 1.19 mmol, 77 %).

^{1}H NMR (400 MHz, DMSO-d_6) δ 12.41 (s, 2H), 8.48 (s, 2H), 8.03 (d, J = 8.7 Hz, 2H), 7.92 (d, J = 1.6 Hz, 2H), 7.42 (dd, J = 8.7, 1.7 Hz, 2H), 3.79 (s, 4H).

^{13}C NMR (101 MHz, DMSO-d_6) δ 172.61, 132.16, 131.01, 130.35, 127.90, 127.47, 125.31, 40.94.

Pyrenylene-1,6-diacetic acid **5d**:

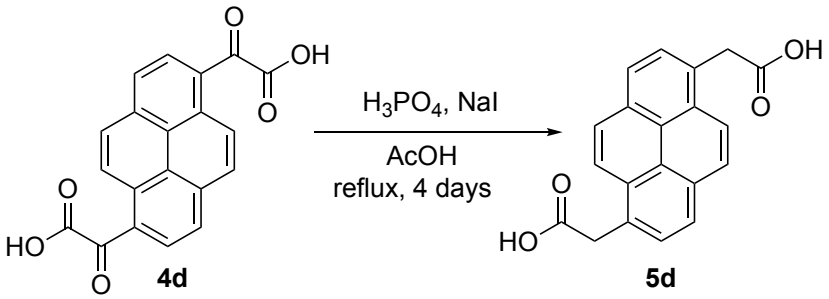

Synthesis according to the general procedure using **4d** (0.45 g, 346.29 g/mol, 1.3 mmol), NaI (0.19 g, 149.89 g/mol, 1.25 mmol), acetic acid (5.7 mL), 50% aqueous H_3PO_2 (0.44 mL, 66 g/mol, 4.0 mmol) and THF (17 mL).

5d was isolated as yellow powder (0.39 g, 1.2 mmol, 94 %).

^{1}H NMR (400 MHz, Chloroform-d) δ 8.26 (d, J = 1.2 Hz, 2H), 8.24 (d, J = 2.7 Hz, 2H), 8.21 (d, J = 9.3 Hz, 2H), 8.00 (d, J = 7.8 Hz, 2H), 4.35 (s, 4H).

^{13}C NMR (101 MHz, DMSO-d_6) δ 172.14, 129.20, 129.00, 128.54, 128.26, 126.88, 124.14, 123.57, 122.71. (methylene carbon hidden by solvent signal [22])

MS (CI) *m/z*: 318 [M + H]. HRMS: calc. for $C_{20}H_{14}O_4$ $[M]^+$: 319.0965, found: 319.0962.

E.1.4 2,6-Dibromoanthracene (2c)

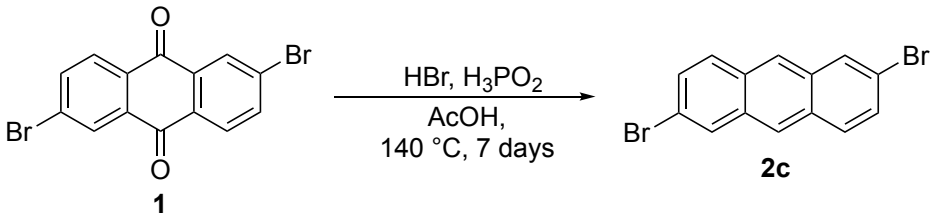

Synthesis according to Kang, Shin [25].

To 2,6-Dibromoanthraquinone **1** (4 g, 366.01 g/mol, 10.9 mmol) was added acetic acid (200 mL), 48 % aqueous HBr (52.8 mL) and 50 % aqueous H_3PO_2 (40 mL). This mixture was heated to reflux for 7 days. After it was cooled to r.t., it was poured onto ice water and the resulting precipitate was filtered off. In order to purify the compound, it was recrystallised from toluene which gave the product as a slightly yellow, shimmering powder (3.1 g, 336.02 g/mol, 84 %).

^{1}H NMR (400 MHz, Chloroform-*d*) δ 8.30 (s, 2H), 8.17 (d, *J* = 1.9 Hz, 2H), 7.87 (d, *J* = 9.0 Hz, 2H), 7.53 (dd, *J* = 9.1, 2.0 Hz, 2H).

MS (CI) *m/z*: 334 [M + H]. HRMS: calc. for $C_{14}H_8Br_2$ $[M]^+$: 333.8987, found: 333.8988.

E.1.5 Diethyl 9,10-anthracenediglyoxalate (3c), diethyl 2,6-anthracenediglyoxalate (3e) and diethyl 2,7-pyrenylenediglyoxalate (3d)

General procedure for **3c**, **3d** and **3e** (according to [24]):

The respective dibromide (1 eq.) was dissolved in anhyd. Et_2O/THF (properly degassed prior to use) and the mixture was kept under nitrogen atmosphere and cooled to -78 °C while stirring using an acetone/dry ice bath. *n*-BuLi (2.5 M in hexane, 6 eq.) was added very slowly. After 1 h at -78 °C the mixture was allowed to warm to r.t. for 2 h. Then it was cooled to -94 °C using an acetone/N_2(liq.) bath and diethyl oxalate (9.9 eq.) was added quickly *via* syringe and the temperature was kept at -94 °C for 1 h, subsequently it was allowed to warm to r.t. for 1 h. The reaction mixture was poured onto 2 M aqueous hydrochloric acid and transferred to a separating funnel. It was extracted with DCM (3x), dried over $MgSO_4$ and the solvent was evaporated under reduced pressure.

Diethyl 9,10-anthracenediglyoxalate **3e**:

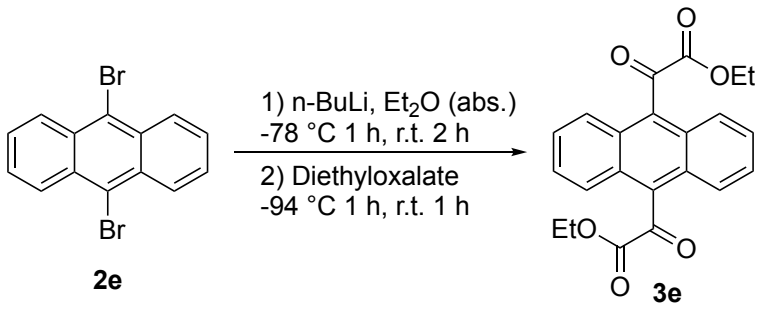

Synthesis according to the general procedure using 9,10-dibromoanthracene **2e** (1.5 g, 336.02 g/mol, 4.5 mmol), anhyd. Et_2O (80 mL), *n*-BuLi (2.5 M in hexane, 11 mL, 26.8 mmol) and diethyl oxalate (6 mL, 146.14 g/mol, 44.2 mmol). As well as 2 M aq. HCl (200 mL) for quenching.

In order to purify the crude product, it was recrystallised from EtOH with gave the product as bright yellow powder (0.93 g, 2.5 mmol, 55 %).

^{1}H NMR (400 MHz, Chloroform-*d*) δ 8.08 – 7.80 (m, 4H), 7.70 – 7.45 (m, 4H), 4.38 (q, *J* = 7.1 Hz, 4H), 1.32 (t, *J* = 7.1 Hz, 6H).

^{13}C NMR (101 MHz, Chloroform-*d*) δ 192.65, 162.62, 134.47, 128.68, 128.16, 125.29, 63.71, 14.44.

MS (CI) *m/z*: 378 [M + H]. HRMS: calc. for $C_{22}H_{18}O_6$ $[M]^+$: 379.1176, found: 379.1174.

Diethyl 2,6-anthracenediglyoxalate **3c**:

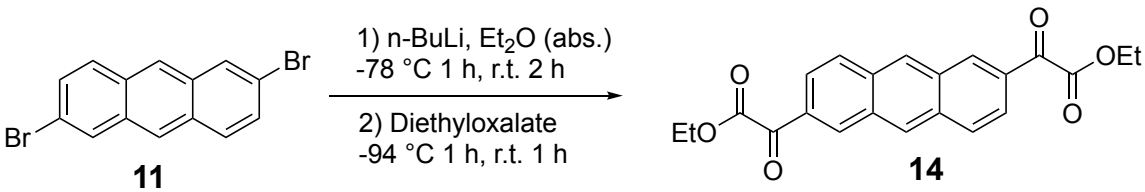

Synthesis according to the general procedure using 2,6-dibromoanthracene **2c** (2.00 g, 336.02 g/mol, 5.95 mmol), anhyd. Et_2O (120 mL), *n*-BuLi (2.5 M in hexane, 9.5 mL, 23.7 mmol) and diethyl oxalate (8 mL, 146.14 g/mol, 58.9 mmol). As well as 2 M aq. HCl (200 mL) for quenching.

For purification, the crude product was filtered over a plug of silica with PE/DCM (1:1) in order to flush out the impurity, then the pure product was eluted using only DCM. After evaporation of the solvent **3c** was isolated as yellow powder (0.69 g, 1.8 mmol, 31 %).

^{1}H NMR (400 MHz, Chloroform-*d*) δ 8.81 (d, *J* = 1.8 Hz, 2H), 8.65 (s, 2H), 8.14 (d, *J* = 8.9 Hz, 2H), 8.07 (dd, *J* = 8.9, 1.7 Hz, 2H), 4.54 (q, *J* = 7.2 Hz, 4H), 1.49 (t, *J* = 7.2 Hz, 6H).
^{13}C NMR (101 MHz, Chloroform-*d*) δ 163.44, 135.00, 133.41, 132.08, 130.80, 129.81, 129.60, 123.17, 62.47, 14.06.
MS (CI) *m/z*: 378 [M + H]. HRMS: calc. for $C_{22}H_{18}O_6$ [M]$^+$: 379.1176, found: 379.1167.

Diethyl 1,6-pyrenylendiglyoxalate **3d**:

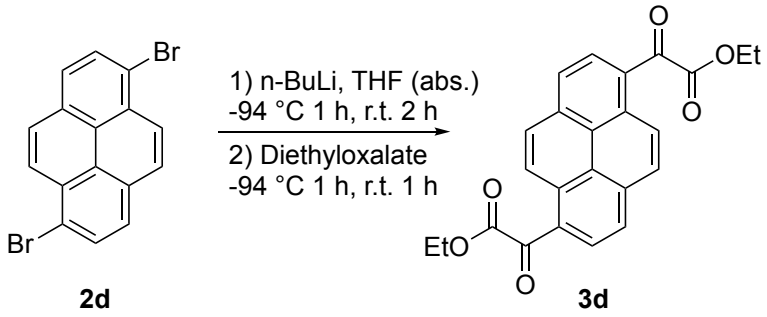

2d **3d**

Synthesis according to the general procedure using 1,6-dibromopyrene **2d** (3.0 g, 360.05 g/mol, 8.3 mmol), anhyd. THF (150 mL), *n*-Buli (2.5 M in hexane, 20.3 mL, 32.5 mmol) and diethyl oxalate (11.2 mL, 146.14 g/mol, 82.5 mmol). As well as 2 M aq. HCl (100 mL) for quenching. For purification, the crude was recrystalised from EtOH which gave the pure product **3d** as orange powder (2.02 g, 5.0 mmol, 61 %).

^{1}H NMR (400 MHz, Chloroform-*d*) δ 9.39 (d, *J* = 9.3 Hz, 2H), 8.43 (d, *J* = 8.1 Hz, 2H), 8.34 (d, *J* = 8.2 Hz, 2H), 8.31 (d, *J* = 9.4 Hz, 2H), 4.56 (q, *J* = 7.1 Hz, 4H), 1.50 (t, *J* = 7.2 Hz, 6H).
13C NMR (101 MHz, Chloroform-d) δ 188.94, 164.51, 134.46, 131.33, 130.53, 130.50, 127.69, 126.55, 125.83, 124.3, 62.71, 14.37.
MS (CI) *m/z*: 402 [M + H]. HRMS: calc. for $C_{24}H_{18}O_6$ [M]$^+$: 403.1176, found: 403.1177.

E.1.6 9,10-Anthrylglyoxylic acid (4e), 2,6-Anthrylglyoxylic acid (4c) and Pyrenylene-1,6-diglyoxylic acid (4d)

General procedure (according to [22]) :
The respective ester (1 eq.) was dissolved in EtOH, $NaHCO_3$ (27 eq.) was dissolved in water and added to the ester while stirring. The mixture was refluxed overnight. Afterwards, the reaction was allowed to cool to r.t. and poured onto 2 M aqueous hydrochloric acid. It was

transferred to a separating funnel and extracted with Et_2O (3 x), after that it was dried over $MgSO_4$ and the solvent was evaporated.

9,10-Anthrylglyoxylic acid **4e**:

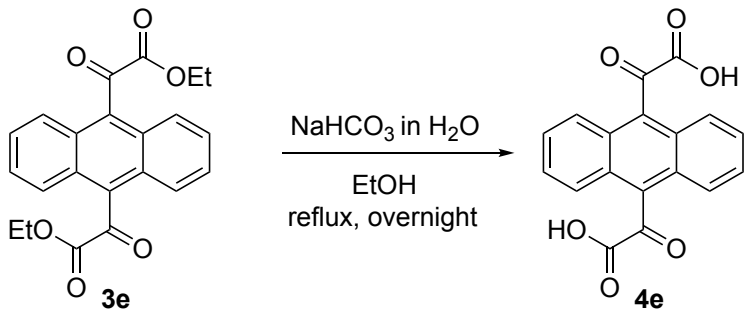

Synthesis according to the general procedure using **3e** (1.83 g, 378.38 g/mol, 4.8 mmol), EtOH (100 mL), and $NaHCO_3$ (10.96 g, 84.0 g/mol, 130.5 mmol) dissolved in water (270 mL). As well as 2 M aq. HCl (200 mL) for quenching.
The pure product was isolated as yellow powder (1.44 g, 4.5 mmol, 93 %) after evaporating the solvent and drying on Schlenk-line.

^{1}H NMR (400 MHz, DMSO-d_6) δ 7.97 – 7.88 (m, 4H), 7.81 – 7.65 (m, 4H).
^{13}C NMR (101 MHz, DMSO-d_6) δ 194.41, 163.57, 134.34, 128.02, 127.10, 124.58.
MS (ESI-TOF) *m/z*: 322 [M - H]. HRMS: calc. for $C_{18}H_{10}O_6$ $[M]^-$: 277.0514, found: 277.0510. (Difference of 45 which corresponds to an carboxylic acid group).

2,6-Anthrylglyoxylic acid **4c**:

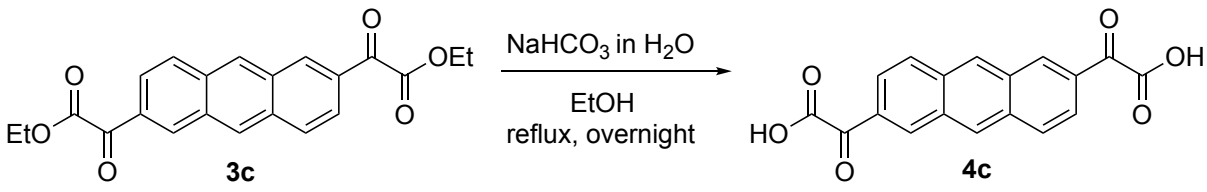

Synthesis according to the general procedure using **3c** (0.44 g, 378.38 g/mol, 1.16 mmol), EtOH (30 mL) and $NaHCO_3$ (2.64 g, 84.0 g/mol, 31.43 mmol) dissolved in water (15 mL). As well as 2 M aq. HCl (150 mL) for quenching.
The reaction yielded **4c** as red powder (0.36 g, 1.1 mmol, 99 %) after dissolving in acetone and evaporating the solvent again.

^{1}H NMR (400 MHz, DMSO-d_6) δ 9.07 (s, 2H), 8.88 (d, J = 1.7 Hz, 2H), 8.31 (d, J = 9.0 Hz, 2H), 7.99 (dd, J = 8.9, 1.7 Hz, 2H).

^{13}C NMR (101 MHz, DMSO-d_6) δ 188.29, 165.70, 134.51, 132.80, 131.49, 129.98, 129.85, 122.37.

MS (ESI-TOF) *m/z*: 322 [M - H]. HRMS: calc. for $C_{18}H_{10}O_6$ [M]$^-$: 321.0399, found: 321.0405.

Pyrenylene-1,6-diglyoxylic acid **4d**:

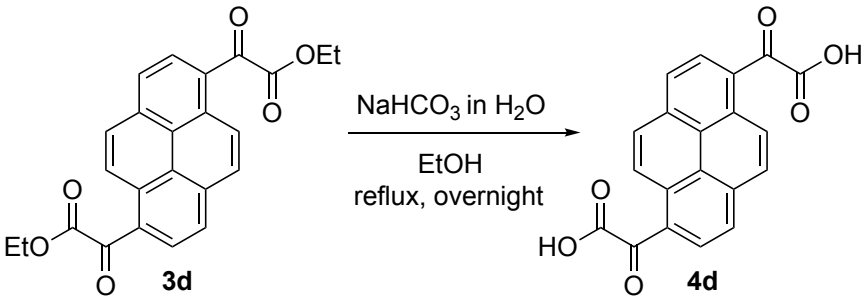

Synthesis according to the general procedure using **3d** (2.3 g, 402.40 g/mol, 5.7 mmol), EtOH (60 mL) and $NaHCO_3$ (13.0 g, 84.0 g/mol, 154.2 mmol) dissolved in water (160 mL). As well as 2 M aq. HCl (200 mL) for quenching.

The reaction yielded **4d** as red powder (1.78 g, 5.1 mmol, 90 %) after the residue was washed out of the sintered funnel with acetone and the solvent was evaporated.

^{1}H NMR (400 MHz, DMSO-d_6) δ 9.24 (d, J = 9.3 Hz, 1H), 8.58 (d, J = 8.2 Hz, 1H), 8.54 (d, J = 3.7 Hz, 1H), 8.52 (d, J = 5.0 Hz, 1H).

^{13}C NMR (101 MHz, DMSO-d_6) δ 191.02, 166.00, 133.46, 130.37, 129.85, 126.46, 126.17, 123.22.

MS (ESI-TOF) *m/z*: 346 [M - H]. HRMS: calc. for $C_{20}H_{10}O_6$ [M]$^-$: 345.0399, found: 345.0405.

E.2 Perkin cyclisations

E.2.1 General procedure for cyclisations [22]

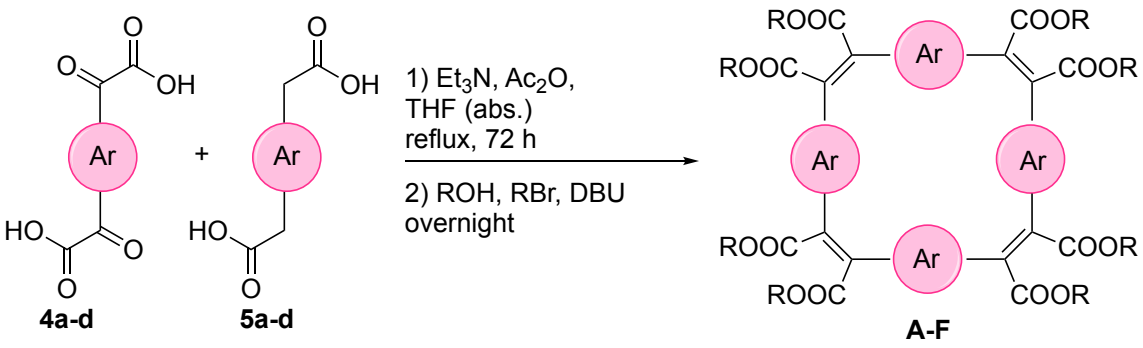

To a mixture of the respective diglyoxylic acid (1 eq.) and diacetic acids (1 eq.) in anhyd. THF (degassed properly priorly) in a 500 mL two-necked flask, triethyl amine (9.5 eq.) and acetic anhydride (15 eq.) were added *via* syringe. The reaction mixture was heated to reflux under nitrogen for 72 h. Afterwards, the respective alkyl bromide (44 eq.), the respective alcohol (82 eq.) and DBU (21 eq.) were added *via* syringe. After another 24 h, the mixture was allowed to cool to r.t. and subsequently poured onto 1 M aqu. hydrochloric acid. It was extracted with $CHCl_3$ (3x) and dried over $MgSO_4$. The crude product was isolated after evaporation of the solvent under reduced pressure.

To separate out the product of the crude mixture of linear and ring-closed species, it was purified on recycling GPC with $CHCl_3$ as eluent.

Variation of general procedure for cyclisation with syringe pump:

To a refluxing mixture of triethyl amine and acetic anhydride in anhyd. THF (degassed priorly) in a 500 mL two-necked flask, the respective diglyoxylic acid (1 eq.) and diacetic acid (1 eq.) were dissolved in 20 mL anhyd. THF (degassed) and added *via* syringe pump over 10 h (2 mL/h). The reaction mixture was refluxed under nitrogen for 72 h in total. The subsequent procedure is consistent with the procedure for the cyclisations without syringe pump.

E.2.2 Benzene macrocycles

E.2.2.1 Benzene macrocycle with ethyl esters (A)

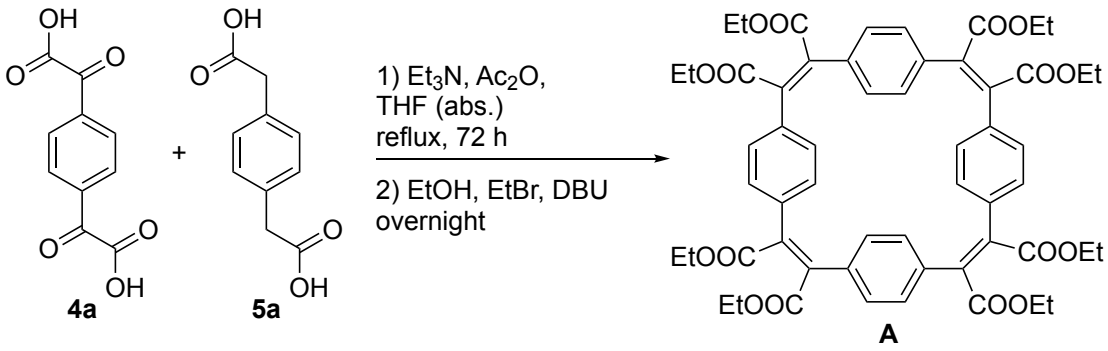

Synthesis of **A** with the use of a syringe pump for addition of monomers:

Synthesis according to general procedure for cyclisation with syringe pump using **4a** (0.250 g, 222.15 g/mol, 1.13 mmol), 1,4-phenyldiacetic acid **5a** (0.219 g, 194.19 g/mol, 1.13 mmol), Et_3N (1.5 mL, 101.19 g/mol, 0.73 g/mL, 10.70 mmol), Ac_2O (1.6 mL, 102.09 g/mol, 1.08 g/mL, 16.89 mmol), anhyd. THF (400 mL), EtOH (5.4 mL, 46.07 g/mol, 0.79 g/mL, 92.33 mmol), EtBr (3.7 mL, 108.97 g/mol, 1.46 g/mL, 49.5 mmol) and DBU (3.5 mL, 152.24 g/mol, 1.02 g/mL, 23.65 mmol).
After purification **A** was isolated as a dark yellow oil that crystallised slowly over time to give yellow crystals (93.6 mg, 0.1 mmol, 17 %).

^{1}H NMR (400 MHz, Chloroform-*d*) δ 6.93 (s, 16H), 4.31 (q, J = 7.1 Hz, 16H), 1.31 (t, J = 7.2 Hz, 26H).
^{13}C NMR (101 MHz, Chloroform-*d*) δ 167.82, 137.53, 134.64, 129.97, 62.11, 14.20.
MS (ESI-TOF) *m/z*: 984 [M + H]. HRMS: calc. for $C_{56}H_{56}O_{16}$ $[M]^+$:1007.3466, found: 1007.3480. (Difference of 23 which corresponds to Na).

Synthesis of **A** without the use of a syringe pump for addition of monomers:

Synthesis according to general procedure for cyclisation without syringe pump:
The amounts of chemicals used is equivalent to the protocol for the cyclisation with syringe pump.

After purification **A** was isolated as a dark yellow oil that crystallised slowly over time to give yellow crystals (87.9 mg, 0.09 mmol, 16 %).

^{1}H NMR (400 MHz, Chloroform-*d*) δ 6.93 (s, 16H), 4.31 (q, *J* = 7.2 Hz, 16H), 1.31 (t, *J* = 7.2 Hz, 24H).

E.2.2.2 Benzene macrocycle with hexyl esters (B)

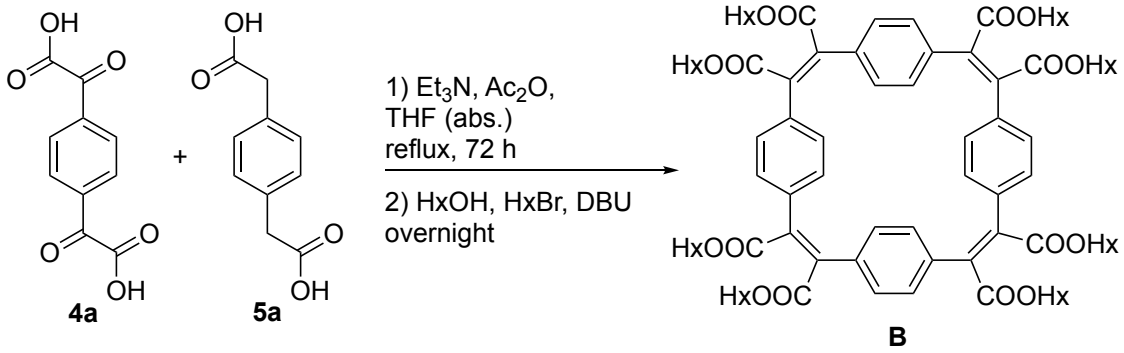

Synthesis of **B** with the use of a syringe pump for addition of monomers:

Synthesis according to general procedure for cyclisation with syringe pump using **4a** (0.250 g, 222.15 g/mol, 1.13 mmol), 1,4-phenyldiacetic acid **5a** (0.219 g, 194.19 g/mol, 1.13 mmol), Et_3N (1.5 mL, 101.19 g/mol, 0.73 g/mL, 10.70 mmol), Ac_2O (1.6 mL, 102.09 g/mol, 1.08 g/mL, 16.89 mmol), anhyd. THF (400 mL), HxOH (11.6 mL, 102.16 g/mol, 0.81 g/mL, 92.33 mmol), HxBr (7.0 mL, 165.07 g/mol, 1.18 g/mL, 49.5 mmol) and DBU (3.5 mL, 152.24 g/mol, 1.02 g/mL, 23.65 mmol).
Purification of the crude product yielded **B** as a brown oil (68.4 mg, 0.05 mmol, 8 %).

^{1}H NMR (400 MHz, Chloroform-*d*) δ 6.92 (s, 16H), 4.23 (t, *J* = 6.8 Hz, 18H), 1.81 – 1.51 (m, 22H), 1.46 – 1.10 (m, 40 H), 0.97 – 0.72 (m, 24H).
^{13}C NMR (101 MHz, Chloroform-*d*) δ 167.56, 137.22, 134.33, 129.62, 65.99, 31.19, 28.17, 25.35, 22.37, 13.85.

E.2.3 Naphthalene macrocycle (C)

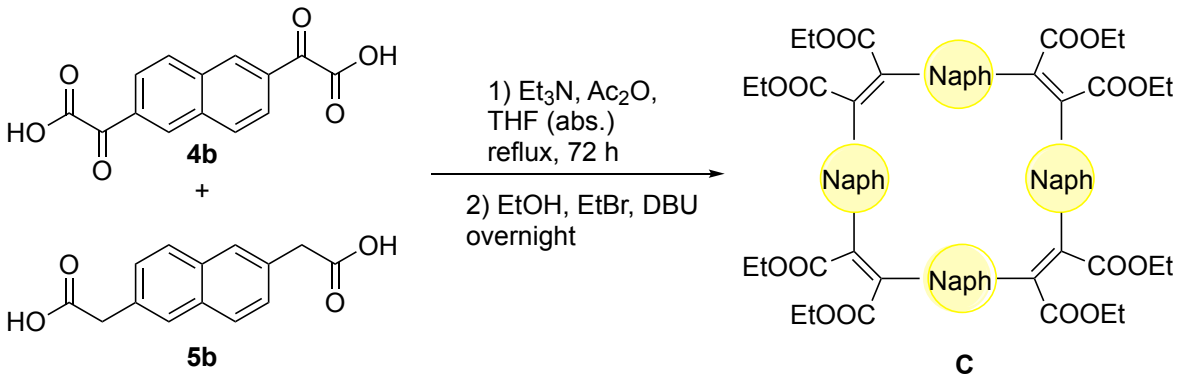

Synthesis according to general procedure for cyclisation without syringe pump using **5b** (0.24 g, 244.25 g/mol, 0.98 mmol), **4b** (0.27 g, 272.21 g/mol, 0.98 mmol), Et_3N (1.3 mL, 101.19 g/mol, 0.73 g/mL, 9.31 mmol), Ac_2O (1.4 mL, 102.09 g/mol, 1.08 g/mL, 14.7 mmol), anhyd. THF (400 mL), EtOH (4.7 mL, 46.07 g/mol, 0.79 g/mL, 80.36 mmol), EtBr (3.2 mL, 108.97 g/mol, 1.46 g/mL, 43.12 mmol) and DBU (3.1 mL, 152.24 g/mol, 1.02 g/mL, 20.58 mmol).

After purification **C** was obtained as yellow powder (46.1 mg, 0.04 mmol, 8 %).

^{1}H NMR (400 MHz, Chloroform-*d*) δ 7.51 (d, *J* = 1.6 Hz, 8H), 7.24 (d, *J* = 8.6 Hz, 8H), 6.88 (dd, *J* = 8.6, 1.7 Hz, 8H), 4.35 (q, *J* = 7.2 Hz, 16H), 1.32 (t, *J* = 7.2 Hz, 24H).

^{13}C NMR (101 MHz, Chloroform-*d*) δ 168.32, 138.71, 133.34, 132.70, 130.03, 128.44, 128.12, 62.43, 14.56.

MS (MALDI-TOF) *m/z*: 1184 [M + H]. MS: found: 1184.

E.2.4 Anthracene macrocycle (D)

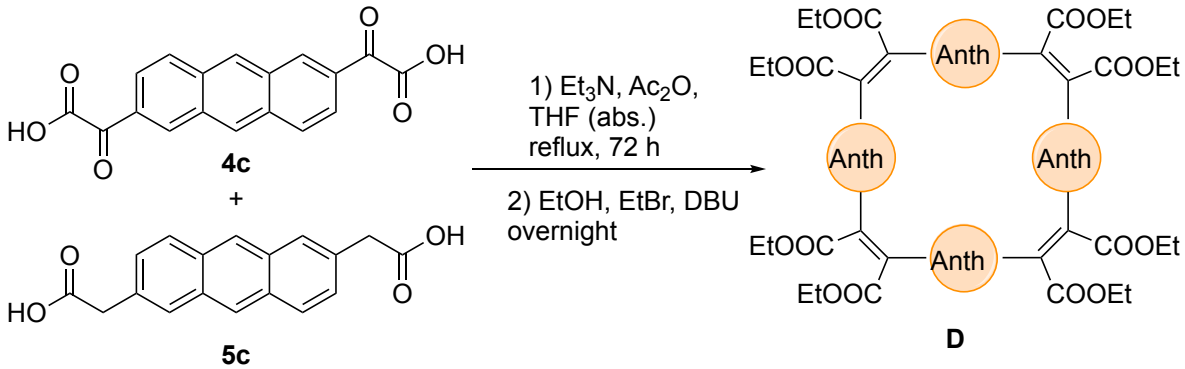

Synthesis according to general procedure for cyclisation without syringe pump using **5c** (0.229 g, 294.30 g/mol, 0.78 mmol), **4c** (0.250 g, 322.27 g/mol, 0.78 mmol), Et_3N (1.0 mL, 101.19 g/mol, 0.73 g/mL, 7.41 mmol), Ac_2O (1.1 mL, 102.09 g/mol, 1.08 g/mL, 11.7 mmol), anhyd. THF (400 mL), EtOH (3.7 mL, 46.07 g/mol, 0.79 g/mL, 63.96 mmol), EtBr (2.6 mL, 108.97 g/mol, 1.46 g/mL, 34.32 mmol) and DBU (2.45 mL, 152.24 g/mol, 1.02 g/mL, 16.38 mmol).

Purification of the crude product yielded **D** as a dark orange powder (36 mg, 0.03 mmol, 7 %).

^{1}H NMR (400 MHz, Chloroform-*d*) δ 8.08 (s, 8H), 7.87 (d, *J* = 1.7 Hz, 9H), 7.61 (d, *J* = 8.9 Hz, 8H), 7.06 (dd, *J* = 8.9, 1.8 Hz, 8H), 4.37 (q, 75H), 1.32 (t, *J* = 7.2 Hz, 24H).

^{13}C NMR (101 MHz, Chloroform-*d*) δ 168.27, 138.23, 132.14, 131.10, 130.38, 128.23, 127.00, 126.94, 62.04, 14.20.

MS (MALDI-TOF) *m/z*: 1386 [M + H]. MS: found: 1386.

E.2.5 Pyrene macrocycles

E.2.5.1 Pyrene macrocycle with ethyl esters (E)

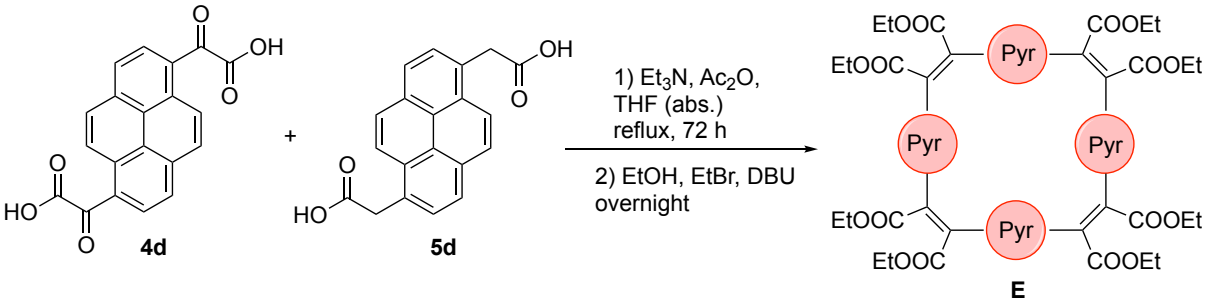

Synthesis according to general procedure for cyclisation without syringe pump using **4d** (0.235 g, 346.29 g/mol, 0.68 mmol), **5d** (0.216 g, 318.33 g/mol, 0.68 mmol), Et_3N (0.9 mL, 101.19 g/mol, 0.73 g/mL, 6.46 mmol), Ac_2O (0.96 mL, 102.09 g/mol, 1.08 g/mL, 10.2 mmol), anhyd. THF (350 mL), EtOH (3.3 mL, 46.07 g/mol, 0.79 g/mL, 55.76 mmol), EtBr (2.2 mL, 108.97 g/mol, 1.46 g/mL, 29.92 mmol) and DBU (2.13 mL, 152.24 g/mol, 1.02 g/mL, 14.28 mmol).

After purification **E** was obtained as orange powder (37.9 mg, 0.03 mmol, 8 %).

^{1}H NMR (400 MHz, Chloroform-*d*) δ 8.24 (d, *J* = 9.2 Hz, 8H), 7.86 (d, *J* = 8.0 Hz, 8H), 7.77 (d, *J* = 8.0 Hz, 8H), 7.70 (d, *J* = 9.2 Hz, 8H), 4.17 (qq, *J* = 7.2, 3.7 Hz, 16H), 1.13 (t, *J* = 7.1 Hz, 24H).

^{13}C NMR (101 MHz, Chloroform-*d*) δ 168.09, 139.65, 130.68, 129.58, 128.85, 127.76, 127.58, 124.70, 124.57, 124.47, 61.83, 13.90.

MS (MALDI-TOF) *m/z*: 1482 [M + H]. MS: found: 1482.

E.2.5.2 Pyrene macrocycle with hexyl esters (F)

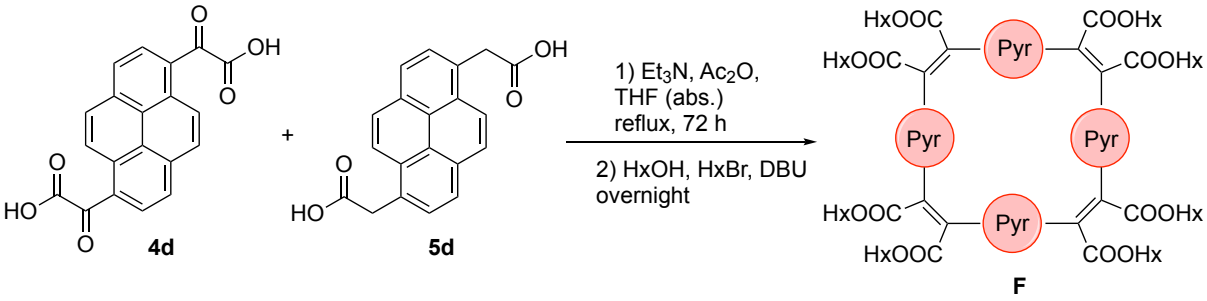

Synthesis according to general procedure for cyclisation without syringe pump using **4d** (0.250 g, 346.29 g/mol, 0.72 mmol), **5d** (0.230 g, 318.33 g/mol, 0.72 mmol), Et_3N (0.95 mL, 101.19 g/mol, 0.73 g/mL, 6.84 mmol), Ac_2O (1.02 mL, 102.09 g/mol, 1.08 g/mL, 10.8 mmol), anhyd. THF (300 mL), hexanol (7.4 mL, 102.16 g/mol, 0.81 g/mL, 59.04 mmol), hexyl bromide (4.45 mL, 165.07 g/mol, 1.18 g/mL, 31.68 mmol) and DBU (2.26 mL, 152.24 g/mol, 1.02 g/mL, 15.12 mmol).

After purification **F** was obtained as red oil (37.5 mg, 0.02 mmol, 5 %).

^{1}H NMR (400 MHz, Chloroform-*d*) δ 8.23 (d, *J* = 9.2 Hz, 7H), 7.86 (d, *J* = 8.0 Hz, 8H), 7.77 (d, *J* = 8.0 Hz, 8H), 7.70 (d, *J* = 9.3 Hz, 8H), 4.25 – 3.77 (m, 18H), 1.46 – 1.37 (m, 22H), 1.05 – 0.86 (m, 40H), 0.65 (t, *J* = 6.2 Hz, 24H).

^{13}C NMR (101 MHz, Chloroform-*d*) δ 168.06, 139.78, 130.62, 129.56, 128.85, 127.73, 127.49, 124.73, 124.46, 124.38, 65.91, 31.15, 28.13, 25.21, 22.26, 13.75.

MS (MALDI-TOF) *m/z*: 1930 [M + H]. MS: found: 1930.

E.3 Model compounds

E.3.1 Perkin model compound and conversions

E.3.1.1 Diethyl (Z)-2,3-diphenylmaleate (8)

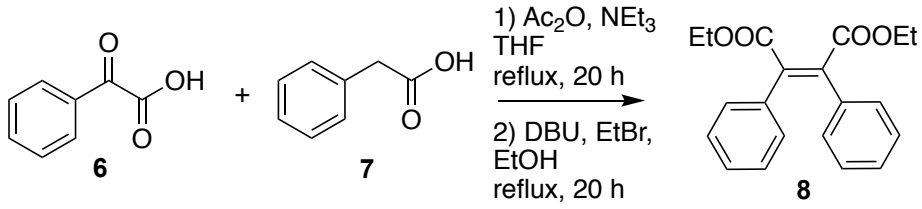

Synthesis according to Cabral et al.[52]

Phenylacetic acid **7** (1.02 g, 136.15 g/mol, 7.5 mmol) and phenylglyoxylic acid **6** (1.12 g, 150.13 g/mol, 7.5 mmol) were dissolved in 30 mL anhyd. THF (properly degassed priorly). While stirring, triethyl amine (2.3 mL, 101.19 g/mol, 2.2 mmol) and acetic anhydride (2.4 mL, 102.09 g/mol, 3.5 mmol) were added *via* syringe and the mixture was heated to reflux under nitrogen for 20 h. After cooling to r.t., DBU (6.13 mL, 152.24 g/mol, 41.1 mmol), ethyl bromide (4.3 mL, 108.97 g/mol, 57.4 mmol) and EtOH (7.9 mL, 46.07 g/mol, 135.5 mmol) were added dropwise and the mixture was heated to reflux under nitrogen for 20 h. The reaction mixture was cooled to r.t. then poured onto 10 % aqueous hydrochloric acid (100 mL). EtOH (20 mL) was added and the solution was stirred for 45 min whereby no precipitate was formed. The mixture was transferred to a separating funnel, extracted with $CHCl_3$ (3 x 50 mL), the combined organic layers were washed with sat. $NaHCO_3$-solution (50 mL), water (50 mL) and brine (50 mL) and dried over $MgSO_4$. The solvent was evaporated, and the crude product was purified on silica gel using DCM/hexane (3:1) which gave the product **8** as slightly yellow/green crystals (1.93 g, 5.95 mmol, 79 %).

^{1}H NMR (400 MHz, Chloroform-*d*) δ 7.21 – 7.14 (m, 6H), 7.12 – 7.07 (m, 4H), 4.30 (q, J = 7.2 Hz, 4H), 1.30 (t, J = 7.1 Hz, 6H).

^{13}C NMR (101 MHz, Chloroform-*d*) δ 168.12, 138.81, 134.81, 129.91, 128.36, 128.23, 61.86, 14.20.

MS (ESI-TOF) *m/z*: 249 [M + H]. HRMS: calc. for $C_{20}H_{20}O_4$ $[M]^+$: 249.0790, found: 249.0795.

E.3.1.2 3,4-Diphenyl-1*H*-pyrrole-2,5-dione (9b)

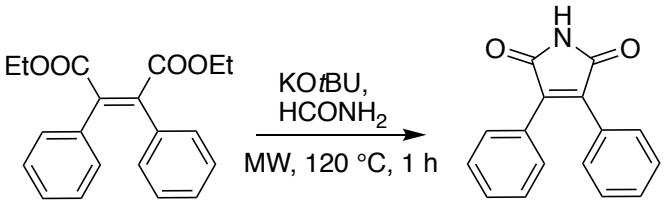

8 **9b**

Synthesis based on Zradni et al.[39]

8 (136 mg, 324.14 g/mol, 0.42 mmol), KO*t*Bu (188 mg, 112.21 g/mol, 1.68 mmol) and formamide (0.5 mL, 45.04 g/mol, 12.6 mmol) were heated to 120 °C for 1 h in the microwave reactor. Acetic acid was added to the reaction mixture at r.t. and the mixture was left to crystallise overnight. The product crystallised as yellow needles which can be filtered off in order to isolate the pure product **9b** (81 mg, 0.30 mmol, 73 %).

^{1}H NMR (400 MHz, DMSO-d_6) δ 11.24 (s, 1H), 7.62 – 7.03 (m, 10H).

^{13}C NMR (101 MHz, DMSO-d_6) δ 171.59, 136.64, 129.60, 129.46, 128.75, 128.36.

MS (ESI-TOF) *m/z*: 249 [M + H]. HRMS: calc. for $C_{16}H_{10}NO_2$ $[M]^+$: 249.0790, found: 249.0795.

E.3.2 Benzoin model compounds

E.3.2.1 5H-dibenzo[*a,d*][7]annulene (12)

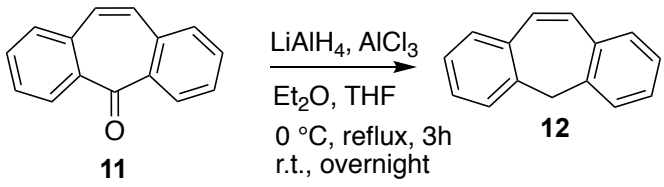

11 **12**

Synthesis according to Schmuck et al.[53]

Anhyd. Et_2O was properly degassed with N_2 for 25 min. $AlCl_3$ (7.63 g, 133.34 g/mol, 57.2 mmol) was suspended in 45 mL Et_2O and $LiAlH_4$ (2.17 g, 37.95 g/mol, 57.2 mmol) was added to 37 mL Et_2O under N_2 atmosphere. The $AlCl_3$ suspension was added to the $LiAlH_4$ solution and stirred at r.t. for 30 min. Afterwards, a solution of 5-Dibenzosuberenone (10.72 g, 206.26 g/mol, 52 mmol) in 50 mL anhyd. THF (degassed priorly) was added to the slurry at

0 °C. After complete addition, the mixture was heated to reflux under nitrogen for 3 h and the reaction was completed by stirring overnight at r.t. (TLC control). Remaining $LiAlH_4$ was quenched with 8 mL *i*-PrOH and 10 mL H_2O, a grey precipitate was formed. The suspension was transferred to a separation funnel and extracted with DCM (3 x 50 mL) and Et_2O (3 x 50 mL), the resulting organic phase was extracted with a sat. solution of $NaHCO_3$ (50 mL), water (50 mL) and brine (50 mL) and dried over $MgSO_4$. Evaporation the solvent gave the product as pure off-white crystalline powder (9.20 g, 47.9 mmol, 92 %).

^{1}H NMR (400 MHz, Chloroform-*d*) δ 7.38 – 7.19 (m, 8H), 7.06 (s, 2H), 3.77 (s, 2H).

E.3.2.2 10,11-Dihydro-5*H*-dibenzo[*a*,*d*]cyclohepten-10-ol (13)

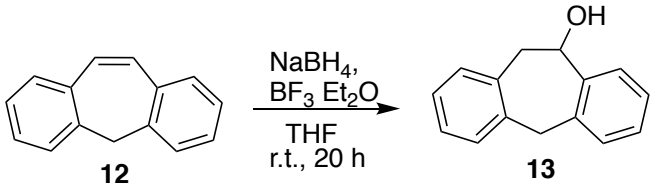

Synthesis according to Slusarczyk et al.[54]

12 (7.69 g, 192.24 g/mol, 40.0 mmol) was partly dissolved in 100 mL andhyd. THF (degassed priorly) and $NaBH_4$ (6.05 g, 37.83 g/mol, 160.0 mmol) was added. The mixture was cooled with an ice bath and $BF_3{\cdot}Et_2O$ (25 mL, 200.0 mmol) was added dropwise *via* syringe. The white suspension was stirred at r.t. under nitrogen for 20 h. Afterwards excess of borohydride was quenched by the slow addition of water (85 mL) and MeOH (85 mL) while cooling with an ice bath. All remaining solid dissolved to result in a homogeneous solution after addition of MeOH. 4 M NaOH (85 mL) and 36 % H_2O_2 solution (75 mL) were added whereas a white precipitate was formed. The resulting reaction mixture was stirred overnight. THF and MeOH were evaporated under reduced pressure and the resulting residue was washed with EA. The organic phase was transferred to a separating funnel and extracted with H_2O (3 x 100 mL) and brine (100 mL). The solvent was evaporated, and the resulting colourless oil was dried in vacuum to give **13** as a white solid (8.203 g, 39.0 mmol, 98 %).

^{1}H NMR (400 MHz, Chloroform-*d*) δ 7.53 (d, J = 7.5 Hz, 1H), 7.38 – 7.16 (m, 7H), 5.16 (br, 1H), 4.31 (d, J = 15.1 Hz, 1H), 3.98 (d, J = 15.0 Hz, 1H), 3.59 (dd, J = 14.5, 3.6 Hz, 1H), 3.28 (dd, J = 14.5, 7.8 Hz, 1H), 2.19 (br, 1H).

E.3.2.3 5,11-Dihydro-10*H*-dibenzo[*a*,*d*]cycloheptene-10-one (14a)

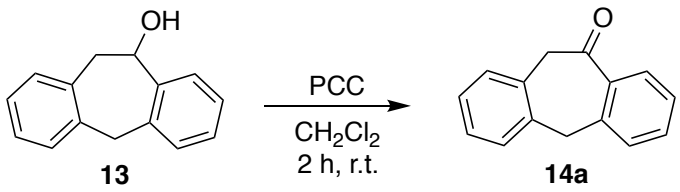

Synthesis according to Slusarczyk et al.[54]

13 (8.2 g, 210.10 g/mol, 39 mmol) was dissolved in 90 mL DCM and NaOAc (52 mg, 82.03 g/mol, 0.6 mmol) was added as well as PCC (25.22 g, 215.56 g/mol, 117 mmol). The colour immediately changed to a dark brown. After stirring at r.t. for 2 h, 220 mL Et_2O were added and the dark brown precipitate was filtered off. The filtrate was concentrated in vacuo which gave the product as brown oil. Purification on silica gel using EA/hexane (95:5) gave pure product **14a** as off-white powder (3.63 g, 17.4 mmol, 45 %).

^{1}H NMR (400 MHz, Chloroform-*d*) δ 8.12 (dd, *J* = 7.9, 1.5 Hz, 1H), 7.45 (td, *J* = 7.4, 1.5 Hz, 1H), 7.39 – 7.27 (m, 4H), 7.23 – 7.15 (m, 2H), 4.28 (s, 2H), 4.19 (s, 2H).
^{13}C NMR (101 MHz, Chloroform-*d*) δ 194.59, 142.86, 140.01, 134.67, 133.45, 132.74, 130.61, 129.99, 129.48, 128.10, 127.60, 127.57, 127.34, 51.37, 42.63.
MS (CI) *m/z*: 209 [M + H]. HRMS: calc. for $C_{15}H_{12}O$ $[M]^+$: 209.0961, found: 209.0966.

E.3.2.4 5*H*-Dibenzo[*a*,*d*]cycloheptene-10,11-dione (14b)

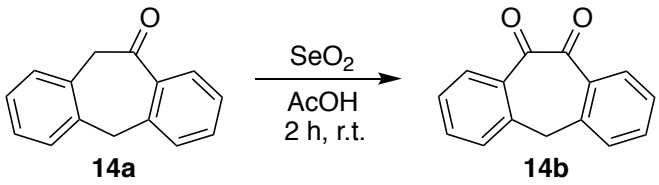

Synthesis according to Slusarczyk et al.[54]

14a (1.00 g, 208.09 g/mol, 4.8 mmol) was dissolved in 20 mL acetic acid under stirring. SeO_2 (0.59 g, 110.96 g/mol, 5.3 mmol) was added and the reaction mixture was refluxed for 2 h whereby the colour rapidly changes from orange to almost black. After cooling to r.t., the solvent was evaporated under reduced pressure, the residue was dissolved in EA and filtered over a pad of silica. The solvent was evaporated under reduced pressure and pure **14b** was isolated as yellow powder (1.06 g, 4.8 mmol, 99 %).

^{1}H NMR (400 MHz, Chloroform-*d*) δ 7.84 (td, *J* = 8.0, 1.5 Hz, 2H), 7.49 (td, *J* = 7.3, 1.5 Hz, 2H), 7.36 (td, *J* = 7.1 Hz, 4H), 4.28 (s, 2H).

^{13}C NMR (101 MHz, Chloroform-*d*) δ 189.51, 140.31, 135.60, 133.90, 131.60, 128.78, 127.94, 40.61.

MS (CI) *m/z*: 223 [M + H]. HRMS: calc. for $C_{15}H_{10}O_2$ $[M]^+$: 223.0754, found: 223.0753.

F Bibliography

1. Hoffmann, R. and H. Hopf, *Learning from Molecules in Distress.* Angewandte Chemie International Edition, 2008. **47**(24): p. 4474-4481.
2. Zhang, B., et al., *Rigid, Conjugated Macrocycles for High Performance Organic Photodetectors.* Journal of the American Chemical Society, 2016. **138**(50): p. 16426-16431.
3. Leger, J., M. Berggren, and S. Carter, *Iontronics: Ionic Carriers in Organic Electronic Materials and Devices*. 2010, Boca Raton, Florida: CRC Press.
4. Golder, M.R. and R. Jasti, *Syntheses of the Smallest Carbon Nanohoops and the Emergence of Unique Physical Phenomena.* Accounts of Chemical Research, 2015. **48**(3): p. 557-566.
5. Iyoda, M., J. Yamakawa, and M.J. Rahman, *Conjugated Macrocycles: Concepts and Applications.* Angewandte Chemie International Edition, 2011. **50**(45): p. 10522-10553.
6. Liu, Y., et al., *Flexibility Coexists with Shape-Persistence in Cyanostar Macrocycles.* Journal of the American Chemical Society, 2016. **138**(14): p. 4843-4851.
7. Ryu, J.-H., N.-K. Oh, and M. Lee, *Tubular assembly of amphiphilic rigid macrocycle with flexible dendrons.* Chemical Communications, 2005(13): p. 1770-1772.
8. Jasti, R., et al., *Synthesis, Characterization, and Theory of [9]-, [12]-, and [18]Cycloparaphenylene: Carbon Nanohoop Structures.* Journal of the American Chemical Society, 2008. **130**(52): p. 17646-17647.
9. Xia, J. and R. Jasti, *Synthesis, Characterization, and Crystal Structure of [6]Cycloparaphenylene.* Angewandte Chemie International Edition, 2012. **51**(10): p. 2474-2476.
10. Aihara, J.-i., *Hückel-like rule of superaromaticity for charged paracyclophanes.* Chemical Physics Letters, 2003. **381**(1): p. 147-153.
11. Shabtai, E., et al., *Charged paracyclophanes behave as annulenes with enhanced anisotropy.* Journal of the Chemical Society, Perkin Transactions 2, 2000(6): p. 1233-1241.
12. Ji, Q., et al., *Cyclotetrabenzoin: Facile Synthesis of a Shape-Persistent Molecular Square and Its Assembly into Hydrogen-Bonded Nanotubes.* Chemistry – A European Journal, 2015. **21**(48): p. 17205-17209.

13. Höger, S., *Shape-Persistent Macrocycles: From Molecules to Materials.* Chemistry – A European Journal, 2004. **10**(6): p. 1320-1329.
14. Shekar, S.C. and R.S. Swathi, *Cation−π Interactions and Rattling Motion through Two-Dimensional Carbon Networks: Graphene vs Graphynes.* The Journal of Physical Chemistry C, 2015. **119**(16): p. 8912-8923.
15. Dinadayalane, T.C., A. Hassan, and J. Leszczynski, *A theoretical study of cation--π interactions: Li+, Na+, K+, Be2+, Mg2+ and Ca2+ complexation with mono- and bicyclic ring-fused benzene derivatives.* Theoretical Chemistry Accounts, 2012. **131**(3): p. 1131.
16. Chandra Shekar, S. and R.S. Swathi, *Rattling Motion of Alkali Metal Ions through the Cavities of Model Compounds of Graphyne and Graphdiyne.* The Journal of Physical Chemistry A, 2013. **117**(36): p. 8632-8641.
17. Baeg, K.-J., et al., *Organic Light Detectors: Photodiodes and Phototransistors.* Advanced Materials, 2013. **25**(31): p. 4267-4295.
18. Malti, A., et al., *An Organic Mixed Ion–Electron Conductor for Power Electronics.* Advanced Science, 2016. **3**(2): p. 1500305.
19. Kim, D.J., et al., *Redox-Active Macrocycles for Organic Rechargeable Batteries.* Journal of the American Chemical Society, 2017. **139**(19): p. 6635-6643.
20. Facchetti, A., *π-Conjugated Polymers for Organic Electronics and Photovoltaic Cell Applications.* Chemistry of Materials, 2011. **23**(3): p. 733-758.
21. Ball, M., et al., *Macrocyclization in the Design of Organic n-Type Electronic Materials.* Journal of the American Chemical Society, 2016. **138**(39): p. 12861-12867.
22. Robert, A., et al., *A carboxyfunctionalized (24)-1,6-pyrenophane-tetraene by glyoxylic Perkin condensation.* Canadian Journal of Chemistry, 2017. **95**(4): p. 450-453.
23. Bock, H., et al., *Complementary Synthetic Approaches to Elongated Polycyclic Arenes with Regioisomeric Carboxylic Substitution Patterns.* European Journal of Organic Chemistry, 2015. **2015**(5): p. 1028-1032.
24. Girotto, E., et al., *Plank-Shaped Column-Forming Mesogens with Substituents on One Side Only.* Chemistry – A European Journal, 2015. **21**(20): p. 7603-7610.
25. Kang, H., et al., *Position Effect Based on Anthracene Core for OLED Emitters.* Journal of Nanoscience and Nanotechnology, 2016. **16**(3): p. 3045-3048.
26. Weidman, J.R., et al., *Structure Manipulation in Triptycene-Based Polyimides through Main Chain Geometry Variation and Its Effect on Gas Transport Properties.* Industrial & Engineering Chemistry Research, 2017. **56**(7): p. 1868-1879.

27. Criswell, T.R. and B.H. Klanderman, *Conversion of 9,10-anthraquinones to anthracenes.* The Journal of Organic Chemistry, 1974. **39**(6): p. 770-774.
28. Baba, H. and T. Takemura, *Spectrophotometric investigations of the tautomeric reaction between anthrone and anthranol—I: The keto-enol equilibrium.* Tetrahedron, 1968. **24**(13): p. 4779-4791.
29. Robert, A., et al., *Non-planar oligoarylene macrocycles from biphenyl.* Chemical Communications, 2017. **53**(84): p. 11540-11543.
30. Moreira, T.S., et al., *Tetracarboxy-Functionalized [8]-, [10]-, [12]-, and [14]Phenacenes.* European Journal of Organic Chemistry, 2017. **2017**(31): p. 4548-4551.
31. Pirrung, M.C. and R.J. Tepper, *Photochemistry of Substituted Benzoylformate Esters. A Convenient Method for the Photochemical Oxidation of Alcohols.* The Journal of Organic Chemistry, 1995. **60**(8): p. 2461-2465.
32. Yao, J., et al., *Palladium-Catalyzed Decarboxylative Coupling of α- Oxocarboxylic Acids with C(sp2)-H of 2-Aryloxypyridines.* Advanced Synthesis & Catalysis, 2013. **355**(8): p. 1517-1522.
33. Trachtenberg, E.N., C.H. Nelson, and J.R. Carver, *Mechanism of selenium dioxide oxidation of olefins.* The Journal of Organic Chemistry, 1970. **35**(5): p. 1653-1658.
34. Gordon, P.E. and A.J. Fry, *Hypophosphorous acid–iodine: a novel reducing system. Part 2: Reduction of benzhydrols to diarylmethylene derivatives.* Tetrahedron Letters, 2001. **42**(5): p. 831-833.
35. Yuan, L.-Z., et al., *Chlorotrimethylsilane and Sodium Iodide: A Useful Combination for the Regioselective Deoxygenation of Arylalkyl-α-Diketones.* Advanced Synthesis & Catalysis, 2017. **359**(15): p. 2682-2691.
36. Kelber, J., et al., *Room-Temperature Columnar Liquid-Crystalline Perylene Imido-Diesters by a Homogeneous One-Pot Imidification–Esterification of Perylene-3,4,9,10-tetracarboxylic Dianhydride.* European Journal of Organic Chemistry, 2011. **2011**(4): p. 707-712.
37. Ruggiero, A., et al., *A 'push–pull' tropylium-fused aminoporphyrazine.* Tetrahedron, 2009. **65**(47): p. 9690-9693.
38. Hoegberg, T., et al., *Cyanide as an efficient and mild catalyst in the aminolysis of esters.* The Journal of Organic Chemistry, 1987. **52**(10): p. 2033-2036.
39. Zradni, F.-Z., J. Hamelin, and A. Derdour, *Synthesis of Amides from Esters and Amines under Microwave Irradiation.* Synthetic Communications, 2002. **32**(22): p. 3525-3531.

40. Ramirez, A., et al., *A Mechanistic Study on the Amidation of Esters Mediated by Sodium Formamide.* The Journal of Organic Chemistry, 2012. **77**(1): p. 775-779.
41. Brand, H., et al., *Salts and Ionic Liquids of Resonance Stabilized Amides.* Chemistry – An Asian Journal, 2009. **4**(10): p. 1588-1603.
42. Slusarczyk, M., et al., *Synthesis and Biological Evaluation of Bridged Analogues of the Platelet Aggregation Inhibitor Trifenagrel.* Letters in Drug Design & Discovery, 2009. **6**(7): p. 478-486.
43. Naimi-Jamal, M.R., et al., *Sodium Tetraalkoxyborates: Intermediates for the Quantitative Reduction of Aldehydes and Ketones to Alcohols through Ball Milling with NaBH4.* European Journal of Organic Chemistry, 2009. **2009**(21): p. 3567-3572.
44. Lin, W., et al., *Selective reduction of carbonyl groups in the presence of low-valent titanium reagents.* Tetrahedron Letters, 2014. **55**(14): p. 2238-2242.
45. Hekmatshoar, R., et al., *Zinc-Promoted Reduction of 1,2-Diketones: A Simple, Efficient, and Mild Approach to a-Hydroxy Ketones.* Monatshefte für Chemie / Chemical Monthly, 2002. **133**(2): p. 195-197.
46. Hayakawa, R., T. Sahara, and M. Shimizu, *Reduction of 1,2-diketones with titanium tetraiodide: a simple approach to α-hydroxy ketones.* Tetrahedron Letters, 2000. **41**(41): p. 7939-7942.
47. Kikuchi, S. and Y. Hashimoto, *Reduction of 1,2-Dicarbonyl Compounds Mediated by the Combination of Phosphine and Lewis Acid.* Synlett, 2004. **2004**(07): p. 1267-1269.
48. Lee, W.Y., C.H. Park, and Y.D. Kim, *Orthocyclophanes. 1. Synthesis and characterization of [14]- and [15]orthocyclophanes and bicyclic biscyclophanes.* The Journal of Organic Chemistry, 1992. **57**(15): p. 4074-4079.
49. Glöcklhofer, F., et al., *A Versatile One-Pot Access to Cyanoarenes from ortho- and para-Quinones: Paving the Way for Cyanated Functional Materials.* Chemistry – A European Journal, 2016. **22**(15): p. 5173-5180.
50. Rimmele, M., et al., *Thioalkyl- and sulfone-substituted poly(p-phenylene vinylene)s.* Polymer Chemistry, 2019. **10**(6): p. 738-750.
51. Naulet, G., et al., *Monoprotection of Arylene-Diacetic Acids Allowing the Build-Up of Longer Aromatic Ribbons by Successive Perkin Condensations.* European Journal of Organic Chemistry, 2018. **2018**(5): p. 619-626.
52. Belarmino Cabral, M.G., et al., *From 1,4-Phenylenebis(phenylmaleate) to a Room-Temperature Liquid-Crystalline Benzo[ghi]perylene Diimide.* ChemPlusChem, 2017. **82**(3): p. 342-346.

53. Schmuck, C. and W. Wienand, *The First Efficient Synthesis and Optical Resolution of Monosubstituted Cyclotribenzylenes.* Synthesis, 2002. **2002**(05): p. 0655-0663.

54. Magdalena, S., et al., *Synthesis and Biological Evaluation of Bridged Analogues of the Platelet Aggregation Inhibitor Trifenagrel.* Letters in Drug Design & Discovery, 2009. **6**(7): p. 478-486.

G Appendix

G.1 Cyclic voltammetry (CV)

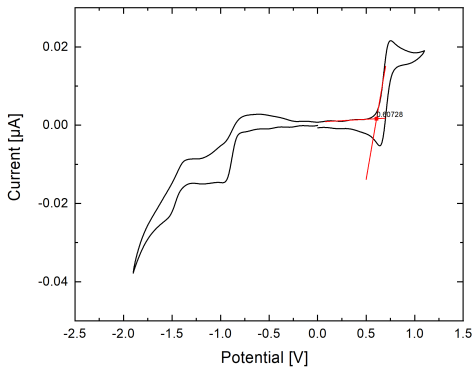

Figure 48: CV plot B-cycle with Fc

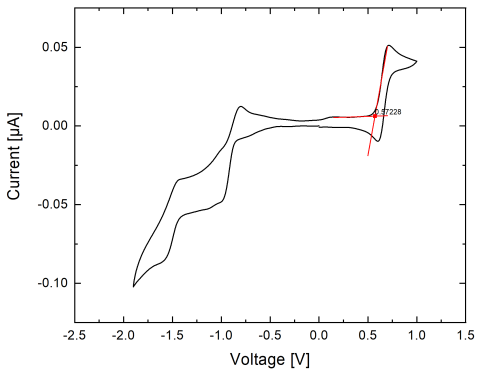

Figure 49: CV plot B-Hx-cycle with Fc

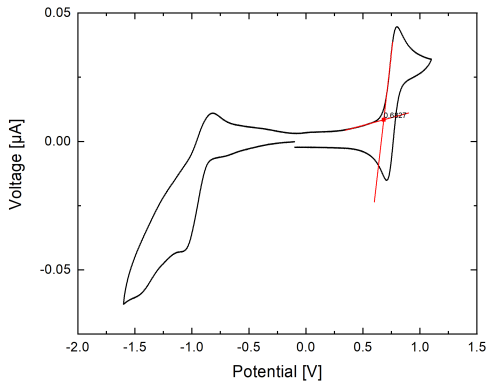

Figure 50: CV plot N-cycle with Fc

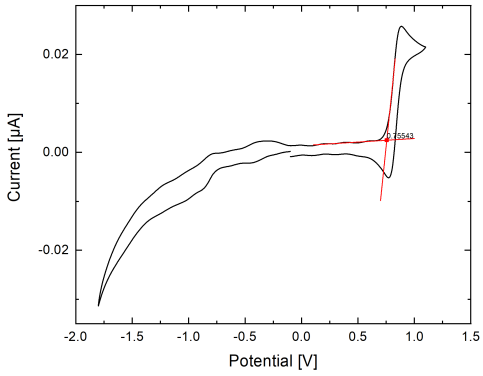

Figure 51: CV plot A-cycle with Fc

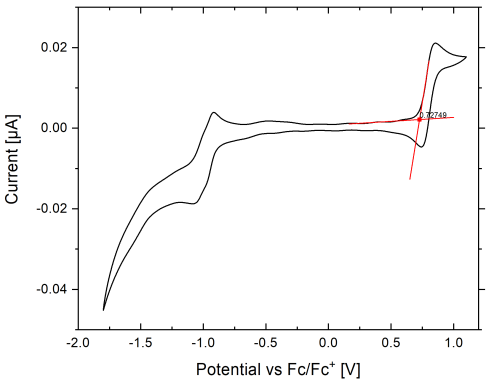

Figure 52: CV plot P-cycle with Fc

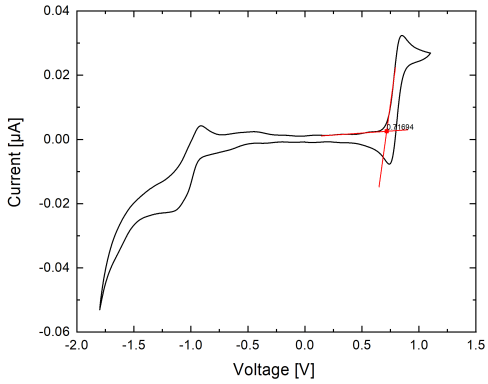

Figure 53: CV plot P-Hx-cycle with Fc

G.2 NMR-spectra

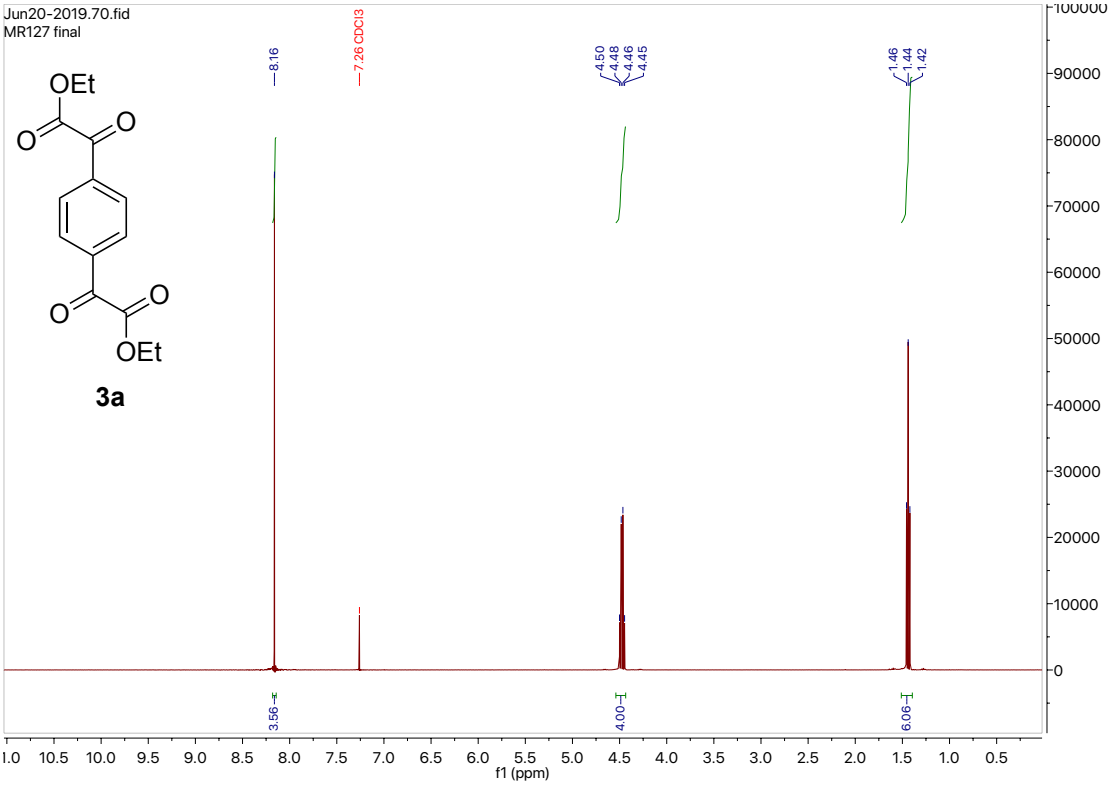

*Figure 54: ^{1}H-NMR (400 MHz, $CDCl_3$) of **3a***

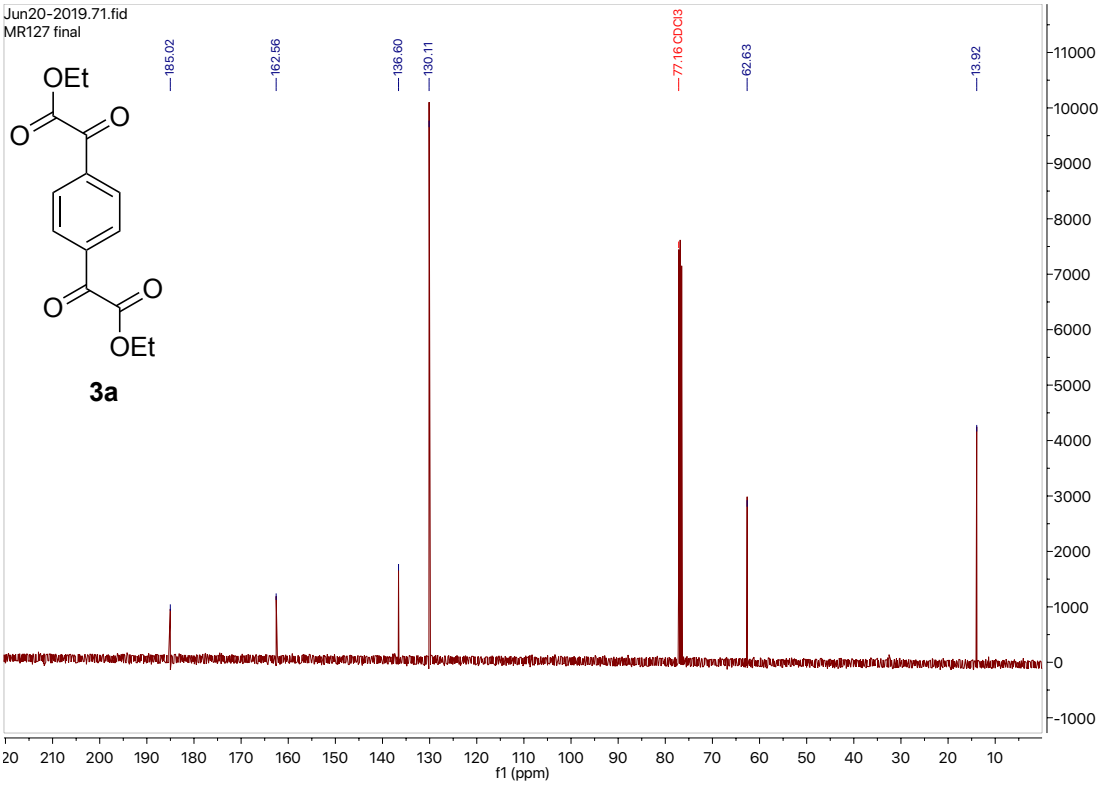

*Figure 55: ^{13}C-NMR (101 MHz, $CDCl_3$) of **3a***

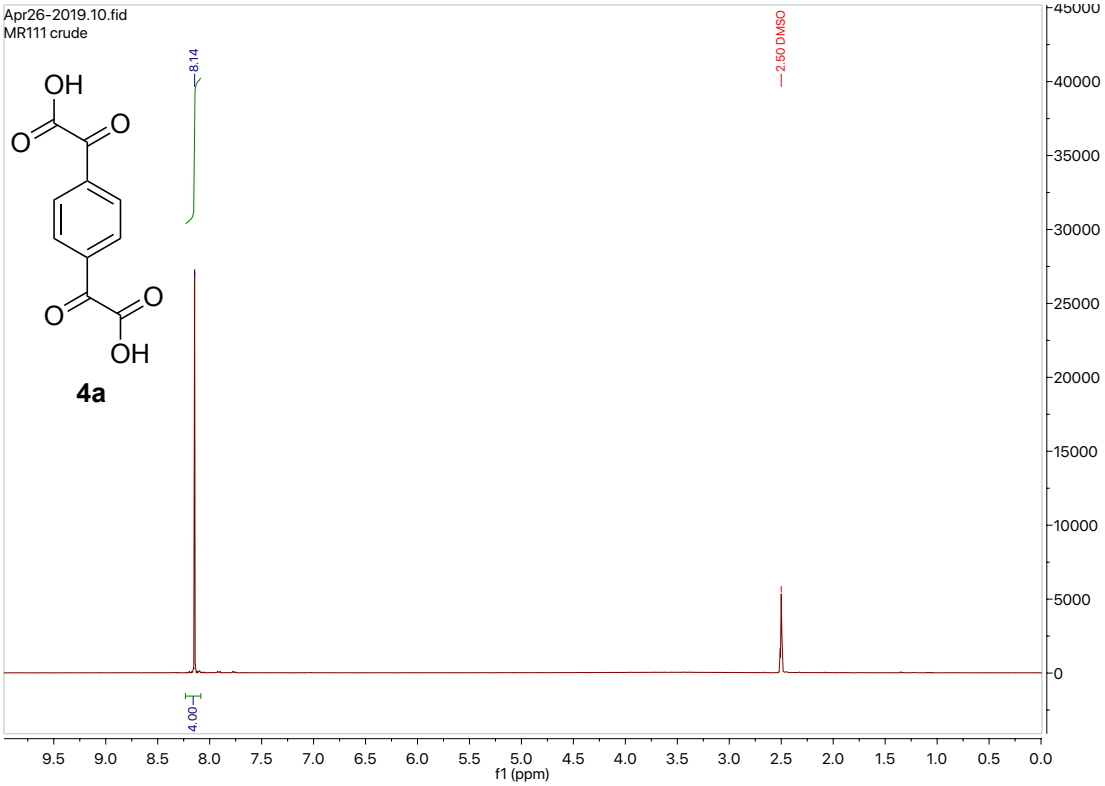

*Figure 56: [1]H-NMR (400 MHz, DMSO) of **4a***

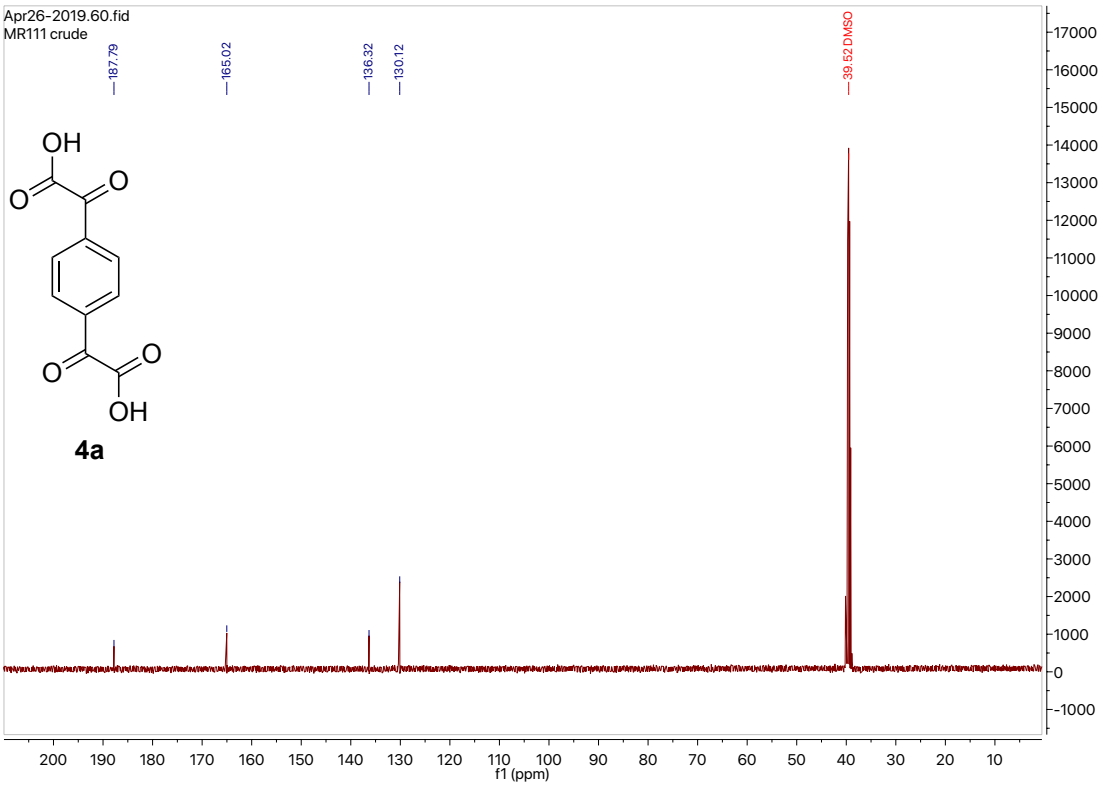

*Figure 57: [13]C-NMR (101 MHz, DMSO) of **4a***

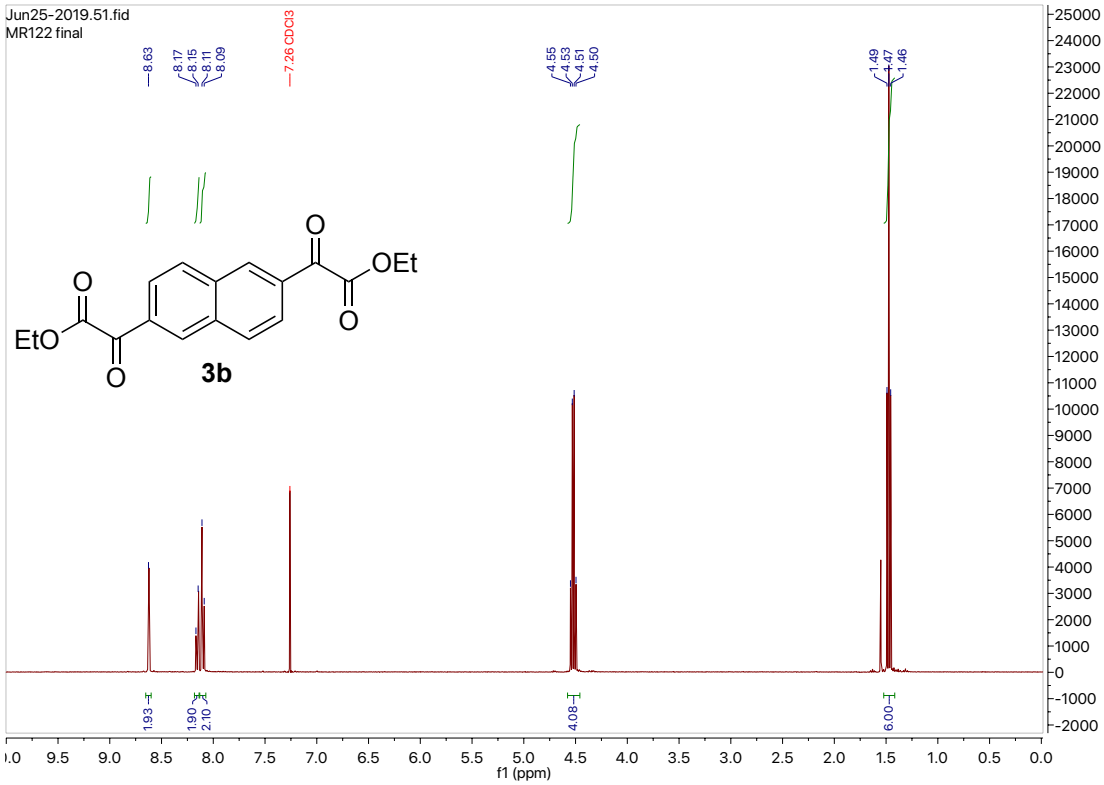

*Figure 58: ^{1}H-NMR (400 MHz, $CDCl_3$) of **3b***

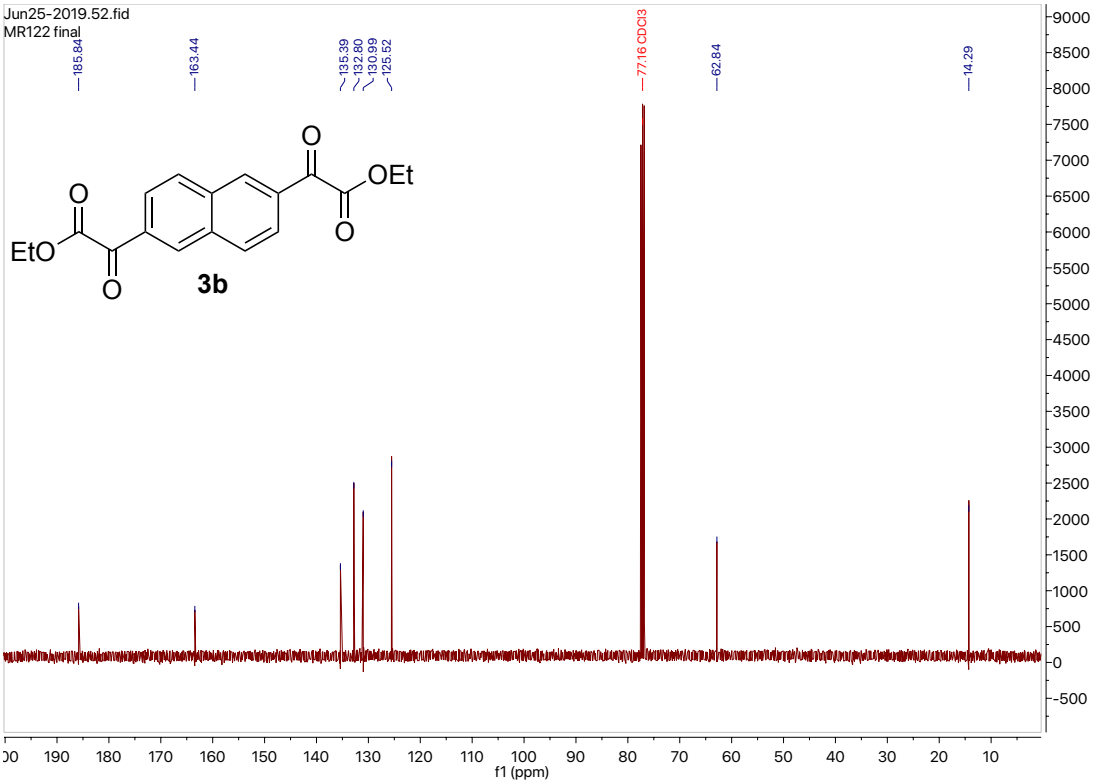

*Figure 59: ^{13}C-NMR (101 MHz, $CDCl_3$) of **3b***

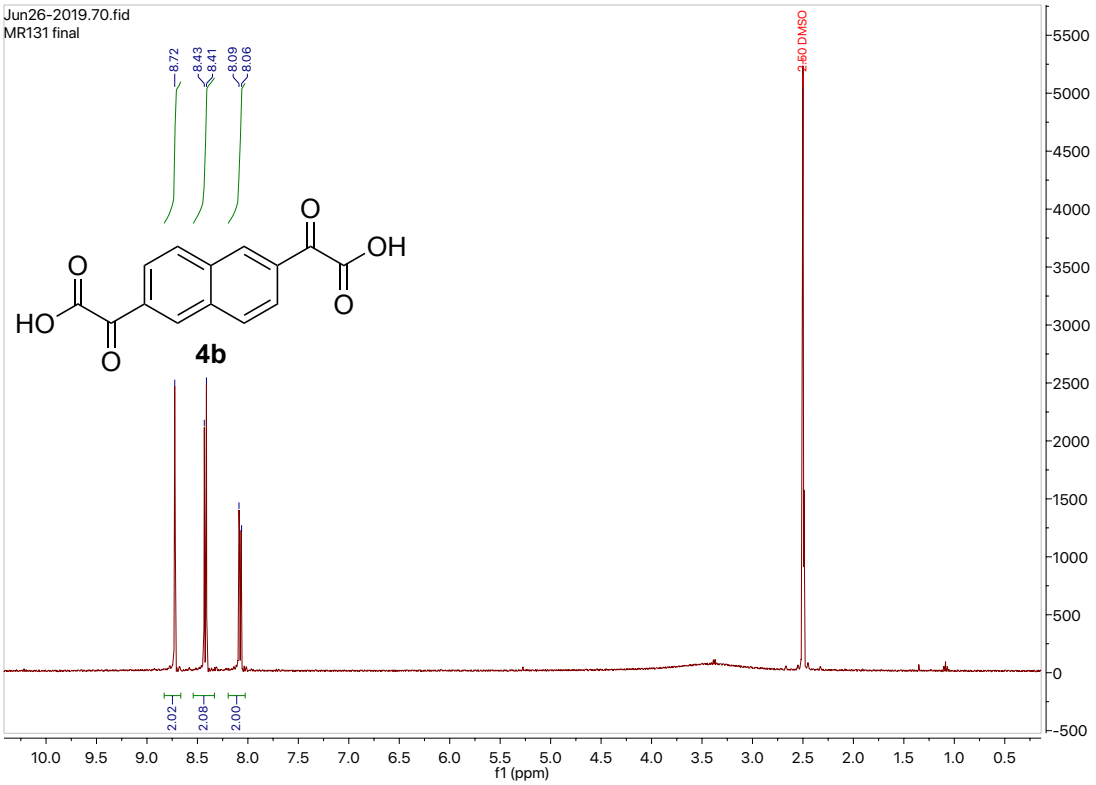

*Figure 60: ^{1}H-NMR (400 MHz, DMSO) of **4b***

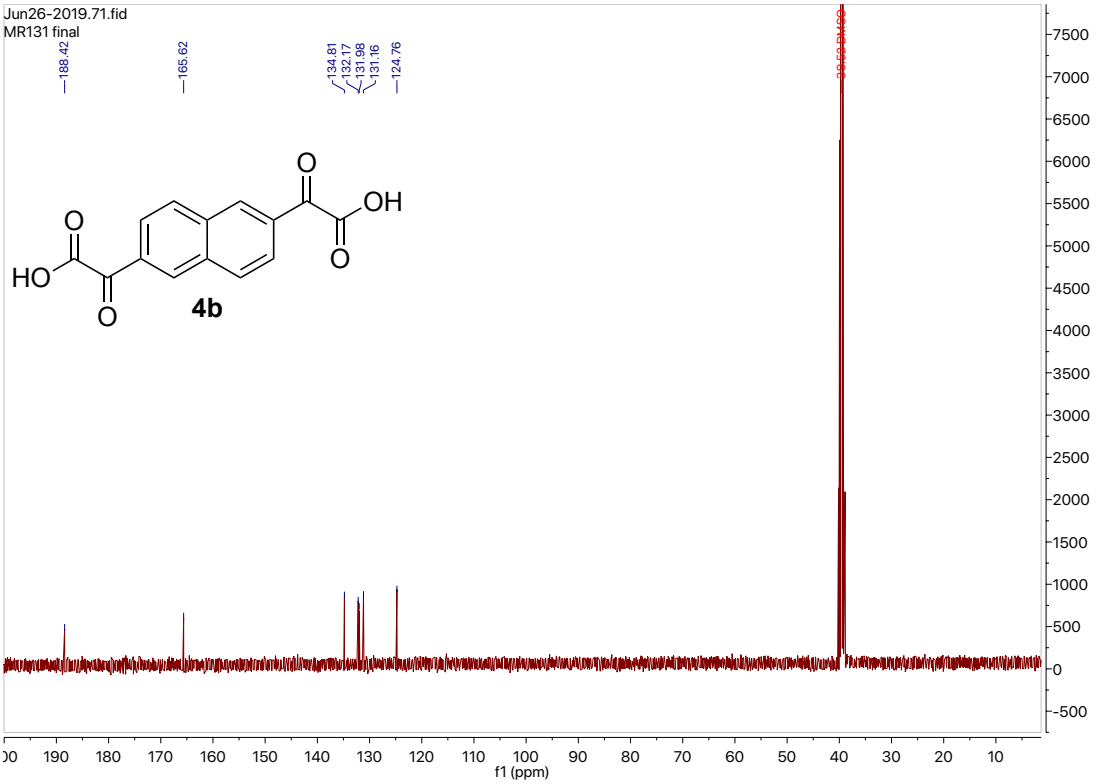

*Figure 61: ^{13}C-NMR (101 MHz, DMSO) of **4b***

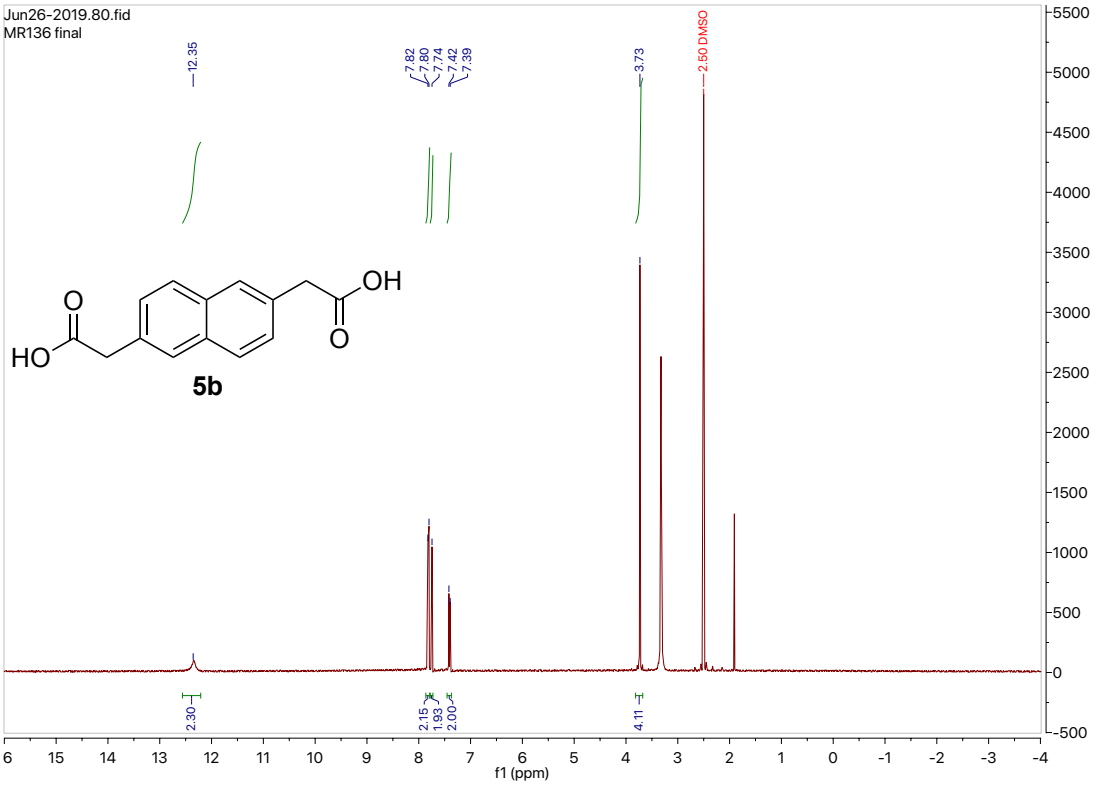

*Figure 62: ^{1}H-NMR (400 MHz, DMSO) of **5b***

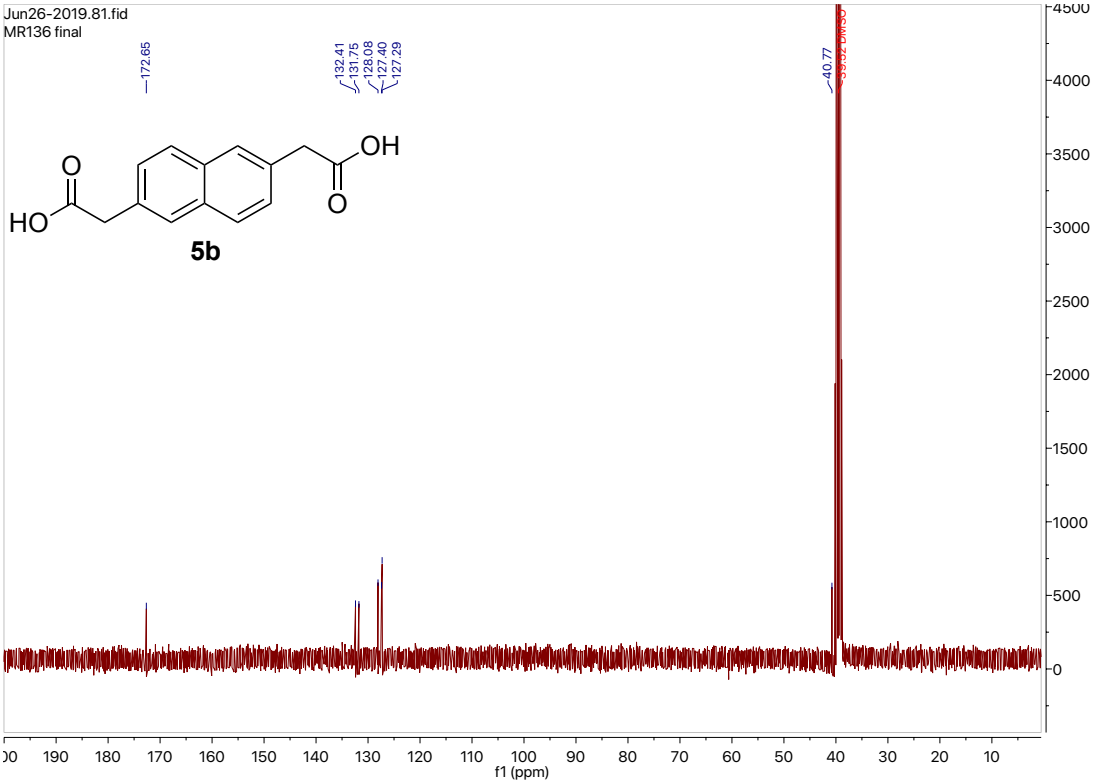

*Figure 63: ^{13}C-NMR (101 MHz, DMSO) of **5b***

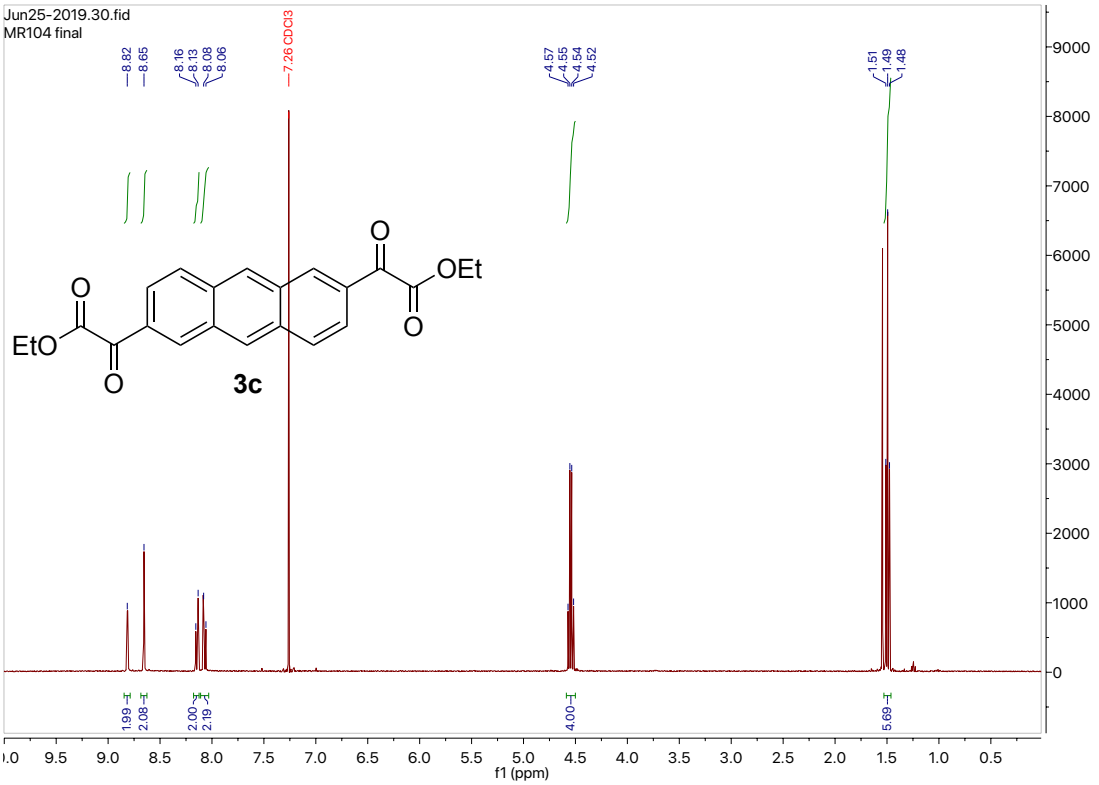

*Figure 64: ^{1}H-NMR (400 MHz, $CDCl_3$) of **3c***

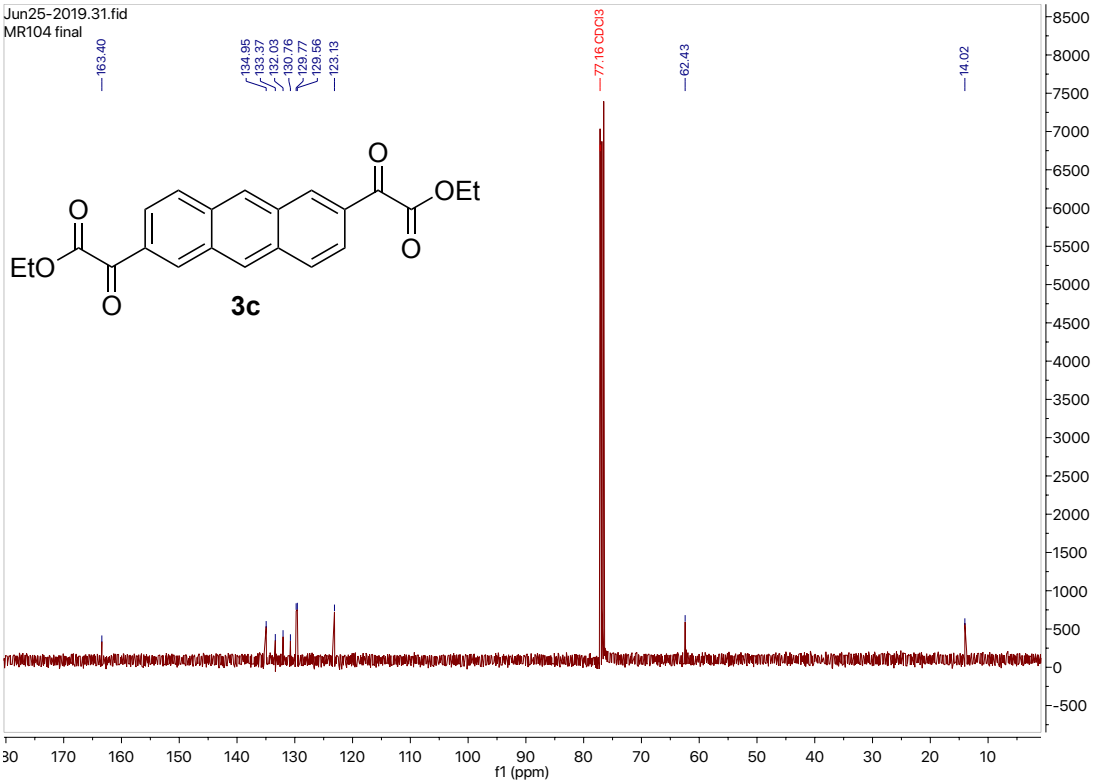

*Figure 65: ^{13}C-NMR (101 MHz, $CDCl_3$) of **3c***

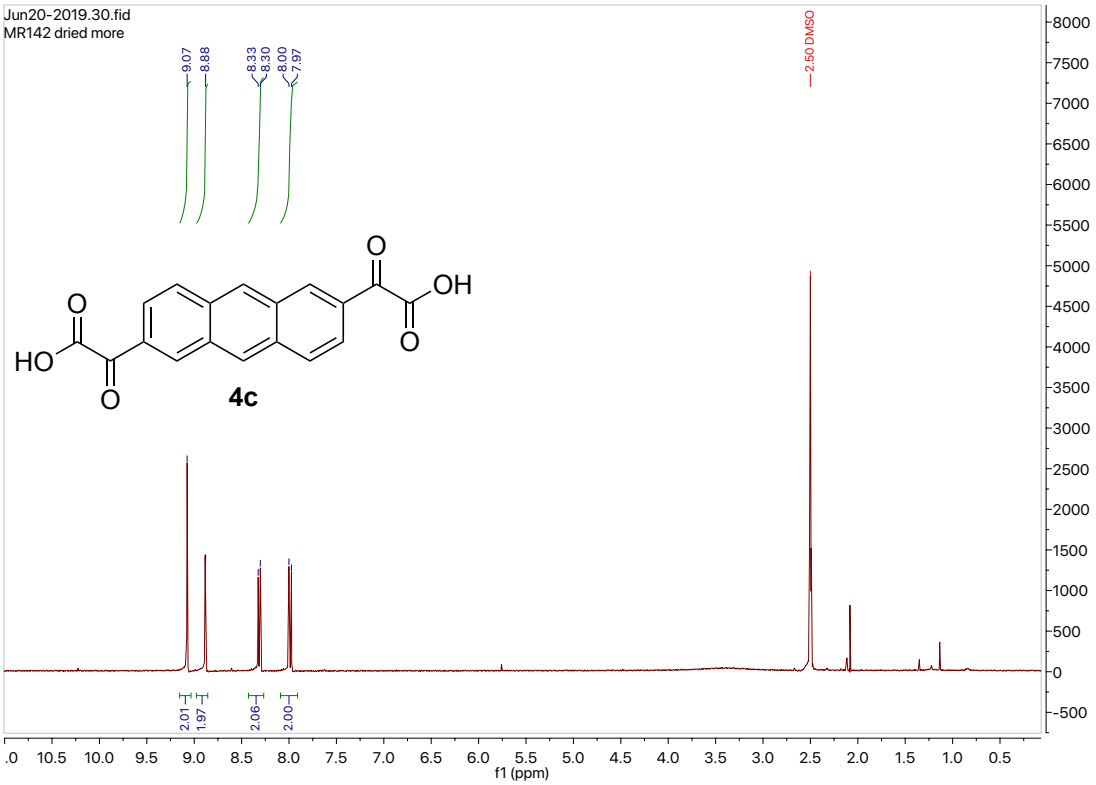

*Figure 66: [1]H-NMR (400 MHz, DMSO) of **4c***

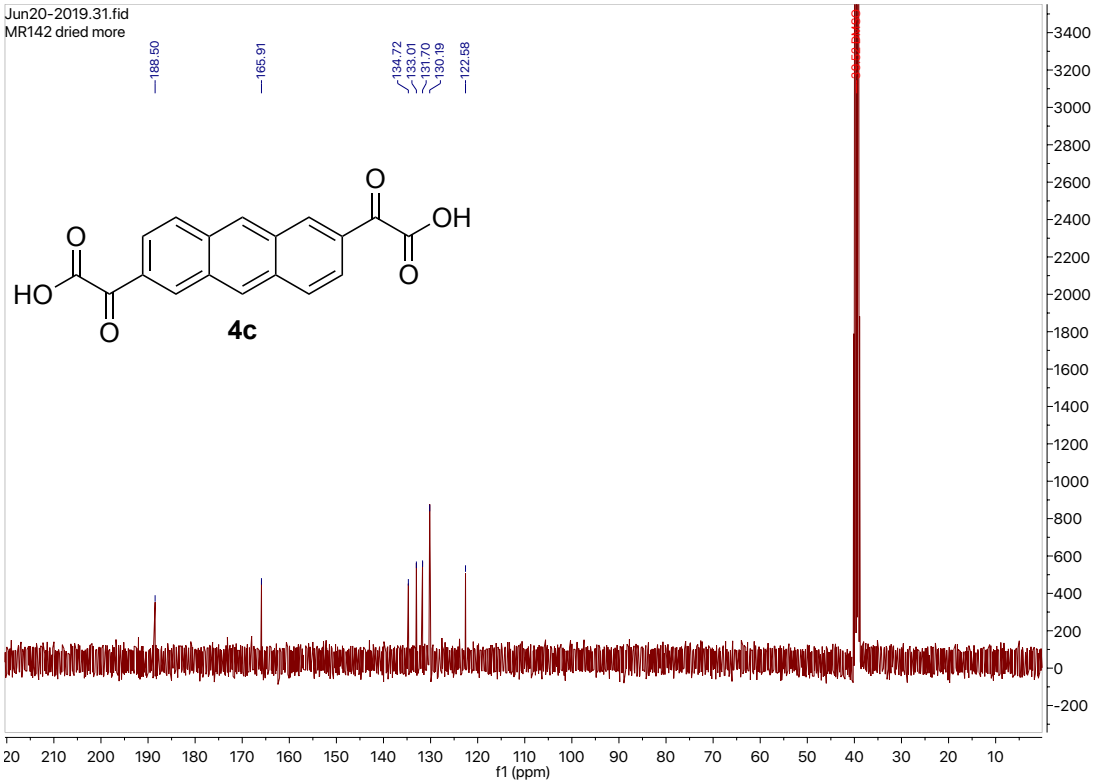

*Figure 67: [13]C-NMR (101 MHz, DMSO) of **4c***

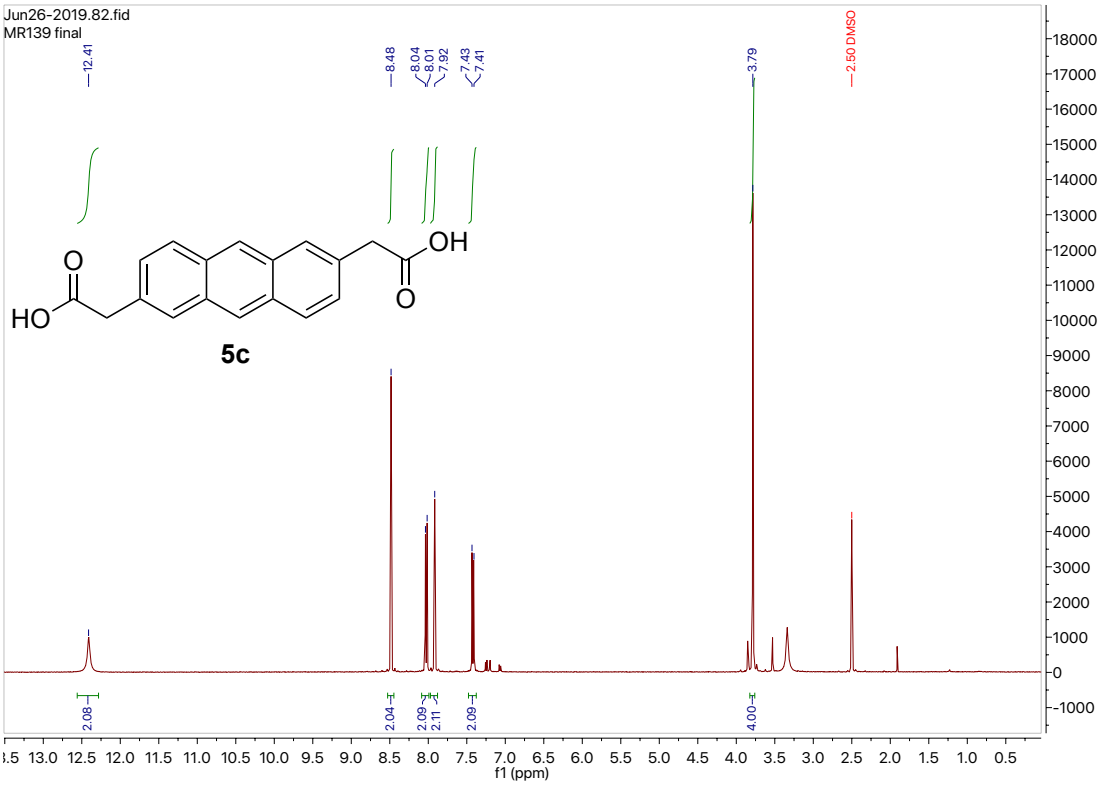

*Figure 68: [1]H-NMR (400 MHz, DMSO) of **5c***

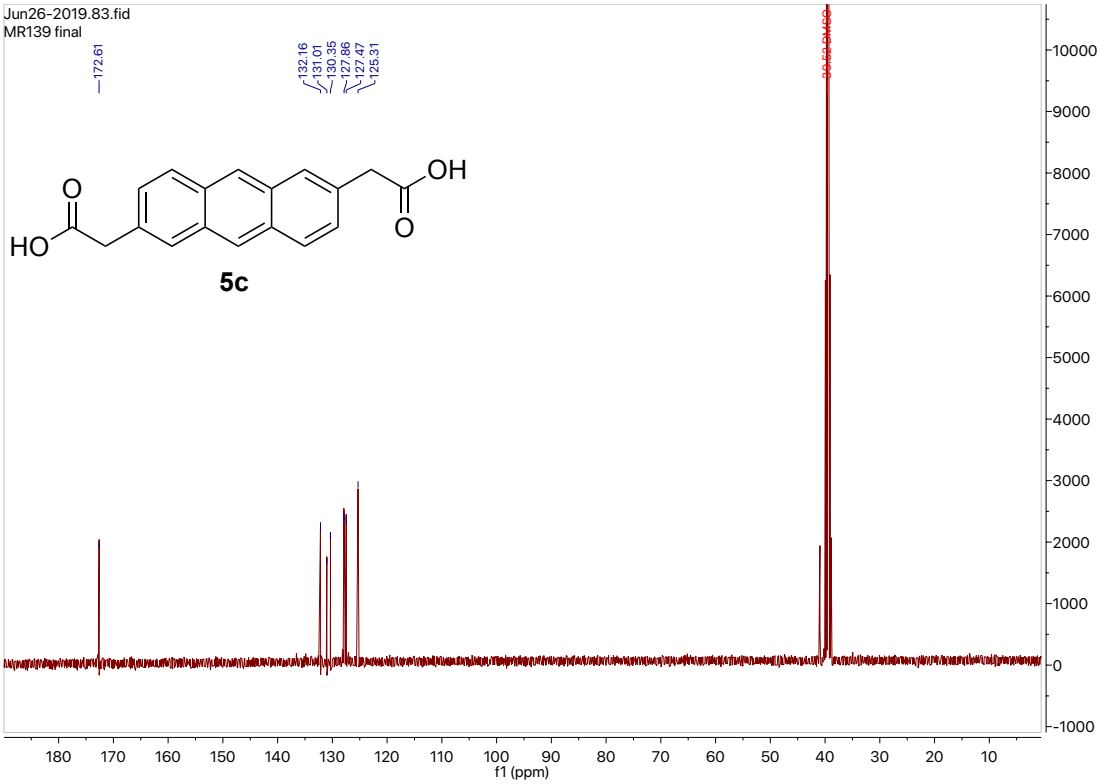

*Figure 69: [13]C-NMR (101 MHz, DMSO) of **5c***

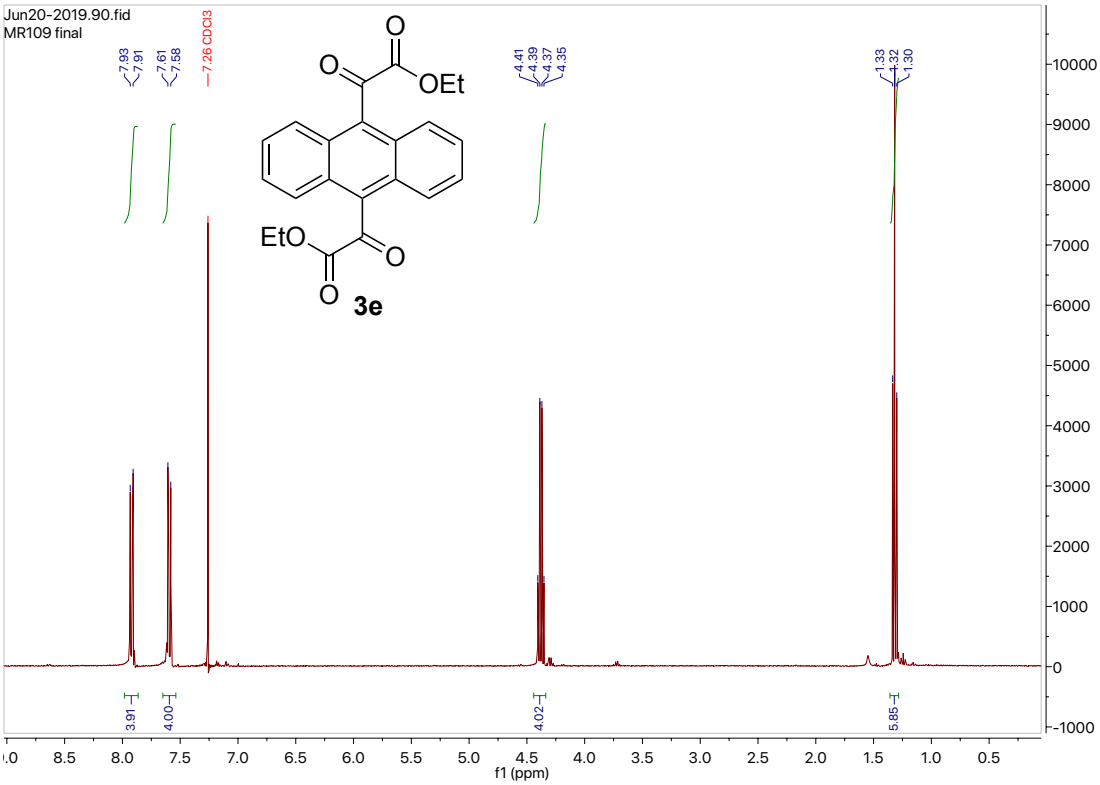

*Figure 70: ^{1}H-NMR (400 MHz, $CDCl_3$) of **3e***

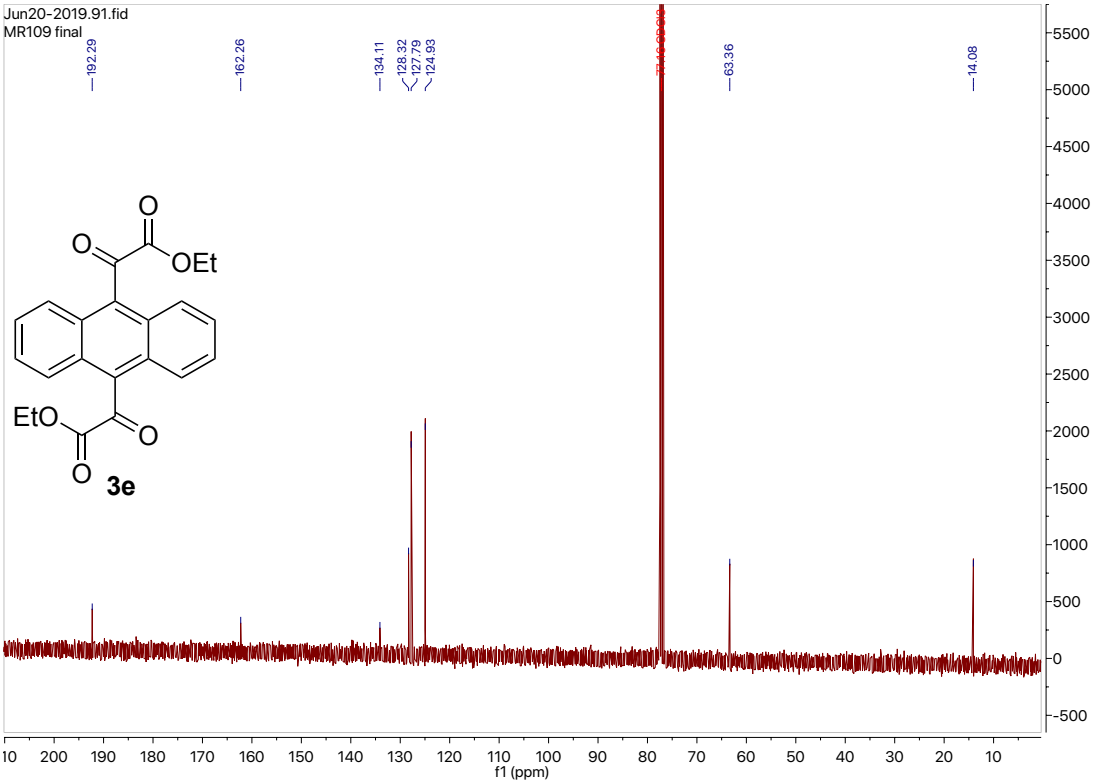

*Figure 71: ^{13}C-NMR (101 MHz, $CDCl_3$) of **3e***

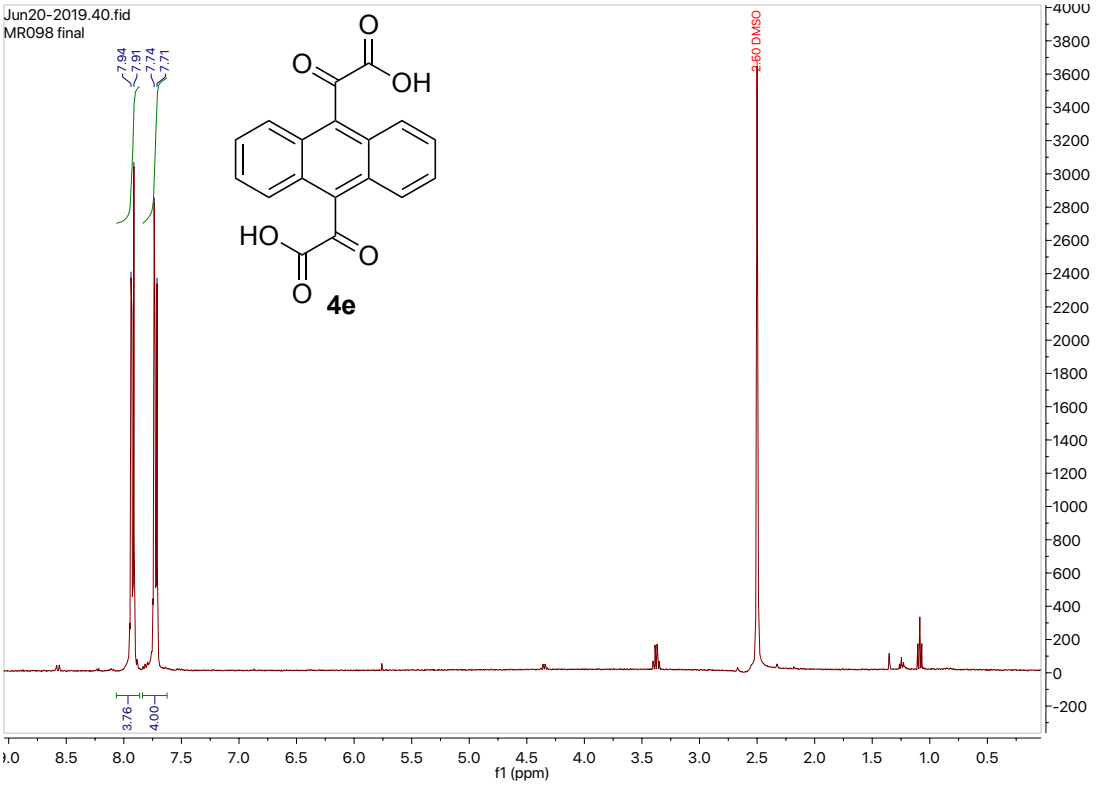

*Figure 72: [1]H-NMR (400 MHz, DMSO) of **4e***

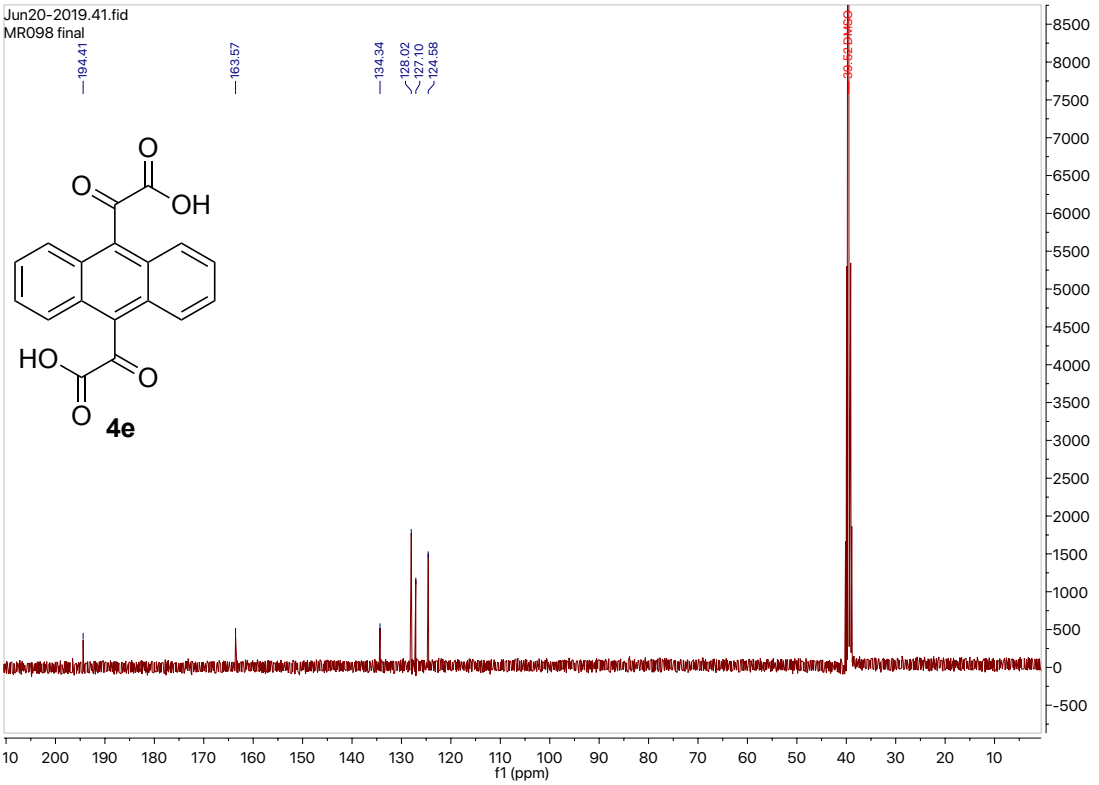

*Figure 73: [13]C-NMR (101 MHz, DMSO) of **4e***

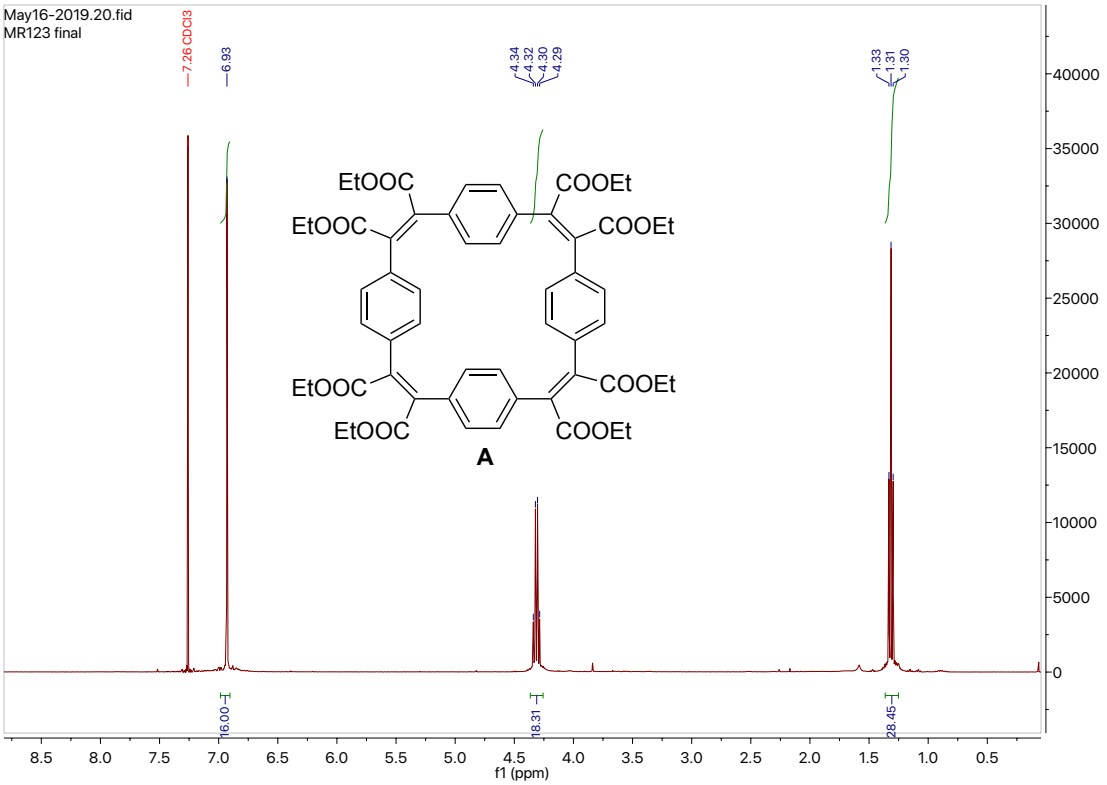

*Figure 74: ^{1}H-NMR (400 MHz, $CDCl_3$) of **A***

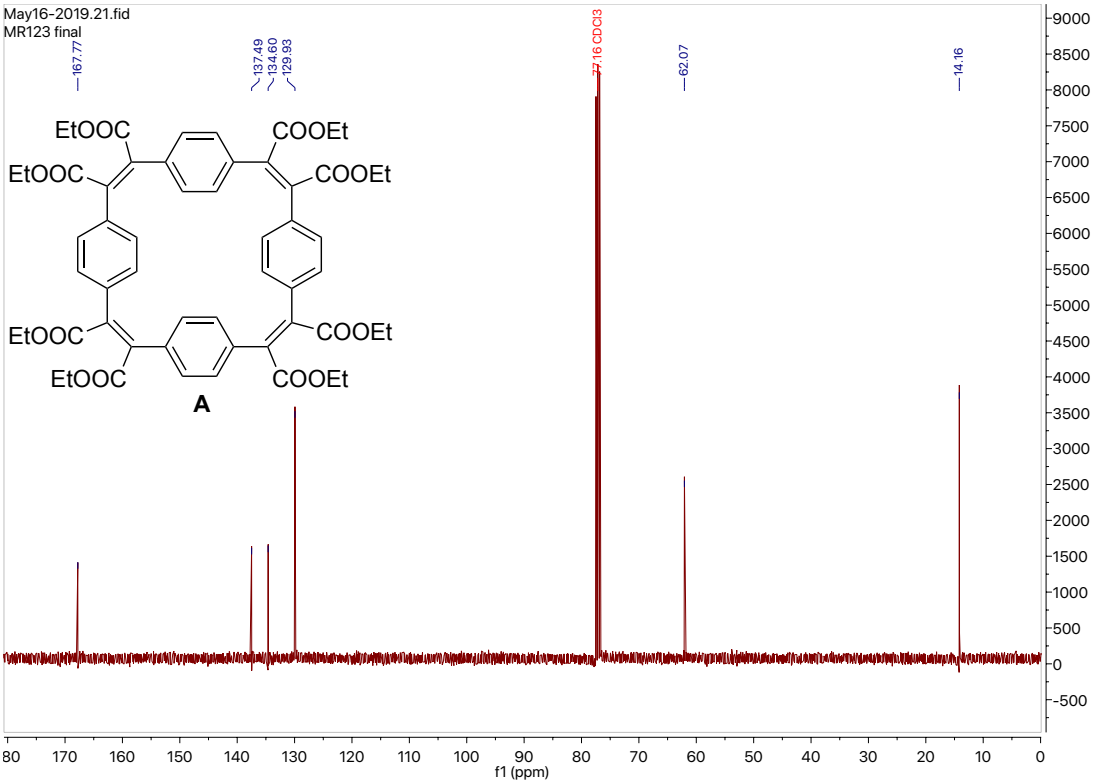

*Figure 75: ^{13}C-NMR (101 MHz, $CDCl_3$) of **A***

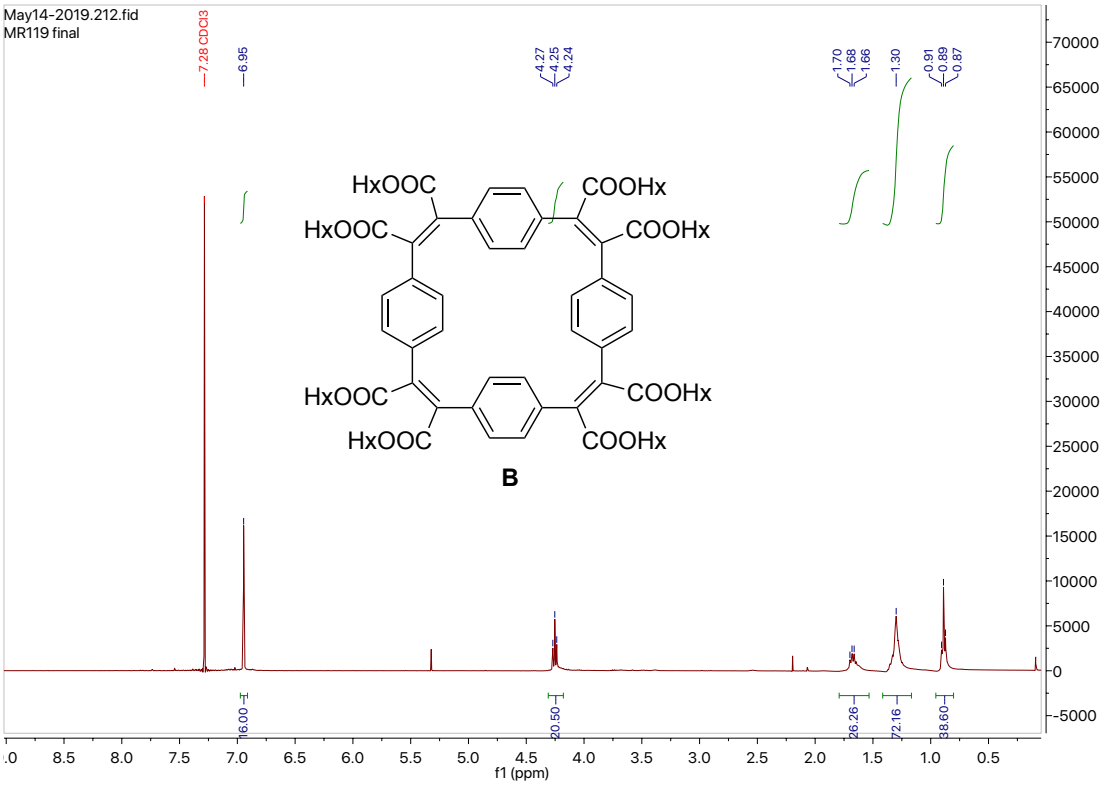

*Figure 76: ^{1}H-NMR (400 MHz, $CDCl_3$) of **B***

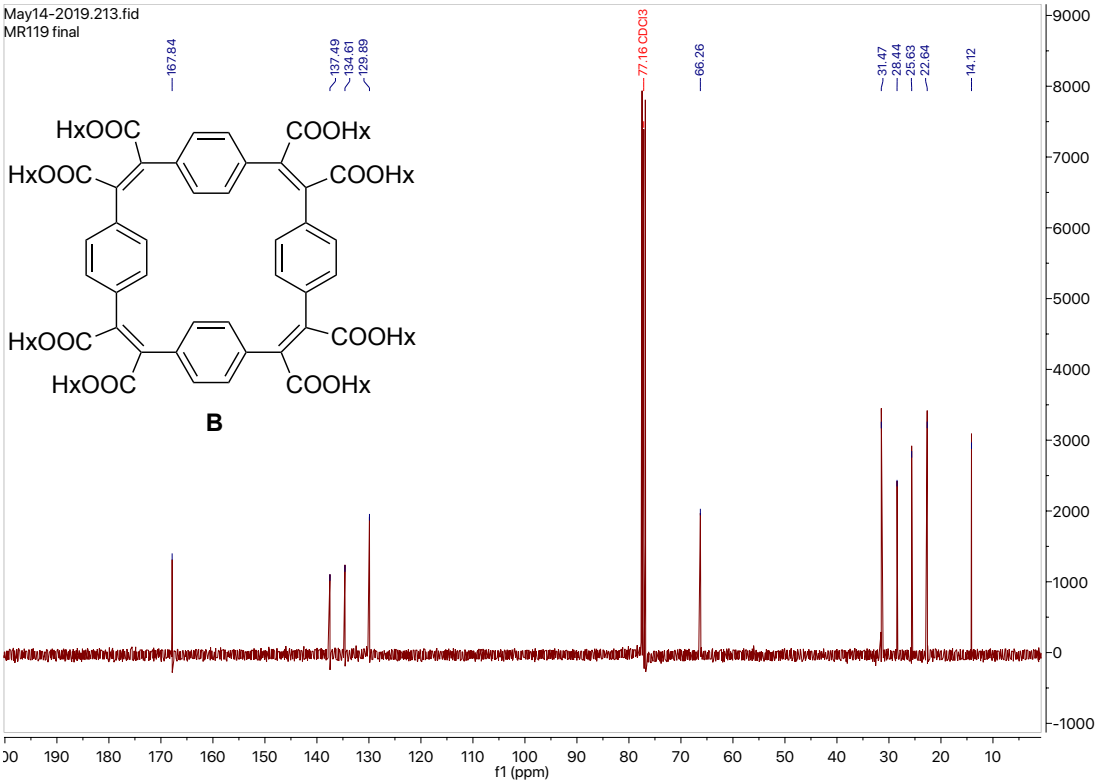

*Figure 77: ^{13}C-NMR (101 MHz, $CDCl_3$) of **B***

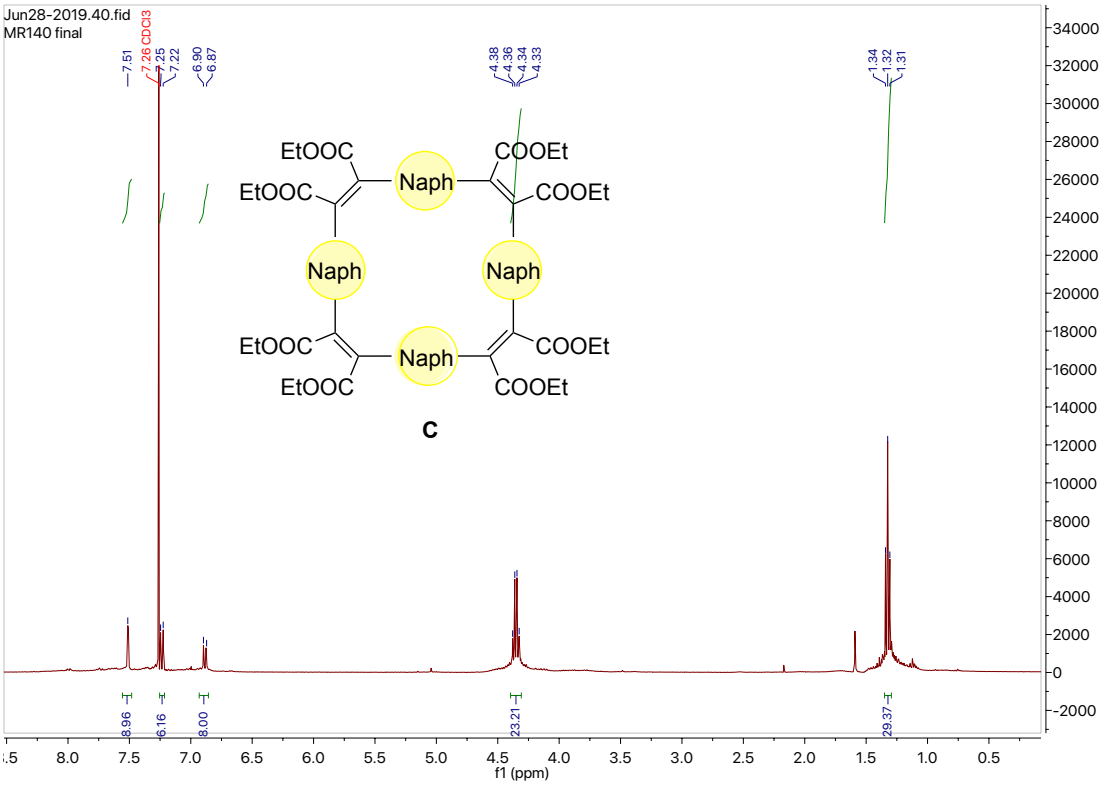

*Figure 78: ^{1}H-NMR (400 MHz, $CDCl_3$) of **C***

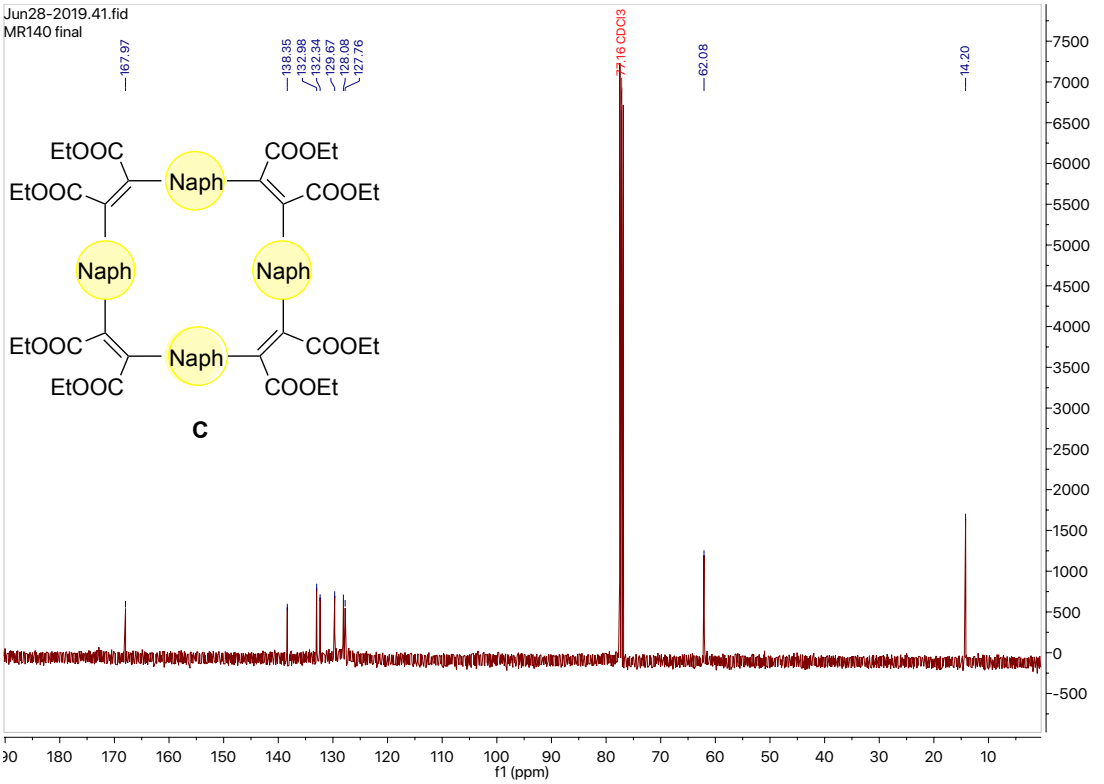

*Figure 79: ^{13}C-NMR (101 MHz, $CDCl_3$) of **C***

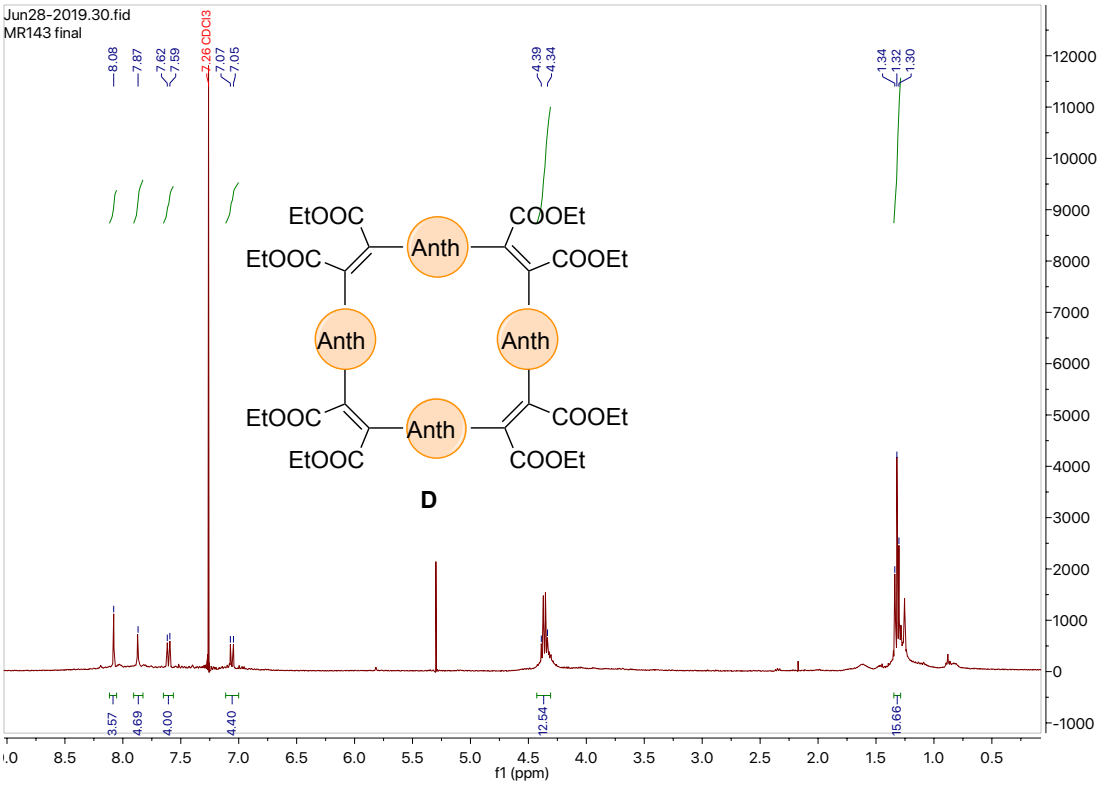

*Figure 80: ^{1}H-NMR (400 MHz, $CDCl_3$) of **D***

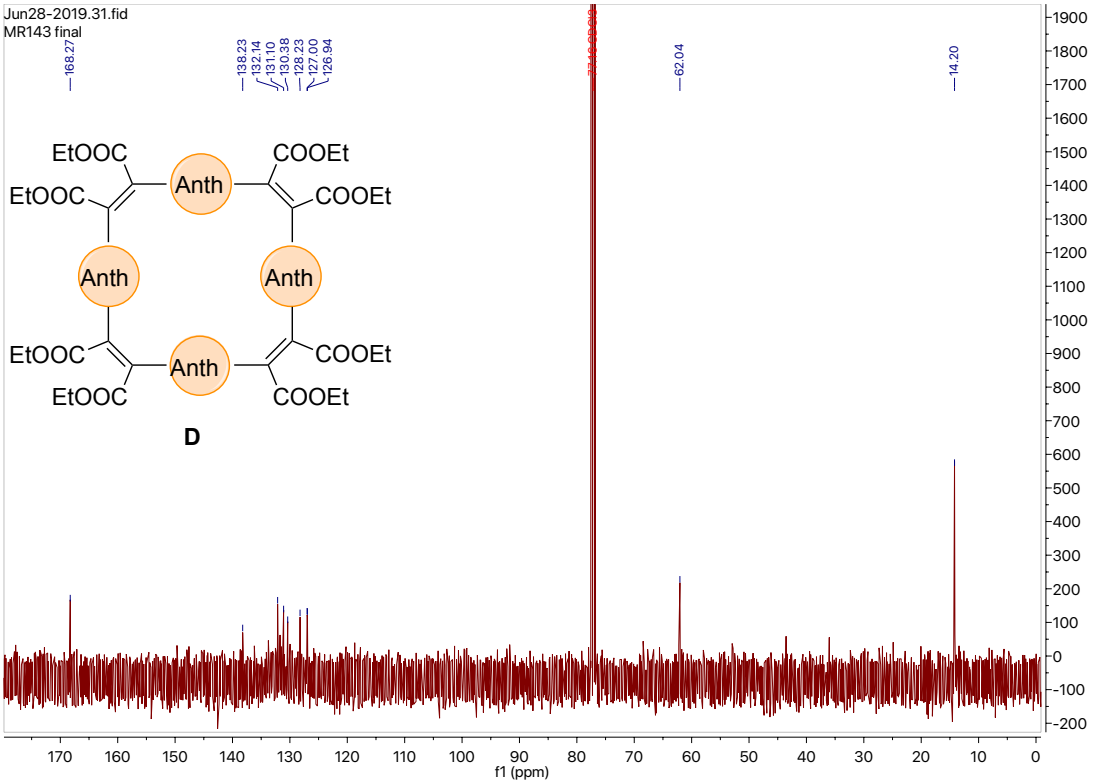

*Figure 81: ^{13}C-NMR (101 MHz, $CDCl_3$) of **D***

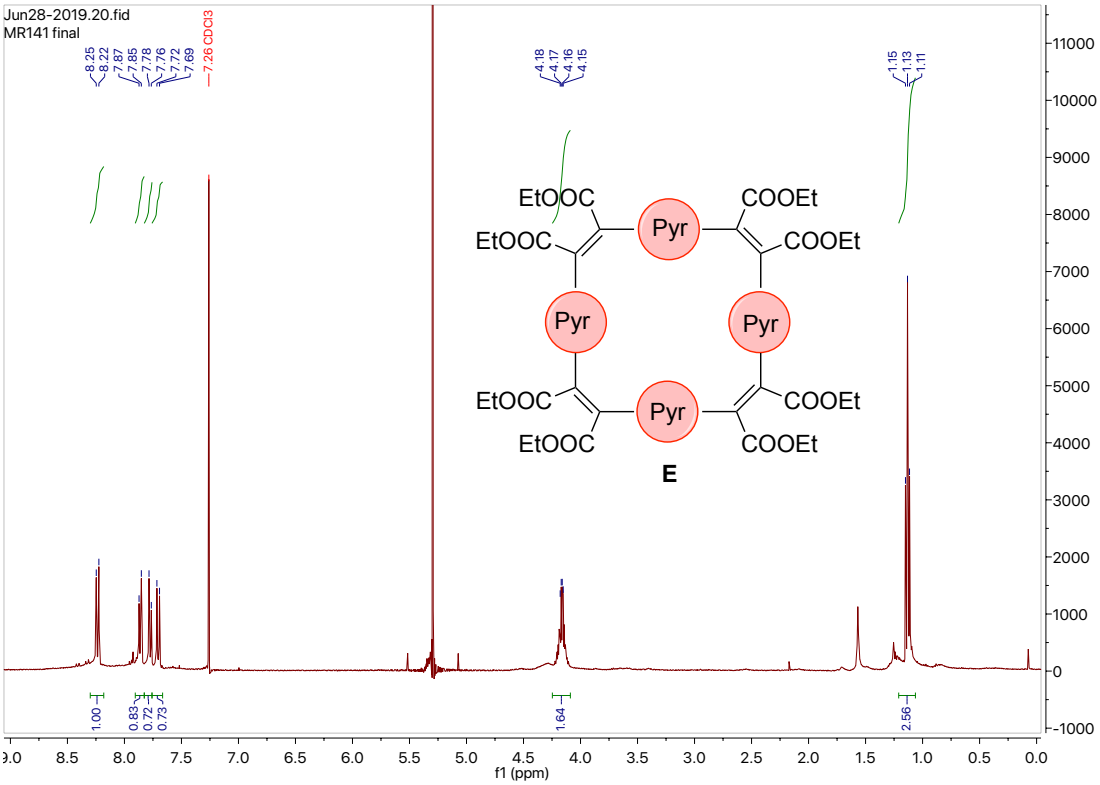

*Figure 82: ^{1}H-NMR (400 MHz, $CDCl_3$) of **E***

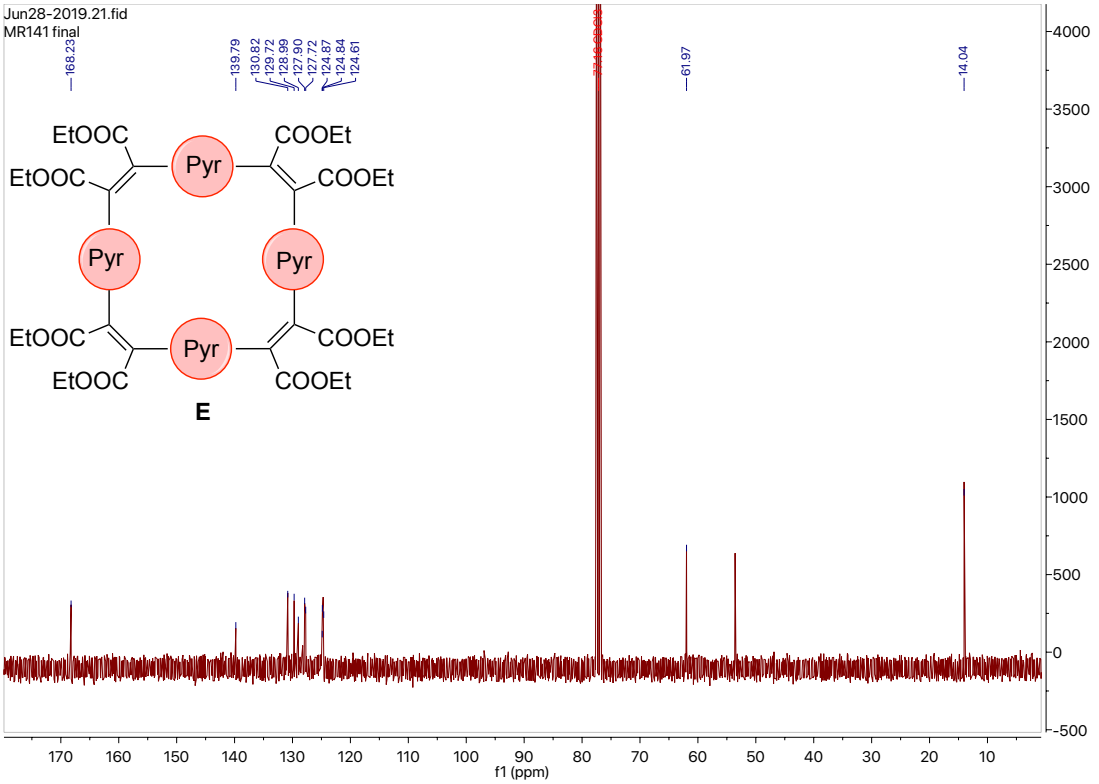

*Figure 83: ^{13}C-NMR (101 MHz, $CDCl_3$) of **E***

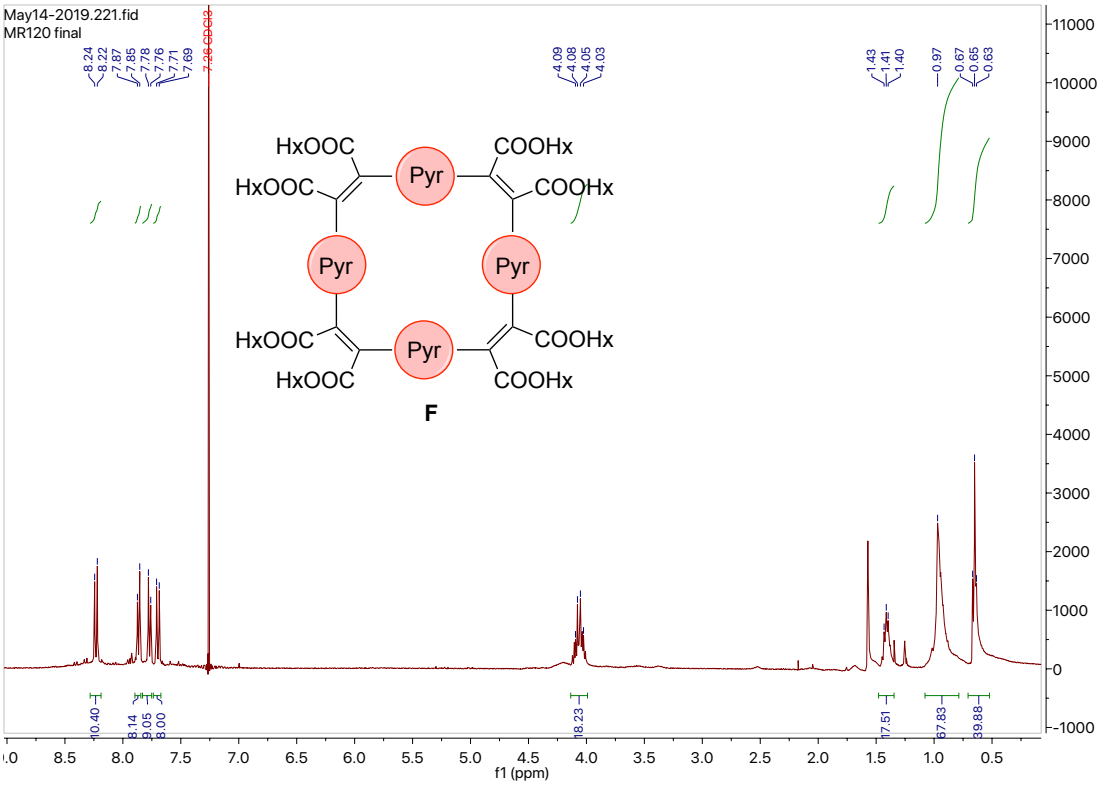

*Figure 84: ^{1}H-NMR (400 MHz, $CDCl_3$) of **F***

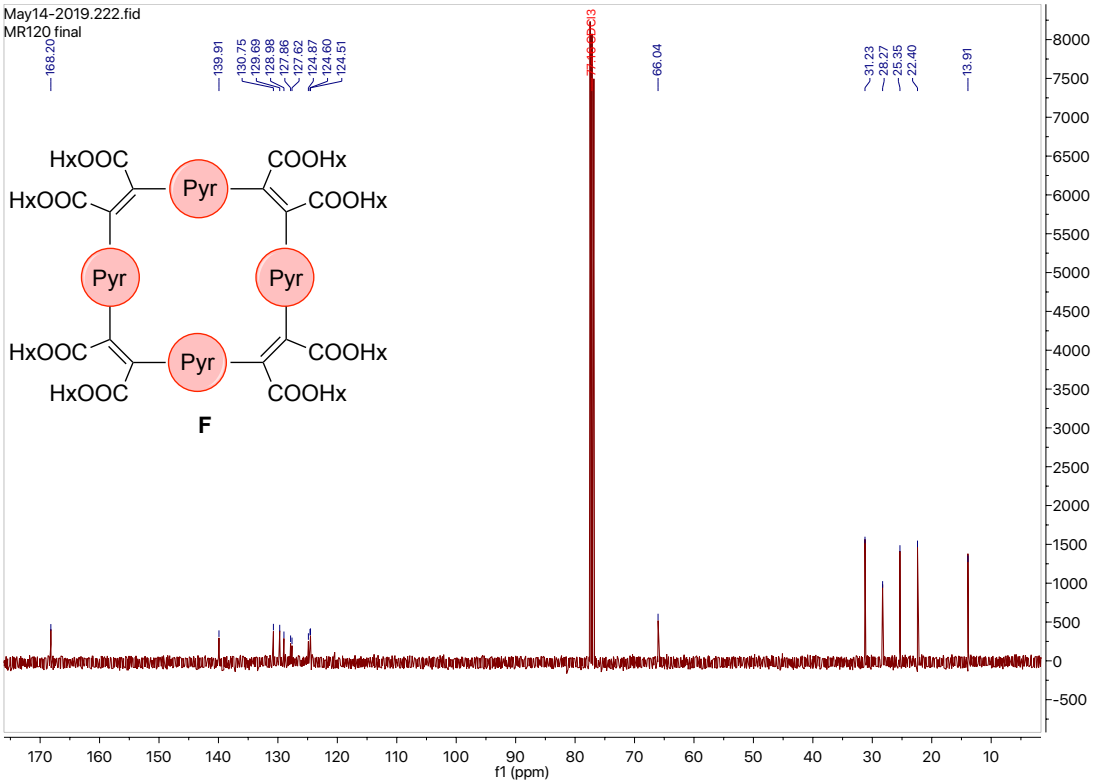

*Figure 85: ^{13}C-NMR (101 MHz, $CDCl_3$) of **F***